



CEEPR

MIT Center for Energy and
Environmental Policy Research

**Working Paper
Series**

Properties of Deeply Decarbonized Electric Power Systems with Storage

Cristian Junge, Cathy Wang, Dharik S. Mallapragada,
Howard K. Gruenspecht, Hannes Pfeifenberger,
Paul L. Joskow, and Richard Schmalensee



FEBRUARY 2022

CEEPR WP 2022-003

Working Paper Series.

Since 1977, the Center for Energy and Environmental Policy Research (CEEPR) has been a focal point for research on energy and environmental policy at MIT. CEEPR promotes rigorous, objective research for improved decision making in government and the private sector, and secures the relevance of its work through close cooperation with industry partners from around the globe. Drawing on the unparalleled resources available at MIT, affiliated faculty and research staff as well as international research associates contribute to the empirical study of a wide range of policy issues related to energy supply, energy demand, and the environment.

An important dissemination channel for these research efforts is the MIT CEEPR Working Paper series. CEEPR releases Working Papers written by researchers from MIT and other academic institutions in order to enable timely consideration and reaction to energy and environmental policy research, but does not conduct a selection process or peer review prior to posting. CEEPR's posting of a Working Paper, therefore, does not constitute an endorsement of the accuracy or merit of the Working Paper. If you have questions about a particular Working Paper, please contact the authors or their home institutions.

Properties of Deeply Decarbonized Electric Power Systems with Storage

Cristian Junge^a, Cathy Wang^a, Dharik S. Mallapragada^a, Howard K. Gruenspecht^a, Hannes Pfeiffenberger^b, Paul L. Joskow^c, Richard Schmalensee^d

ABSTRACT

The final version of this paper will appear as Chapter 6 in the forthcoming MIT Energy Initiative study, The Future of Storage. Chapters referred to in this paper will be included in that study when it is published. In order to illuminate the role of energy storage in future decarbonized electric power systems, we construct detailed models, calibrated to mid-century, of optimal assets and hourly operation of power systems under a range of assumptions about generation and storage technologies' availability and cost. We model three US regions: The Northeast, the Southeast, and Texas. These regions differ in many dimensions, notably in the quality of their variable renewable energy (VRE, wind and solar) resource and load profiles. We find that nearly complete decarbonization of all three systems using only VRE generation and (very little) natural gas, along with Lithium-ion storage, can be achieved without reduced reliability or very large increases in system average electricity cost. The incremental cost of going to complete decarbonization of the electric power system without any offsets from other sectors is very high, however, comparable or higher than estimated costs of negative emissions technologies. If technologies more suitable for long-duration storage are available, they optimally substitute for dispatchable natural gas capacity and, under plausible assumptions, produce only moderate reductions in system average electricity cost. Substantial industrial demand for hydrogen would make its use for storage in the electric power system more attractive. In decarbonized power systems, the distribution of the hourly marginal value of energy (MVE), which corresponds roughly to the wholesale spot price, will be drastically different from the distributions of spot prices in current systems: there will be more hours of high MVEs and many more hours of very low MVEs. In order to encourage efficient economy-wide decarbonization, wholesale markets and retail rate structures will need to be significantly modified. In addition, research in the design, operation, and regulation of decarbonized systems should be a high priority.

a. MIT Energy Initiative, Massachusetts Institute of Technology

b. The Brattle Group, Cambridge, MA

c. Department of Economics, Massachusetts Institute of Technology

d. MIT Sloan School of Management and Department of Economics, Massachusetts Institute of Technology

Email addresses: Junge@mit.edu (Junge), cathyxw@mit.edu (Wang), dhariik@mit.edu (Mallapragada), hkg@mit.edu (Gruenspecht), Hannes.pfeiffenberger@brattle.com (Pfeiffenberger), [pjokow@mit.edu](mailto:pjoskow@mit.edu) (Joskow), rschmal@mit.edu (Schmalensee).

6.1 Introduction

6.1.1 Chapter Overview

As policy makers across the world design and implement policies to achieve long-term deep decarbonization of the power sector, the share of variable renewable energy (VRE) generation (i.e., wind and solar) is expected to grow substantially in the next few decades.¹ Unlike “dispatchable” generation that can be turned up and down by the system operator to balance supply and demand, VRE generation increases and decreases with exogenous variations in wind speed and direction and solar irradiation. The large-scale integration of wind and solar generation is contingent on designing flexible power systems that can balance variations in wind and solar output to continuously meet electricity demand, consistent with reliability criteria. Today, dispatchable generation (e.g., natural gas, nuclear, coal, and reservoir hydropower) provides this kind of balancing service. But in low-carbon systems dominated by VRE generation, the availability of dispatchable resources will be severely limited.

In such systems, power system flexibility can be enhanced by deploying energy storage along with other enhancements to legacy electric power systems: (1) transmission network expansion to increase the geographic footprint of balancing areas and better exploit spatiotemporal variations in demand and weather-driven VRE resource availability; (2) demand flexibility and demand response; and (3) deployment or retention of some dispatchable zero or low-carbon generation. Here, we use systems modeling approaches to examine the value of energy storage for achieving the deep decarbonization of the electric sector and the implications for storage technology development and electricity market design under a wide range of technological and economic assumptions. The findings in this chapter focus on the role for grid-scale storage in developed country settings, such as the United States, with relatively high levels of grid reliability, universal access to electricity, well-developed wholesale electricity markets or regulated vertically integrated utilities, and increases in electricity demand driven by the electrification of segments of the transportation, buildings, and industrial sectors that currently use fossil fuels.

Specifically, we analyze power system evolution in three U.S. regions—the Northeast, Southeast and Texas, as well as, with less detail, at a national level. All these regions, and the United States as a whole, experienced significant reductions in carbon dioxide (CO₂) emissions from electricity generation between 2005 and 2018—both in absolute terms (tons CO₂) and in terms of emissions intensity (grams CO₂ per kilowatt-hour or gCO₂/kWh). These reductions reflect the combined effects of stagnant electricity demand; a large reduction in coal-fired generation in favor of natural gas generation, largely for economic reasons; and significant increases in VRE generation, importantly (but not exclusively) driven by public policy. Notwithstanding these trends, electricity generation remains a major source of energy-related CO₂ emissions in the United States, accounting for roughly 31% of the nation’s total energy-related CO₂ emissions in 2018 (EIA, 2021).²

¹ For example, the International Energy Agency’s Roadmap to Net Zero by 2050 assumes that solar PV and wind will account for 70% of global electricity generation in 2050 (IEA, 2021). Strictly speaking, run-of-the-river hydroelectric generation is also both variable and renewable. We do not model it here because it is not expected to expand significantly in coming decades in developed countries, and its primarily seasonal variability does not pose the sort of challenges associated with wind and solar generation, which are our focus.

² In addition to CO₂, there are also other greenhouse gases (GHG) that contribute to global warming, including methane (CH₄) (10% of U.S. GHG emissions in 2019); nitrous oxide (N₂O) (7%); and hydrofluorocarbons (HFCs), perfluorocarbons (PFCs), sulfur hexafluoride (SF₆), and nitrogen trifluoride (NF₃) (2.8%) (EPA, 2021).

Given the central role for electrification in long-term U.S. decarbonization efforts, the model-based findings in this chapter primarily rely on electricity demand projections from a high-electrification scenario developed by the National Renewable Energy Laboratory (NREL) for its 2018 Electrification Futures (EFS) study. In NREL's high-electrification scenario, U.S. electricity consumption increases by a factor of 1.6 by 2050 relative to the 2018 level of roughly 4,000 terawatt-hours (TWh) (Mai, et al., 2018). Subject to these demand assumptions, which in turn rest on assumptions regarding policy support for electrification of other sectors, we analyze power system evolution for different 2050 power system decarbonization targets, defined in terms of CO₂ emissions produced per kWh of electricity dispatched, for three different regions of the country in 2050. In our study, we focus on four emissions constraints: 0 gCO₂/kWh, 5 gCO₂/kWh, 10 gCO₂/kWh, and 50 gCO₂/kWh. We also consider an unconstrained ("No Limit") case that provides a consistent benchmark to compare the impact of imposing different emissions constraints; additionally, we include some modeling runs with a 1 gCO₂/kWh constraint for Texas. Since we do not consider technologies for removing CO₂ from the atmosphere (sometimes called "negative emissions technologies"³), the 0 gCO₂/kWh case represents a stricter constraint compared to the more common goal of achieving a "net-zero" power system, where a net-zero system could allow for the deployment of one or more negative emissions technologies that we do not include in our analysis.

When contemplating the common goal of "net-zero" carbon energy systems, where the term "net-zero" is understood to allow for the inclusion of negative emissions technologies, the 5 gCO₂/kWh or even the 10 gCO₂/kWh emissions constraint modeled here is likely more informative than the very strict 0 gCO₂/kWh constraint. At the 2018 level of electricity demand, reducing the average carbon intensity of generation for the U.S. electricity grid to 5 gCO₂/kWh or 10 gCO₂/kWh from the nation-wide average of 449 gCO₂/kWh in 2018 (Table 6.1) would result in total U.S. CO₂ emissions from electricity generation of 21 million metric tons (MMT) or 42 MMT respectively, delivering reductions of 99.2% or 98.3% respectively relative to 2005 electricity sector emissions of 2,544 MMT (EIA, 2021).⁴ To meet a higher, 6,700-TWh level of demand (the load projected for 2050 in NREL's EFS high-electrification scenario), these same intensity targets would deliver reductions of 98.7% or 97.4%, respectively, relative to emissions if average intensity remained at the 2005 level. While our analysis focuses on grid decarbonization by 2050, achieving zero or net-zero carbon emissions from electricity generation sooner than 2050, say by 2035 (consistent with some decarbonization goals), would require more rapid shifts in the generation mix and possibly an expanded role for energy storage (for both short-duration and long-duration uses). It could involve much higher costs than those modeled here since our analysis incorporates significant reductions in the costs of VRE generation and storage by 2050. These cost reductions are unlikely to be realized by 2035. Accordingly, if 2035 is the target year for "net-zero" emissions it would likely have to be achieved with higher-cost technologies than those incorporated into our analyses for 2050.

³ Examples of such technologies include biomass for energy production coupled with carbon capture and sequestration (CCS) or systems that capture CO₂ directly from the ambient air (sometimes called 'direct air capture') (Daggash et al. 2019; Fajardy et al. 2021).

⁴ The United States, Canada, Japan, Australia, and many other countries use 2005 as the baseline year for emission reduction commitments. Many European countries use 1990 as their baseline year.

	2005		2018	
Electricity Generation				
	TWh	% 2050	TWh	% 2050
U.S. Total	4,055	61%	4,178	62%
Northeast	283	62%	238	52%
Southeast	824	115%	834	117%
Texas	397	27%	477	33%
Electricity-Related CO₂ Emissions				
	MMT	gCO ₂ /kWh	MMT	gCO ₂ /kWh
U.S. Total	2,544	627	1,874	449
Northeast	118	416	55	232
Southeast	485	589	327	392
Texas	261	659	230	482

Table 6.1: Electricity generation and electricity-related emissions (U.S. total and three regions modeled in this study). Regional figures are based on summing up emissions for the various states part of each region. Data source: “U.S. Electric Power Industry Estimated Emissions by State” (EIA, 2021).

6.1.2 Roles of Storage in Power Systems

There is growing interest in deploying energy storage for a variety of applications on the electricity grid. For example, the U.S. Energy Information Administration (EIA) classifies battery projects based on 11 leading applications that overlap to some extent, including frequency regulation as well as other ancillary services (e.g., spinning reserves, voltage support), storage for excess wind and solar generation, load management, system peak shaving, transmission and distribution network deferral, backup power, and energy arbitrage (where arbitrage involves effectively moving the electricity from one time period to another) (DNV GL 2017; EIA 2020). The latter enables time-shifting of energy supply and is functionally central to the other grid applications provided by energy storage. The model results presented in this chapter focus on the value of energy storage enabled by its arbitrage function in future electricity systems. Energy storage makes it possible to defer investments in generation and transmission, reduce VRE curtailment, reduce thermal generator startups, and reduce transmission losses.

While these use cases are likely to have the greatest long-term impact on grid evolution, there are other valuable use cases for energy storage that we do not consider. These include: (1) deployment of storage at the level of the distribution network for operational or investment deferral reasons, which can be valuable, but generally represent context-specific opportunities that cannot be easily generalized; and (2) consumer adoption of storage to reduce consumption during peak demand hours, which can enable large users to manage demand charges that may constitute a significant part of their total bill and which can also increase the value of rooftop photovoltaics (PV) for all types of customers under alternative tariff structures (Neubauer and Simpson 2015; Darghouth, et al. 2020). These use cases are strongly affected by available retail tariff structures as well as by the methods used to value rooftop PV injections back to the grid; thus, they cannot be generalized. A third use case we do not consider is storage to provide a variety of ancillary services that are required to meet reliability criteria at the bulk power system level. These reliability needs tend to be smaller than capacity requirements for electricity supply and thus are mainly important as short-term drivers for storage value and deployment. The distribution network and customer-level use cases for storage are partly addressed in Chapter 7 in the context of developing country settings.

6.2 Systems Modeling Approach

6.2.1 Capacity Expansion Modeling (GenX)

Our analysis uses an open-source capacity expansion model (CEM) called GenX (MITEI and Princeton University, 2021). GenX takes the perspective of a cost-minimizing central planner to determine the optimal generation, storage, and transmission investments needed to meet a pre-defined time-path of system demand, while adhering to various grid operational constraints, resource availability limits, and other imposed policy/environmental constraints. Similar to other state-of-art CEMs (Brown, Hörsch and Schlachtberger; Johnston, et al. 2019; Kuepper, Teichgraeber and Brandt 2020), GenX incorporates a detailed temporal resolution of power sector operations, based on modeling either representative periods or one or more years at an hourly resolution, depending on the model configuration. As noted by recent inter-model comparison studies (Mai, Barrows, et al. 2015; EPRI and RFF 2017; Cole, et al. 2017; Mallapragada, et al. 2018), increasing temporal resolution and preservation of chronology in CEMs allow for improved characterization of the temporal variability of demand or “load,” VRE generation, and the inter-temporal dynamics of various generators and energy storage technologies. GenX can also be used to model the available suite of demand- and supply-side resources and has the capability to represent non-electric energy demand and its impact on the power sector.

Several major grid operating constraints are activated in GenX for this study. The first is demand and supply balance for each hour at the zonal level, considering inter-zonal imports and exports as well as the option of shedding load in each zone at a value of lost load (VoLL) equal to \$50,000/MWh. A high VoLL was chosen to minimize instances of involuntary load shedding and incentivize investment in more capacity to meet demand within the energy-only market framework implemented in the model. Other operating constraints in the model include linearized unit commitment (start-up/shut-down) decisions,⁵ and minimum up/down times and hourly ramping limits for thermal generators; transmission capacity limits and linear line losses,⁶ where applicable; inter-temporal constraints governing storage state-of-charge and capacity constraints on maximum hourly charge/discharge and stored energy; and renewable resource (both VRE and hydropower) availability limits in each hour. To model system evolution to meet the decarbonization targets mentioned previously, we include constraints to enforce upper limits on annual average CO₂ emissions intensity that account for generation and storage discharge as well as storage losses. The long-run system-level optimization approach employed by GenX and other state-of-art CEMs (Brown, Hörsch and Schlachtberger; Johnston, et al. 2019; Kuepper, Teichgraeber and Brandt 2020) captures the declining marginal value of all resources, including energy storage, and their resulting least-cost equilibrium penetration levels. The shadow prices on the carbon emission limits imposed within the CEM can be thought of as carbon prices that are included in system prices when carbon-emitting generation is on the

⁵ Many thermal generators have a non-zero minimum stable power output level below which the plant needs to be shut down in case its power output needs to be lowered further. This discontinuity in power output is typically captured in power systems models using binary variables that are either 1 or 0 depending on the plant’s commitment status (1=committed, 0=not committed). Several operational constraints can be formulated using the commitment variable, but these constraints add significantly to computational complexity. Linearized unit commitment refers to implementations where the integrality of plant commitment variables is relaxed but the associated operational constraints are still enforced. Previous work has shown that this approximation provides a reasonable balance between computational tractability and accuracy in power systems planning models (Palmintier 2013; Poncelet, Delarue and D’haeseleer 2020).

⁶ Generally, transmission losses scale as a quadratic function of power flows. To maintain model linearity and thus, computational tractability, we approximate transmission losses to be a linear function of power flow across the line in each time interval (Brown, et al., 2020).

margin (Brown & Reichenberg, 2021). This makes the model suitable for evaluating the impact of technology and system drivers on the role for energy storage in future power systems. Like most other CEMs, GenX models only bulk power supply and considers the costs of generation and storage, as well as additions to the transmission grid, where applicable. It seems likely that existing fossil-fuel generating plants will have retired by 2050, so greenfield conditions are assumed for this study, with the exception of hydro (Northeast, Southeast) and some existing nuclear (Southeast), where available. We do not model distribution costs or compute estimates of retail rates.

Like any single-stage CEM, GenX outputs include cost-optimal installed capacities of generation, storage, and transmission assets, as well as their hourly utilization to meet the modeled load. Constant returns to scale are assumed—that is, investment costs for a facility are assumed to be proportional to its capacity. The objective function of the GenX model includes the sum of annualized investment cost and operating cost for all resources as well as the cost of non-served energy, if any. These outputs can be used to compute a metric called the system average cost of electricity (SCOPE). SCOPE is defined as the total annualized investment and operational cost of the modeled system (i.e., the objective function of the GenX model), divided by the total annual electricity demand served (Heuberger, Staffell, Shah, & Dowell, 2017). SCOPE is distinct from the levelized cost of energy (LCOE) or levelized cost of storage (LCOS), both of which are technology-specific cost metrics that are computed with a static view of the power system and that require specifying a fixed dispatch profile for the resource in question, which often leads to misleading inter-technology cost comparisons. By contrast, the SCOPE metric is computed as an output of the CEM—thus, changes in SCOPE across different scenarios provide a view of the system impact of various technology and policy drivers under assumptions of perfect foresight, constant returns to scale, and optimal investment and operation. Further details on the formulation and implementation of the GenX model can be found elsewhere, including in prior publications that use GenX (MITEI and Princeton University, 2021) and in the open-source model itself (MITEI and Princeton University, 2021).

The modeling results presented here should not be viewed as predictions or forecasts. We view GenX as a platform for performing a set of internally consistent experiments that in turn reflect alternative but realistic assumptions about the attributes of technologies, including their costs and availabilities, as well as the level and flexibility of demand and other factors. This allows us to examine how variations in these assumptions affect the optimal portfolios of technologies, their costs, and implicit bulk system electricity prices. Importantly, the modeling results shed light on which variations seem likely to be important and which do not.

6.2.2 Modeling Energy Storage in GenX

Energy storage technologies are differentiated in the GenX model based on their design as well as their assumed cost and performance characteristics. In terms of design, GenX includes two broad representations of storage technologies. The first category includes technologies that have equal charging and discharging power capacity (e.g., lithium-ion or other electrochemical flow batteries, pumped hydro); for these technologies, energy storage capacity and charging/discharging power capacity are the two independent design variables and feasible ranges for the ratio of energy capacity to power capacity can be specified.⁷ The second category includes technologies where both charging power and discharging power capacity, as well as

⁷ This classification includes the special case where the ratio of energy capacity to power capacity, or storage duration, is held constant, either due to lack of data or other factors, so there is only one independent design variable.

energy storage capacity, are independent design variables (e.g., thermal or hydrogen storage). Depending on this classification, storage technologies are characterized by one, two, or three independent capital and fixed operations and maintenance (FOM) cost parameters (Table 6.2). For technologies where energy storage capacity is an independent design variable, we constrain the storage duration (ratio of energy to discharging power capacity) to be less than 300 hours, but this constraint is never binding for the results reported here. Additionally, due to data limitations, we model pumped hydro storage with fixed storage duration (12 hours) and assume total capital costs scale with power capacity alone (Brown, et al. 2020; U.S. Department of Energy 2018).

Type	Independent design variable	Dependent design variable	Classification of storage technologies modeled here
1	Discharge power capacity	Charge power capacity, energy capacity	Pumped hydro
2	Discharge capacity, Energy capacity	power Charge power capacity	Li-ion, Redox Flow batteries, Metal-air batteries
3	Discharge capacity, Energy capacity, Charge power capacity	power -	Thermal energy storage, H ₂ storage

Table 6.2: Design variables for different types of storage technologies modeled in this study.

The inter-temporal operation of storage technologies is modeled using several parameters, highlighted in Table 6.3, including the hourly self-discharge rate and the variable O&M cost for charging and discharging. We also model energy losses during charging and discharging, by parametrizing charging and discharging efficiency for each technology. As with other CEMs, to manage computational tractability, we do not model degradation of energy capacity with use, or dynamic charging or discharging efficiency as functions of the state of charge of storage. This approach, which is similar to the approach taken in other modeling studies, may overestimate the benefits of electrochemical storage technologies relative to other storage technologies that are less affected by these considerations (Jafari 2020; Sakti 2017). In our analysis, the impact of this modeling simplification is partly mitigated by accounting for the periodic replacement of energy components in the FOM costs (Cole and Frazier 2020) for the electrochemical energy storage technologies considered here. This is akin to paying a fixed annual maintenance fee to guarantee a certain level of performance (further details are discussed in Chapter 2).

	Tech		Discharging Capital Cost (\$/kW)	Charging Capital Cost (\$/kW)	Storage Capital Cost (\$/kWh)	FOM (\$/kW- year)	FOM (\$/kWh- year)	VOM (\$/kWh)	Efficiency Up (%)	Efficiency Down (%)	RTE (%)
[1]	PHS	Mid	1,966	-	0.0	41.0	0.0	0.0	89%	89%	80%
[2]	Li-ion	Low	32	-	70.9	0.3	1.4	0.0	92%	92%	85%
[3]	Li-ion	Mid	110	-	125.8	0.8	2.2	0.0	92%	92%	85%
[4]	Li-ion	High	154	-	177.0	1.4	3.2	0.0	92%	92%	85%
[5]	RFB	Low	297	-	15.5	4.1	0.0	0.0	92%	88%	80%
[6]	RFB	Mid	396	-	48.0	4.1	0.0	0.0	92%	88%	80%
[7]	RFB	High	530	-	102.2	4.1	0.0	0.0	92%	88%	80%
[8]	Metal-air	Low	595	-	0.1	14.9	0.0	0.0	70%	59%	41%
[9]	Metal-air	Mid	643	-	2.4	16.1	0.1	0.0	73%	63%	46%
[10]	Metal-air	High	950	-	3.6	23.7	0.1	0.0	72%	60%	43%
[11]	Hydrogen	Ultra-Low	1,190	479.3	1.1	11.0	0.0	0.0	77%	65%	50%
[12]	Hydrogen	Low	1,150	356.1	6.0	11.0	0.1	0.0	80%	70%	56%
[13]	Hydrogen	Mid	1,190	479.3	7.0	11.0	0.1	0.0	77%	65%	50%
[14]	Hydrogen	High	1,230	602.4	8.0	11.0	0.1	0.0	60%	60%	36%
[15]	Thermal	Low	494	3.3	2.9	3.9	0.0	0.0	100%	55%	55%
[16]	Thermal	Mid	736	3.3	5.4	3.9	0.0	0.0	100%	50%	50%
[17]	Thermal	High	1,226	3.3	9.0	3.9	0.1	0.0	100%	46%	46%

Table 6.3: Storage Costs and Operational Assumptions. Values from the Future of Storage technical teams; refer to previous chapters for detailed description of individual technologies: hydrogen (Chapter 5); thermal (Chapter 4); metal-air, RFB and Li-ion (Chapter 2). PHS = Pumped Hydro Storage, RFB = Redox Flow Battery. Round-trip efficiency (RTE) is the fraction of energy used to charge a device that is available to be discharged; it is the product of Efficiency Up and Efficiency Down similarly expressed. Hourly self-discharge rates for storage technologies are also considered in the modeling but are very small at 0.002% for Li-ion and metal-air systems and 0.02% for thermal systems. Low-, mid-, and high- cost assumptions for hydrogen assume above-ground storage, while ultra-low-cost reflects cost assumptions for geological storage. PHS cost data sourced from the 2016 Hydropower Vision report (U.S. Department of Energy 2016).

Our analysis focuses on modeling the supply–demand balance within the bulk power system enforced at an hourly resolution for each balancing area within the region considered. Storage contributes to the supply–demand balance as both a supply-side resource (via discharging) and as a demand-side resource (via charging). In addition, as previously noted, storage can contribute to the procurement and supply of grid ancillary services such as operating reserves. Since we do not model system operating reserve requirements, however, the benefit of providing these services is not captured in our valuation of energy storage technologies. Previous research using GenX that included operating reserve requirements has shown that the ability to satisfy reserve requirements does contribute significantly to the value of storage when storage is deployed at low levels. However, this incremental benefit is lost with increasing storage penetration (Mallapragada, Sepulveda, & Jenkins, 2020). This suggests that long-run valuations of alternative storage technologies may not be much affected by ignoring their participation in operating reserve markets.

6.2.3 Regional Modeling

Selection of Model Regions

We focus on three U.S. regions in 2050: the Northeast, the Southeast, and Texas. We do not seek to develop detailed trajectories of the evolution of the resource mix in these regions, as this evolution will be affected by a range of factors, including the turnover of the existing generation fleet, market design, state incentives, permitting rules, etc. Instead, we focus on the effects of differences in VRE resource quality and the availability of long-lived, existing low-

carbon hydro and nuclear generation assets, and pumped hydro storage assets, assuming cost-efficient investment and operation. The three selected regions differ across several key attributes that affect the potential costs and benefits of achieving various decarbonization goals, including: (1) wind speeds and solar irradiation, land availability, and resulting installed costs of wind and solar generation; (2) hydroelectric and potential hydrogen (H₂) storage resources; and (3) industry structure and regulation and associated implications for nuclear power development. As noted above, we also assume that the existing stock of fossil-fuel generating capacity retires by 2050, so that our analysis basically examines a "greenfield" system developed to meet 2050 demand, utilizing existing transmission assets and some other existing non-fossil assets, with some regional differences (as detailed below). New fossil generating capacity may be selected depending on its costs, utilization rates in an optimal system, and the stringency of the system-wide carbon constraint.

The **Northeast** region (New England and New York) is characterized by strong legislative and regulatory support for renewable generation, offset by siting difficulties that translate, in some cases, into increased infrastructure costs (Wiser & Bolinger, 2018). Most states in this region have pledged to reduce their economy-wide greenhouse gas (GHG) emissions by at least 80% by 2050, with a few states committing to more ambitious targets.⁸ The region is largely restructured with competitive wholesale markets managed by two independent system operators (ISO-NE and NYISO) that govern system operations and partially govern investment in new generation and transmission capacity. The region has relatively low-quality solar, but high-quality onshore and offshore wind. However, siting difficulties have plagued onshore VRE and transmission developments, which may explain some of the recent, state-mandated procurements of relatively expensive offshore wind and supporting requirements for new transmission infrastructure investments. The region also imports non-trivial amounts of hydropower from Canada and has its own hydro resources that can help to support VRE integration. While the Northeast's electricity demand profile currently peaks in the summer, penetration of electric space heating anticipated to meet decarbonization commitments (and included in the NREL high electrification demand scenario), may transform the Northeast into a winter-peaking region (Mai 2018; N. A. Sepulveda 2021). All the region's nuclear power plants are merchant plants that must cover their going-forward costs with wholesale market revenues to break even. Because many of these plants are financially challenged, and currently depend on state subsidies to continue operating, their licenses are unlikely to be renewed beyond their current license periods. Accordingly, we assume that all existing nuclear units retire by 2050 (in other words, that they do not renew their current operating licenses) and that new nuclear plants are not deployed by 2050 based on available information about the technology's cost and public acceptance challenges. We also assume that the existing stock of fossil generating capacity retires by 2050, but that existing hydro and pumped storage resources continue to be operational in 2050.

The **Southeast** region (Tennessee, Alabama, Georgia, North and South Carolina, and Florida) is characterized by the presence of regulated, vertically integrated utilities; the absence of organized wholesale markets; prevalence of winter-peaking demands for some states within the region; and an extensive nuclear generation fleet, which contributed 28% of the region's power

⁸ For example, the Massachusetts' Global Warming Solutions Act of 2008 requires at least an 80% reduction in carbon emissions by 2050 (below a 1990 baseline level) (Massachusetts Executive Office of Energy and Environmental Affairs, 2021). New York has a mandated goal to achieve zero-emissions electricity by 2040, including 70% renewable energy generation by 2030, and to reach economy-wide carbon neutrality by 2050 (NYSERDA, 2021).

generation in 2018.⁹ While nuclear plant economics have been adversely impacted in other parts of the United States that are currently served by wholesale electricity markets, the economics of nuclear generation remain more favorable in the regulated, vertically integrated utility environment of the U.S. Southeast (U.S. DOE 2017; Szilard 2017). Continued reliance on this regulatory structure in the U.S. Southeast, combined with greater public acceptance of nuclear energy, makes it more likely that nuclear plant operators will apply for, and be granted, second license renewals that extend the remaining life of the region's existing plants beyond 2050. Thus, our analysis includes existing nuclear plants in the region with an initial operating date of 1975 or later, which could operate to or beyond 2055 with a second license renewal (see Appendix Table A-1). We assume that 25 gigawatts (GW) of existing nuclear capacity will still be online through 2055 (assuming an 80-year lifetime for nuclear plants). Nuclear, as a dispatchable low-carbon resource, could partially mitigate the need for VRE resources and storage technologies and has the potential to lower the system costs of achieving deep decarbonization (Buongiorno 2018; Sepulveda 2018). The political environment in the Southeast is also more conducive to building new nuclear plants; indeed, the only two nuclear units currently under construction in the United States (Plant Vogtle) are in Georgia.¹⁰ The Southeast region is also endowed with relatively good-quality solar resources. While offshore wind may be a possibility in this region, we have not modeled its availability due to a lack of reliable data to characterize the resource. Thus, we model the Southeast as a mostly a "greenfield" system in 2050, but for the continued operation of significant existing nuclear capacity and any existing hydroelectric resources.

Texas is characterized by high-quality wind and solar resources, an organized wholesale market serving a restructured electricity sector, summer-peaking demand with a strong component of relatively inflexible air conditioning demand, significant penetration of weather-sensitive electric heating, proximity and access to CO₂ sequestration sites, and strong industrial energy demand. Notably, the petrochemical industry, which uses almost all the hydrogen produced today for feedstock purposes, is concentrated in Texas and the other Gulf Coast states. As economy-wide decarbonization advances, there may be additional demand for hydrogen in energy applications. Supplying this incremental demand using electrolyzers¹¹ coupled with hydrogen storage could add demand flexibility to the grid. Texas also has underground salt caverns, which can serve as a cheaper medium than above-ground tanks for the long-duration storage of hydrogen. This allows us to use Texas to test our hydrogen storage cost sensitivities and hydrogen-as-a fuel sensitivities. We assume that the state's two existing merchant nuclear plants (four units) retire and are not replaced by 2050. The only brownfield resources are Texas's (minimal) existing hydroelectric resources, which are assumed to continue operating in 2050.

As we will see in later sections, the availability of dispatchable low-carbon resources and the relative resource quality of solar and wind have significant implications for modeled system costs and for the optimal amount of storage. Differences across the three modeled regions and obvious differences between these regions and other parts of the United States (i.e., exceptional-quality solar in the Southwest and extensive hydro in the Northwest) mean that there is no credible way to generalize or aggregate our regional results to produce national totals.

⁹ Total electricity generation (866 TWh), and nuclear generation (241 TWh) from the U.S. EIA (2021).

¹⁰ We assume these units will be part of the 2050 existing nuclear fleet for the Southeast.

¹¹ Electrolysis technologies considered here generally split water at or near ambient conditions and are capable of flexible operation over nearly the entire range of power loadings. Further description of electrolyzer technologies can be found in a 2019 IEA report, *The Future of Hydrogen* (IEA 2019).

Regional Commonalities in Modeling

In GenX, each scenario is characterized by zonal hourly VRE capacity factors and demand, investment and operational parameters (e.g., costs, ramp rates, minimum generation levels) for each technology, and different carbon emission constraints (Table 6.4). Across all three regions, we use the latest mid-range EIA fuel-price projections for 2050 and NREL’s Annual Technology Baseline 2020 (ATB) to characterize the capital cost of various generation technologies (Table 6.5) as well as lithium-ion (Li-ion) battery storage.¹²

Key Inputs	Key Outputs
<ul style="list-style-type: none"> Solar PV and wind hourly capacity factor 2050 hourly demand profile from NREL Electrification Futures Study Fixed (capital and O&M) and variable (O&M and fuel) costs for each resource technology Operational parameters for each technology Fuel parameters such as CO₂ emissions rate and cost 	<ul style="list-style-type: none"> Optimal installed electricity generation capacity mix Total system cost Hourly operation of each resource technology System carbon emissions Energy contribution and capacity factor for each technology

Table 6.4: Inputs and Outputs of the GenX Model. See Figure 6.2 and Appendix A for further details.

	Tech	Capital Cost (\$/kW)	FOM (\$/kW-year)	VOM (\$/MWh)	Modeled in Regions
[1]	Onshore Wind	1,085	34.6	0.01	NE, SE, TX
[2]	Offshore Wind	2,179	58.8	0.01	NE
[3]	Utility-Scale Solar	725	8.5	0.00	NE, SE, TX
[4]	Distributed Solar	924	8.0	0.00	NE
[5]	CCGT	936	12.9	2.16	NE, SE, TX
[6]	OCGT	854	11.4	4.50	NE, SE, TX
[7]	CCGT_CCS	2,080	27.0	5.72	NE, SE, TX
[8]	Allam	1,929	48.0	2.07	TX
[9]	Nuclear	6,048	119.0	2.32	SE

Table 6.5: Mid-cost assumptions for VRE and natural gas generating resources. The “Modeled in Regions” column indicates where the technologies are assumed to be available. Projected costs from NREL ATB 2020. For onshore wind, we applied a 1.5x multiplier in the Northeast to reflect difficulties in siting and interconnection. “Allam” refers to the supercritical CO₂-based oxy-combustion power concept, also referred as the “Allam-Fetvedt” cycle (Weiland and White 2019).

Per our (mostly) greenfield modeling assumption, we restrict investment to the following technologies: utility-scale solar and onshore wind (as well as offshore wind and distributed solar in the Northeast); natural gas-fired plants (open cycle gas turbine (OCGT) and combined cycle gas turbine (CCGT)), with and without amine-based carbon capture and storage (CCS)

¹² We assume 2045 technology costs from the 2020 NREL Annual Technology Baseline (ATB) database, reflecting the fact that the stock of resources in 2050 will likely have been built/financed a few years earlier.

technology; and hydro resources where they play a major role (Northeast, Southeast).¹³ We do not consider coal as a viable generating technology in 2050 in the United States, given its declining cost-competitiveness and diminishing role in the U.S. power mix over the past few years, as well as its high carbon emissions. The exceptions to greenfield modeling are for existing hydro and pumped hydro storage in the Northeast and Southeast, existing nuclear in the Southeast that would still be operational in 2050 under an assumed 80-year lifetime (see Table A-1 in Appendix A), and existing transmission capacities in the Northeast and Southeast. As discussed below, we modeled Texas as a single transmission zone. In stand-alone regional case studies, we also assess the impact of new nuclear and emerging natural gas-based power generation technologies with CCS (e.g., Allam-Fetvedt cycle (Weiland and White 2019), and hydrogen for industrial uses).

The model characterizes hourly demand for each region using the 2050 demand profiles developed by NREL for its EFS study (specifically, NREL’s high-electrification-with-moderate-technology-advancement scenario) (Mai, et al., 2018). These demand profiles correspond to 2012 weather year variations.¹⁴ They assume a high degree of electrification in residential and commercial buildings (e.g., 61% of space heating, 52% of water heating, and 94% of cooking services) and transportation (e.g., plug-in electric vehicles account for 84% of light-duty vehicle stock in 2050), which collectively results in electricity providing 41% of final U.S. energy demand in 2050 as compared to 19% in 2016. We take as given that policies necessary to encourage these levels of electrification have been implemented and consider the incremental effects of limits on carbon emissions from the power sector. The projected demand profiles are also available with a breakdown of hourly demand among various end-use segments, which we use to explore the impact of demand flexibility for certain end uses, such as electric vehicle (EV) charging.

To represent PV and wind resources at a high level of spatial and temporal resolution, we follow the approach documented by Brown and Botterud (2021): (1) we develop supply curves of available land area for PV and wind development (excluding water bodies, national parks, urban areas, mountain ranges, and Native American territories) and (2) we quantify the cost of spur lines to connect new VRE generation to existing transmission infrastructure. For each site, the hourly capacity factor (CF) for PV is simulated assuming a horizontal one-axis-tracking PV system and using 2007–2013 satellite data from the National Solar Radiation Database (NSRDB). The hourly CF for wind is simulated using climate reanalysis data from the WIND Toolkit and manufacturer power curve data for the Gamesa G126/2500 turbine at 100-meter height. We develop different “quality bins” for VREs (based on the levelized cost of energy, considering generation and interconnection costs) by aggregating over these individual sites. Further details are provided in the Supplemental Information (Note S2) to Brown and Botterud (2021).

Regional Differences in Modeling

Since the sources of storage value we are trying to capture are highly sensitive to temporal resolution, we opted to model operational decisions on an hourly basis, to better capture the

¹³ Many of our capital cost assumptions were taken from the 2020 edition of the NREL annual technology baseline (ATB) report (National Renewable Energy Laboratory (NREL), 2020). In the 2021 edition of the ATB, mid-cost projections for Li-ion battery power capital costs were higher than the values in the 2020 edition, while energy capital costs were lower. Using projections from the 2021 edition of the ATB would presumably increase the duration of Li-ion storage deployment across the scenarios evaluated in this study.

¹⁴ Presumably, the NREL load projections do not account for the impacts of climate change on electricity demand, which, according to recent literature, could be important to consider in system planning, along with climate change impacts on generation (Ralston Fonseca, et al. 2021; Steinberg, et al. 2020).

power system's inter-temporal ramping and balancing needs with high VRE penetration and to estimate how these needs affect the value of different storage resources. Our emphasis on high temporal resolution leads to necessary trade-offs between the level of chronological and network detail we consider in the analysis to keep the model computationally tractable.

About 90% of electricity supply in Texas is managed by a single ISO, the Electric Reliability Council of Texas (ERCOT). Because ERCOT is almost completely electrically isolated from the rest of the country and because transmission capacity between wind-rich areas (designated as "Competitive Renewable Energy Zones") in the northwestern and western portions of the state and demand centers in eastern and southern Texas have relatively recently been greatly expanded (Hulbert, Chernyakhovskiy, & Cochran, 2016), we decided to model all of Texas as a single zone. With this simplified spatial resolution, we were able to include the maximum temporal resolution of grid operations in the CEM, limited only by data availability: seven years at hourly resolution.

In contrast, the Northeast and Southeast regions of the United States are relatively large and geographically diverse, and they have well-documented intra-regional transmission constraints. This makes it important to consider intra-regional transmission expansion. For these two regions, we elected to use a spatially resolved network representation, which in turn meant that we had to use a lower temporal resolution to keep the model computationally tractable. We model annual grid operations in these two regions based on 35 representative periods of 10 days each (corresponding to 8,400 hours), which are sampled from the available time series data of seven years at an hourly resolution. Such a time-domain reduction approach is often employed in CEM studies to balance spatial/temporal resolution and level of operational detail (Heuberger, Staffell, Shah, & Dowell, 2017; Kotzur, Markewitz, Robinius, & Stolten, 2018; Mallapragada, Papageorgiou, Venkatesh, Lara, & Grossmann, 2018). (Mallapragada, Papageorgiou, Venkatesh, Lara, & Grossmann, 2018)The selection of 35 representative periods (350 days x 24 hours/day) follows an iterative clustering approach, as further described in Appendix B.

We also consider other regional differences with respect to resource quality and regulatory environment. Notably, we apply a 50% cost premium to onshore wind development in the Northeast to reflect well-documented siting challenges—this multiplier is consistent with regional multipliers for the Northeast used in other studies (Brown, et al., 2020). To reflect difficulties in expanding transmission into and out of the New York City area (zone 4 in Figure 6.2), we apply a two-times (2x) expansion limit, based on existing transfer capacities. Finally, we include offshore wind as a viable technology with no limits on maximum deployable capacity in the Northeast, due to favorable water depths and supportive deployment policies at the state level.

As described previously, we use the NREL EFS high-electrification load scenario in our base case (other assumptions in our base case are discussed in the next section), to reflect the levels of electrification needed to achieve deep decarbonization on an economy-wide basis by 2050. The high-electrification load scenario assumes an increased role for electricity in meeting final energy demand compared to the reference scenario (41% vs. 23% in 2050). Regional differences arise due to local weather conditions and electrification potential. For example, in comparison to the NREL EFS reference load scenario case, the high-electrification load scenario has a 65% higher system peak and 52% higher annual demand in the Northeast region, and a 36% higher system peak and 32% higher annual demand in Texas (Table 6). Under the high-electrification scenario, winter electricity consumption increases most substantially in the Northeast, due to a greater role for electrified space heating via cold-climate heat pumps. This partly explains the

larger impact of electrification (high vs. reference scenario) on peak and annual electricity demand for the Northeast as compared to Texas (Figure 6.1).

	System Peak (GW)		Annual Demand (TWh)	
	High-electrification	Reference-electrification	High-electrification	Reference-electrification
Northeast	94	57	454	298
Texas	151	111	715	543
Southeast	298	205	1,457	1,051

Table 6.6: EFS 2050 demand assumptions for the Northeast, Southeast, and Texas. Hourly system peak (GW) and total annual demand (TWh) are shown for both the high and reference electrification scenarios.

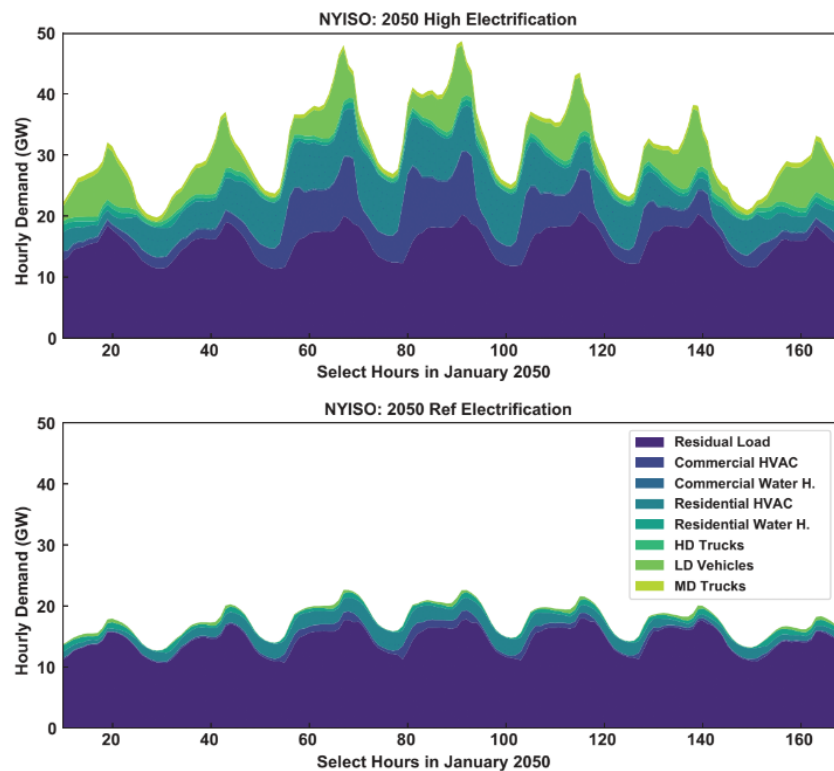


Figure 6.1: Example electricity demand in New York State in select hours in January 2050. High electrification includes higher levels of electrified space heating (commercial and residential HVAC) and transportation (mainly light-duty electric vehicles). H Electrification = high electrification scenario; R Electrification = Reference electrification. HVAC = Heating Ventilation & Air Conditioning. HD = Heavy-duty, LD = Light-duty; MD = Medium-duty. Data source: NREL Electrification Futures Study (Mai, et al., 2018)

6.2.4 Model Limitations

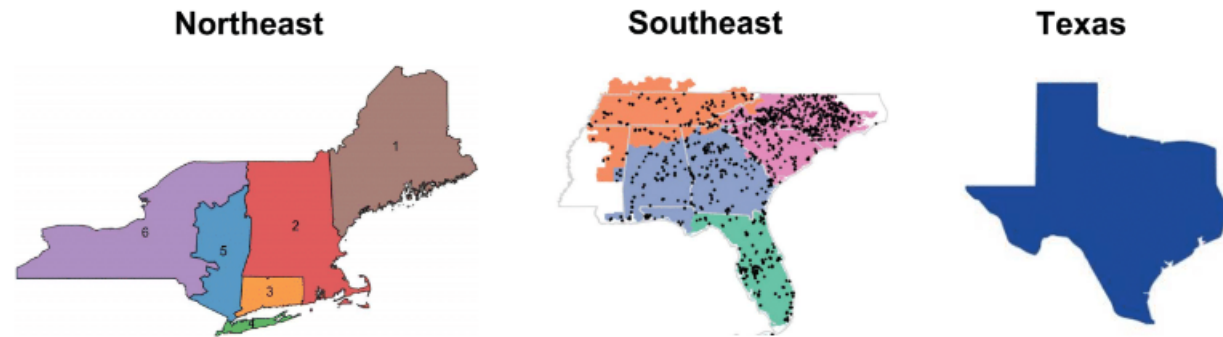
Before describing our results and key findings, we note some limitations in our modeling approach. Our use of historical weather to simulate multi-year VRE capacity factors provides range and variation for VRE availability; however, it does not capture correlations between the effects of extreme weather events on generation and their effects on demand. Thus, we can only partly capture events like the ERCOT outages experienced in Texas in February 2021. As with most other capacity expansion models, our hourly supply–demand balance assumes perfect foresight with respect to VRE availability and demand—in reality, forecasting is not perfect, and technologies that provide flexibility (e.g., storage) will be needed to manage short-term deviations from forecasts. The assumption of perfect foresight thus serves to produce a lower bound on storage capacity requirements. A second limitation is that we model intra-regional transmission in a highly aggregated manner based on a “pipe-and-bubble” formulation

(Mai, et al., 2015).¹⁵ We also do not model sub-hourly VRE variability or planning reserve margins that mimic capacity markets in some jurisdictions. These simplifications have operational and cost implications and point to areas that should be considered in future work. Finally, it is important to keep in mind that this analysis relies on an optimization model that is designed to derive efficient solutions. The model does not account for real-world market imperfections, regulatory imperfections, or public policies that may favor one technology over another—all of which are likely to make it very difficult to achieve least-cost solutions in practice. Nonetheless, our analysis provides a useful benchmark against which real-world results can be compared for policy evaluation.

¹⁵ Pipe-and-bubble or transport models for transmission are often used in investment planning to simplify the modeling. In these formulations, the transmission of electricity is represented in the same manner as the transport of mass, instead of using the more complex laws of physics (Kirchoff's laws) that actually govern electricity flows.

Assumptions & Sources

- **After-tax WACC:** 4.5%
- **Load:** NREL Electrification Futures Study (2012 weather year) – high electrification
- **VRE resource:** NREL WIND Toolkit, National Solar Radiation Database (PV) (2007-2013)
- **Generation costs:** NREL Annual Technology Baseline (ATB) 2020
- **Storage costs:** Technical teams + NREL ATB 2020 for Li-ion + other literature sources
- **Gas price:** EIA Annual Energy Outlook 2020 estimate for 2050 - \$4.16/MMBtu (2019: \$2.88/MMBtu)
- **Transmission capacity:** EPA Integrated Planning Model's existing capacity (Northeast, Southeast)
- **Existing generation:** Hydro & pumped hydro (Northeast, Southeast), distributed PV (Northeast), nuclear (Southeast)
- **Hydropower:** Oak Ridge National Laboratory database + EIA 923 + Canada energy board



	Northeast	Southeast	Texas
Variable renewables	Wind: Onshore (50% cost premium) + offshore PV: Utility + distributed	Wind: Onshore PV: Utility	Wind: Onshore PV: Utility
Hydro	Yes (domestic + imports)	Yes (domestic)	No
Spatial resolution	6 zones with existing intra-zonal transmission capacity	4 zones with existing intra-zonal transmission capacity	Single zone
Temporal resolution	35 representative periods of 10 days from 2007-2013 weather years, including "extreme" periods (8,400 hours)	35 representative periods of 10 days from 2007-2013 weather years, including "extreme" periods (8,400 hours)	2007-2013 weather years (61,314 hours)

Figure 6.2: Summary of regional modeling features and differences across the Northeast, Southeast, and Texas. Further details available in Appendix A.

6.3 Findings from the Modeling Analysis

6.3.1 Near-Complete Decarbonization with VRE, Natural Gas, and Li-ion Battery Storage

In our “base case” scenario only today’s commercially available technologies, namely lithium-ion (Li-ion) battery storage, wind and solar generating capacity, and natural gas, with and without CCS, can be deployed in 2050, all subject to 2050 mid-cost assumptions. Wind, solar, and storage technologies, which have experienced significant cost reductions in recent years and are expected to become even less expensive in the future, play a greatly expanded role in this scenario even absent power system decarbonization goals—as reflected in our results for an emissions policy with no carbon limit.¹⁶ For the base case and “No Limit” emissions policy, for example, wind and solar account for 73% of generation in Texas in 2050, compared to only 16.5% of generation in ERCOT in 2018.

Since we do not model negative emissions technologies, and since the incremental cost of driving emissions to zero in our models exceeds the likely per-ton cost of these technologies, we emphasize the findings for our 5 gCO₂/kWh case as being most representative of an extreme decarbonization scenario. Figure 6.3 and Figure 6.4 summarize the key modeled system outcomes for scenarios with tightening CO₂ limits across the three regions. System impacts can be observed in the trade-offs between technology-level installed capacities and system costs, and between storage capacities and VRE curtailment.

Base Case Summary System Impacts

As CO₂ limits tighten across the three regions, natural gas generating capacity is incrementally replaced by larger buildouts of VRE and Li-ion battery storage, as well as by the deployment of gas capacity with CCS. Notably, the capacity factor of CCGTs (without CCS) declines from 36% in Texas, 54% in Southeast, and 66% in Northeast under the No Limit case to 2%–5% across the three regions in the 5 gCO₂/kWh case (see Table D-1 in Appendix D). Relative to the already very substantial VRE capacity increases modeled in the No Limit policy scenario, VRE capacity increases by 48% (Texas), 139% (Southeast), and 257% (Northeast) in the 5 gCO₂/kWh case, and by 185% (Texas), 281% (Southeast), and 500% (Northeast) in the 0 gCO₂/kWh case.

¹⁶ As noted above, this case does assume that government policies outside the power sector have been implemented to support the substantial electrification assumed in the NREL demand scenario we employ.

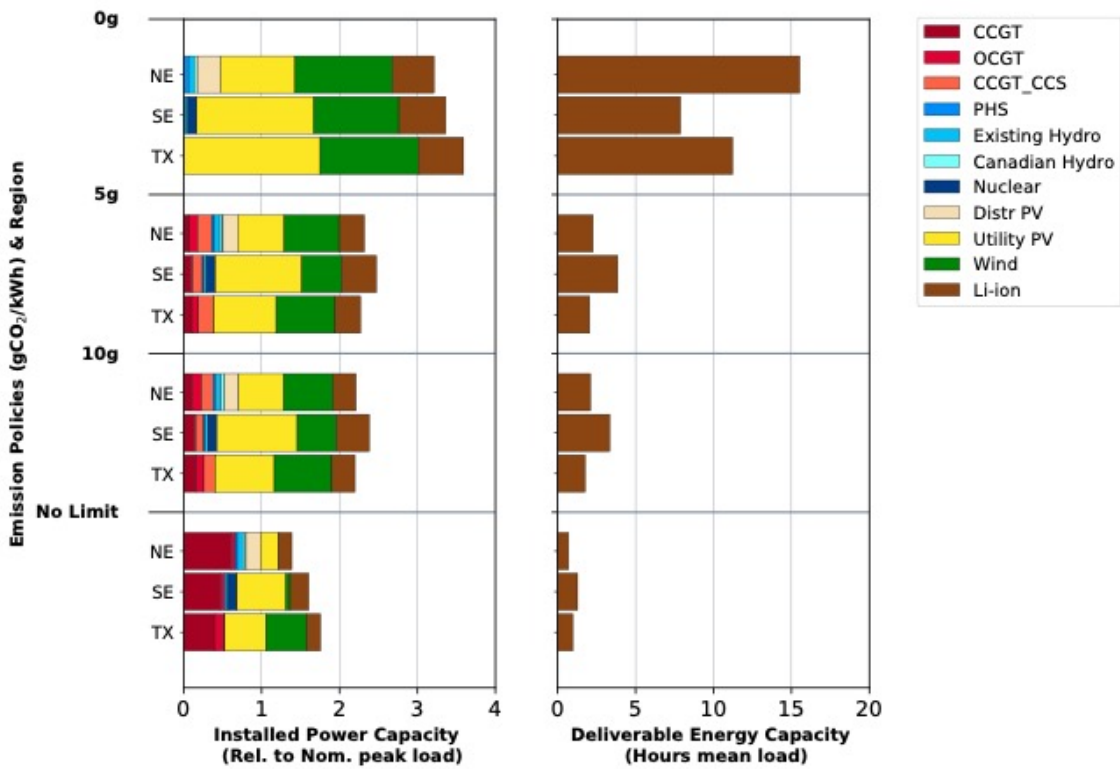


Figure 6.3: Installed capacities in the Northeast (NE), Southeast (SE), and Texas (TX) under tightening CO₂ emissions constraints. Left side: installed power capacities (relative to the region's 2050 peak electricity demand); right side: deliverable storage energy capacity to the grid (i.e., product of energy capacity and discharge efficiency, relative to the region's annual electricity demand). Capacity factors of CCGTs can be found in Appendix D (Table D-1). For the Northeast, "Wind" represents the sum of onshore and offshore capacity.

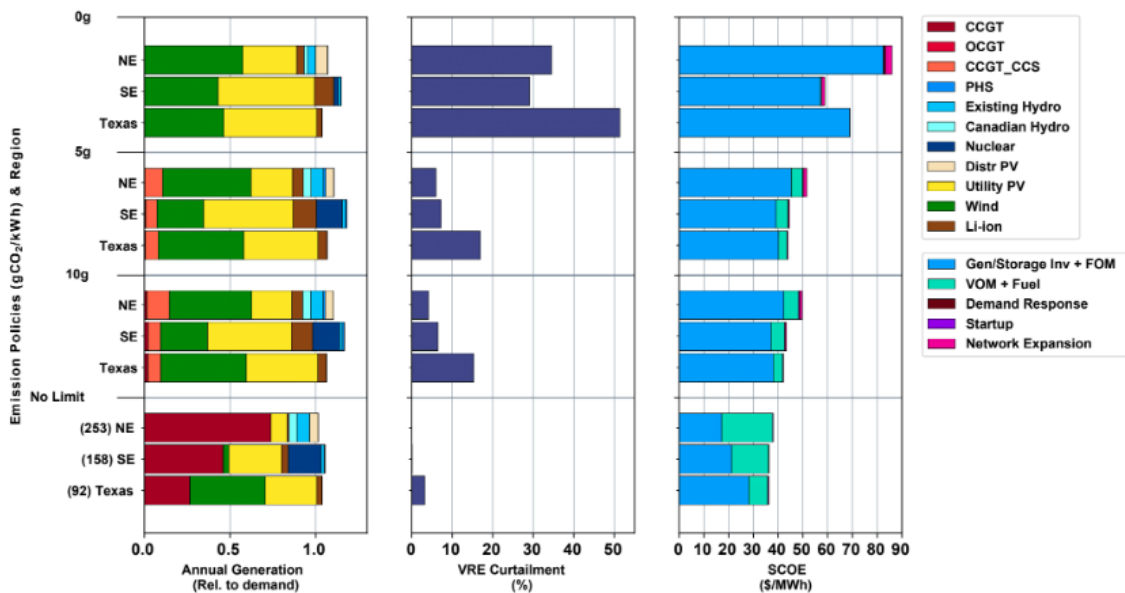


Figure 6.4: Annual generation, VRE curtailment, and system average cost of electricity (SCOE) in the Northeast (NE), Southeast (SE), and Texas (TX) under tightening CO₂ emissions constraints. SCOE includes total annualized investment, fixed O&M, and operational costs of generation, storage, and transmission, as well as any non-served energy penalty. Emissions intensity under the No Limit policy case is noted in parentheses in the bottom panel. For the Northeast region, "Wind" represents the sum of onshore and offshore wind generation.

Across the three regions, the variability of VRE generation is managed in the base case via three mechanisms: (1) flexible operation of natural gas generation to handle long periods of low VRE output, (2) deployment and utilization of energy storage for shorter periods of low VRE output, (3) optimization of the relative capacities of wind and solar generation, and (4) VRE deployment in excess of peak load. Use of the latter approach, often referred to as “overbuilding”, makes it cost-optimal to limit energy storage capacity to 2–4 hours of mean system load¹⁷ in the 5 gCO₂/kWh case. In the regions where the model allows for intra-region transmission expansion, we also see 46 GW (Southeast) and 55 GW (Northeast) of added transmission capacity in the 5 gCO₂/kWh scenario to enable maximum utilization of high-quality VRE resource sites to serve high-demand areas. In the Southeast region, for example, transmission capacity expands to connect VRE sites in Florida to load in Georgia.

The optimal VRE curtailment level depends on the study region’s resource mix and VRE quality (Figure 6.4); in the 5 gCO₂/kWh scenario, we observe 6%–7% VRE curtailment in the Southeast and Northeast regions, respectively, and 17% curtailment in Texas (where VRE generally accounts for a larger portion of generation because of higher-quality wind and solar resources). Curtailment involves “turning down” VRE generation using administrative or market mechanisms. The relatively high capacity cost of Li-ion energy storage under the mid-cost assumptions explains why the cost-optimal deployment of this technology has a storage duration (i.e., ratio of deliverable energy capacity to discharge power capacity) of less than five hours for the 5 gCO₂/kWh scenario.

Tightening the emissions constraint down to 5 gCO₂/kWh is accompanied by higher costs relative to having no CO₂ emissions limit (the “No Limit” policy case). In the base case, the percentage increase in SCOE to achieve an average grid carbon intensity of 5 gCO₂/kWh (relative to the SCOE for the No Limit case) depends on resource availability and load variations and differs across the three regions, from 21% in Texas to 23% in the Southeast and 36% in the Northeast. This translates into an average CO₂ abatement cost¹⁸ relative to the “No Limit” policy case of \$54–\$88 per metric ton of CO₂ and marginal abatement costs of \$333–\$644 per metric ton of CO₂ (Table 6.7). These high marginal costs point to the value of reducing the cost of negative emissions technologies and/or long-term storage. They are also, effectively, measures of the carbon prices that would be required, absent other policies, to provide sufficient incentives for achieving these levels of decarbonization. Across all regions, an increase in investment costs for capital-intensive resources like VRE and storage is partly offset by a reduction in operating costs as the role of thermal generation resources declines.

Marginal Cost (\$/metric ton CO ₂)			Average Cost (\$/metric ton CO ₂)		
50g	10g	5g	50g	10g	5g

¹⁷ Hours of mean system load is computed by taking the ratio of total storage deliverable energy capacity (i.e., the product of storage energy capacity multiplied by discharge efficiency) and mean annual system power demand. It is a measure of how long storage can serve mean system power demand when fully charged. In absolute terms, the deliverable storage capacity of installed Li-ion batteries corresponds to 167–639 GWh in the 5 gCO₂/kWh case.

¹⁸ Average CO₂ abatement cost to achieve an emissions target is computed by dividing the increase in SCOE (relative to the “No Limits” policy case) by the reduction in annual CO₂ emissions (relative to the “No Limits” policy case). Marginal CO₂ abatement costs are obtained as the shadow price of the carbon emissions constraint imposed in the capacity expansion model (which is a linear program).

Northeast	88	237	644	35	48	55
Southeast	67	181	333	23	48	54
Texas	48	246	516	19	73	88

Table 6.7: Marginal and average costs of carbon abatement for various emission policy constraints.¹⁹

Additionally, the model results show no major effect on non-served energy events (i.e., involuntary curtailments of demand) from decarbonizing the grid with VRE and Li-ion battery storage, at least when considering the demand and supply balance from an hourly perspective. With an assumed value of unserved load of \$50,000/MWh, non-served energy events for the modeled grid decarbonization scenarios were generally quite small (e.g., 0.0003% of annual demand for Texas, as shown in Table 6.8). As described earlier, these findings are based on modeling seven years of hourly VRE resource variability with perfect foresight of load (non-coincident with renewable resource variability) and generation, but they do not account for the impact of extreme weather events (e.g., extreme heat waves and cold snaps) on correlated load and generation outages. Appendix B describes the approach used in our modeling to ensure reliability (measured in terms of non-served energy events) in the Northeast and Southeast regions when using representative periods in the CEM.

In the 0 gCO₂/kWh scenario, deployment of Li-ion storage increases significantly, to 8–16 hours of mean system load across the three regions.²⁰ SCOE also increases (relative to the No Limit case), by 62% in the Southeast, 91% in Texas, and 127% in the Northeast. This cost increase corresponds to average CO₂ abatement costs of \$143–\$358 per metric ton CO₂ and substantially higher marginal abatement costs compared to the 5 gCO₂/kWh emissions constraint. In the Northeast and Southeast, where pumped hydro storage (PHS) can be expanded, we also observe increases in installed PHS capacity (with a fixed duration of 12 hours) of 107% and 16% respectively, in the 0 gCO₂/kWh case. However, as noted above, this scenario represents a strict definition of zero-carbon power systems that excludes both any use of natural gas generation, even with existing CCS technologies (<100% capture rate), and any use of negative emissions technologies. Hence, we emphasize our findings for the 5 gCO₂/kWh scenario as more representative of a realistic strategy for the deep decarbonization of power systems. The results for our 0 gCO₂/kWh scenario highlight the value of natural gas or some other dispatchable generation capacity, used very sparingly, in moderating the cost of near-zero carbon electricity systems with Li-ion batteries as the sole form of energy storage to be expanded. These results also illustrate the potential value of low-cost negative emissions technologies. Overall, the analysis for our base case indicates that the near-complete decarbonization of electricity systems will be feasible, from the perspective of balancing hourly energy supply and demand, with bulk power cost increases from 21% to 36% compared to the No Limit case, based on projected technology cost declines by 2050.

CO ₂ Constraint (gCO ₂ /kWh)	Number of NSE events	Max duration of a single event (hours)	Total NSE (GWh)	Max hourly demand loss (%)	Total NSE as fraction of nominal load
0	0	0	0	0	0
5	0	0	0	0	0

¹⁹ We ran experiments at 1 gCO₂/kWh in the Texas region and found that the marginal costs of carbon abatement at that level are eight times the marginal cost of abatement at the 5 gCO₂/kWh emissions limit.

²⁰ Based on modeled demand across the three regions, this corresponds to 797–1,307 GWh of deliverable Li-ion storage capacity.

10	0	0	0	0	0
50	1	2	4.2	3.9	<10 ⁻⁶
NL	1	2	14.0	6.4	<10 ⁻⁵

Table 6.8: Base case reliability results in Texas. Non-served energy events are identified in the dispatch decisions optimized over the full 2007–2013 period. Appendix B describes the reliability simulation approach used for the Northeast and Southeast regions, and associated reliability results.

Finding: Near-complete decarbonization of electricity systems appears feasible, from an hourly energy supply and demand balance perspective, using renewables, natural gas, and Li-ion battery storage alone, without creating significant reliability issues or very large increases in system average cost.

Base Case Regional Differences

It is interesting to note that in the absence of any CO₂ emissions policy, the three U.S. regions studied here achieve very different CO₂ emission intensities, based on our 2050 technology cost assumptions and demand projections, which are based on NREL’s high-electrification scenario (Mai, et al., 2018) for end-uses. The difference between actual emissions intensity in 2018 and modeled emissions intensity in 2050 in the No Limit case can be explained by three factors: (1) we are not modeling existing thermal generation assets that are assumed to retire by 2050; (2) even with no carbon constraint, deployment of new VRE and natural gas generation is economically favorable and is expected to largely replace existing assets; and (3) electricity demand in 2050 is projected to be much higher than demand in 2018 and is also expected to have a different temporal profile owing to the electrification of additional end-uses. The precise share of VRE generation in the No Limit policy case is driven both by the quality of wind and solar resources in each region and by changes in demand profiles and overall demand as a result of expanded electrification of end-uses in sectors such as transportation and heating.

The level of electrification affects VRE penetration and subsequent needs for energy storage. Relative to NREL’s reference-electrification scenario, the high-electrification scenario results in increased power and storage capacity requirements, but it has only minor impacts on VRE curtailment and average system cost (Figure 6.5). For instance, we observe only a 5% increase in SCOE for the 5 gCO₂/kWh policy case. The impact of electrification on emissions intensity is most notable when there are no emission constraints. In our No Limit case, average system-wide emissions in the Northeast under the high-electrification demand scenario are 253 gCO₂/kWh—11% higher than in the reference-electrification case (228 gCO₂/kWh). The change in demand profile due to increasing electrification of space heating and transportation reduces the value of VRE resources and increases the optimal level of dispatchable natural gas generation, which leads to higher system-average emissions intensity.

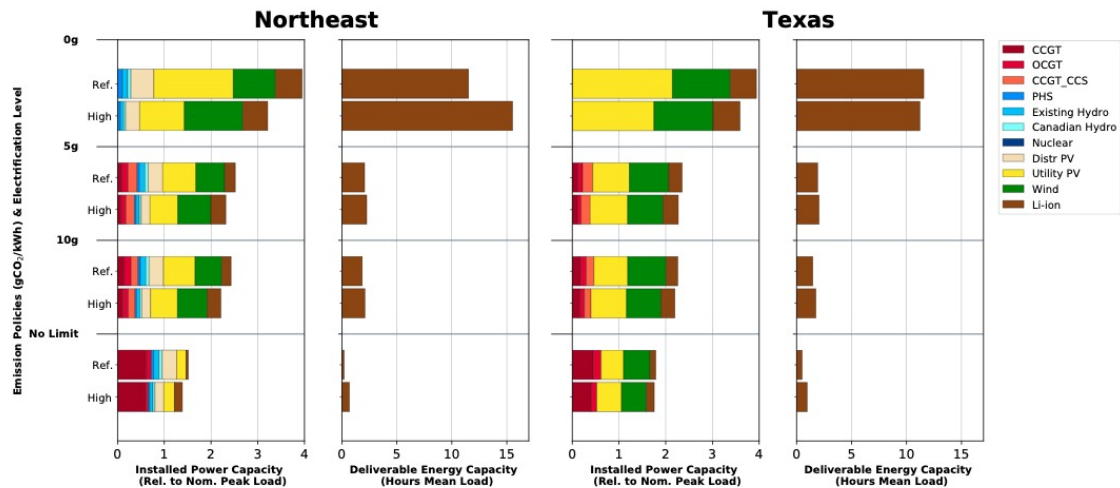


Figure 6.5: System impacts of varying levels of electrification in the Northeast and Texas. Scenarios show the impacts of assuming the NREL EFS reference- vs. high-electrification load scenarios on installed power capacity, storage capacity, and VRE curtailment, across a range of CO₂ emission policies. Under the high-electrification load assumptions, both system peak and annual demand are higher (see Table 6 for details).

With high-electrification load assumptions, we observe the following regional emission intensities in our No Limit policy case: 92 gCO₂/kWh in Texas, 158 gCO₂/kWh in the Southeast, and 253 gCO₂/kWh in the Northeast. Based on these results, the amount of decarbonization predicted to occur by mid-century, even without any carbon constraints, is particularly striking in Texas, where modeled emissions intensity in 2050 is 81% lower than (actual) 2018 emissions intensity (Table 6.9). This is because, in Texas, low-cost VRE technologies combined with good-quality VRE resources drive the displacement of higher-capital-cost thermal generators based on economics alone. In the Northeast, by contrast, modeled 2050 emissions intensity in the No Limit case is 2% higher than actual emissions intensity in 2018. This could partly be due to a substantial increase in annual demand, including a shift from summer peaking to winter peaking; the relatively small role for coal-based power generation in the region’s power mix as of 2018;²¹ the presumed retirement of existing nuclear generation by 2050; and the lower quality and higher cost of VRE resources in the Northeast (based on historic patterns, we assume the region’s VRE capital costs are 50% greater than in Texas and the Southeast).

Achieving an emissions intensity goal of 5 gCO₂/kWh requires a 98% reduction in power sector CO₂ emissions from 2018 levels and 90% carbon-free electricity in the Northeast by 2050; a 99% reduction in carbon emissions from 2018 levels and 93% carbon-free electricity in the Southeast by 2050; and a 99% reduction in carbon emissions from 2018 levels and 92% carbon-free electricity in Texas by 2050. Table 6.9 shows how these model results translate into other commonly used metrics of decarbonization (such as percentage emission reductions relative to historic emissions and low-carbon generation as a share of total generation).

²¹ For instance, coal contributed 1% of total annual electricity supply in ISO-New England in 2018 (ISO New England 2020).

	gCO ₂ /kWh	NL	50	10	5	0
Relative to 2018 Levels						
Northeast	249	-2%	80%	96%	98%	100%
Southeast	387	59%	87%	97%	99%	100%
Texas	418	78%	88%	98%	99%	100%
Relative to No-Limit Levels						
Northeast	253	0%	80%	96%	98%	100%
Southeast	158	0%	68%	94%	97%	100%
Texas	92	0%	46%	89%	95%	100%
Carbon-Free Generation						
Northeast	-	26%	85%	86%	90%	100%
Southeast	-	54%	85%	91%	93%	100%
Texas	-	74%	85%	91%	92%	100%

Table 6.9: Modeled emissions results for different decarbonization targets summarized using alternative metrics commonly used in policy discourse: (1) reductions relative to 2018 (current) emissions levels; (2) emission reductions relative to the No Limit policy case; and (3) carbon-free generation relative to modeled annual generation. For presentation purposes, carbon-free generation is defined in the table to include VRE, nuclear, and hydro resources, but does not include CCGT + CCS.²²

The Southeast differs from other regions because of the possibility that significant nuclear capacity (25 GW) will be available for some years beyond 2050, assuming an 80-year lifetime for existing plants.²³ Figure 6.6 compares modeling results for scenarios where (1) most existing nuclear capacity is retained (as a zero-carbon dispatchable resource) and (2) all existing nuclear capacity is retired. We see that in the former case, the availability of existing nuclear reduces system-wide cost in the Southeast by 6% in the No Limit scenario, 11% in the 5 gCO₂/kWh scenario, and 15% in the 0 gCO₂/kWh scenario, compared to a scenario where existing nuclear is retired. Benefits are derived from the displacement of new capital investments in VRE resources (mainly solar) that are not dispatchable. These results are consistent with prior research findings on the benefit of dispatchable low-carbon generation in terms of reducing the cost of power sector decarbonization (Buongiorno, Corradini, Parsons, & Petti, 2018; Sepulveda, Jenkins, de Sisternes, & Lester, 2018).

²² If CCGT + CCS were to be included in the definition, the resulting emissions intensity will be lower at emission constraints more stringent than 10 gCO₂/kWh. At that level, the percentage of “carbon-free” generation is 98% across the three regions for 10 gCO₂/kWh (compared to 86%-91% without CCS).

²³ Specifically, these are nuclear plants whose current licenses expire in 2055, assuming a second license extension (to 80 years of operating life).

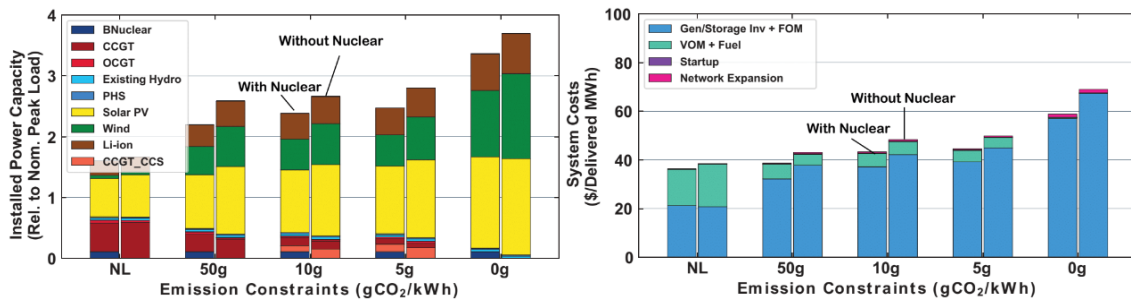


Figure 6.6: System impacts of nuclear availability in the Southeast. The two scenarios compare optimal generation capacity deployed and SCOE under two assumptions: (1) existing nuclear plants remain part of the portfolio and can be dispatched to meet demand; and (2) all existing nuclear plants retire by 2050, and no new nuclear is added.

Finding: In the absence of any CO₂ constraint on the power sector, the three U.S. regions studied here (Texas, the Northeast, and the Southeast) achieve very different CO₂ emission intensities for the same set of 2050 technology cost assumptions. These differences primarily result from regional variations in renewable resource quality and load profiles.

6.3.2 Impacts of Adding Long-Duration Energy Storage (LDES)

As the penetration of VRE resources increases, needs for grid balancing on longer time scales (i.e., days and weeks) will grow. This could potentially create value for long-duration energy storage (LDES) technologies. Compared to Li-ion battery storage, the LDES technologies available in 2050 are projected to have lower energy capacity cost, higher power capacity cost, and lower overall round-trip efficiency (RTE) (Figure 6.7).

Our analysis considers four distinct LDES technologies, as defined in the earlier, technology-focused chapters of this report: redox flow batteries (RFBs, Chapter 2), metal-air batteries (Chapter 2), hydrogen storage (Chapter 5), and thermal storage (Chapter 4). These technologies, which span a range of electrochemical, chemical, and thermal storage systems, are at varying levels of maturity; thus, our experimental design is aimed at understanding the relative merits of different classes of storage technology rather than identifying the most favorable technology within each class. Figure 6.7 highlights the classification of storage technologies based on two out of three key design attributes: Class 1 technologies have the lowest power capacity cost, relatively high energy capacity cost, and high RTE (e.g., Li-ion batteries); Class 2 technologies have mid-range power and energy capacity costs and RTE (e.g., current and future RFBs); and Class 3 technologies have high power capacity costs, low energy capacity costs, and low RTE (e.g., emerging LDES options including metal-air batteries, hydrogen, and thermal storage).

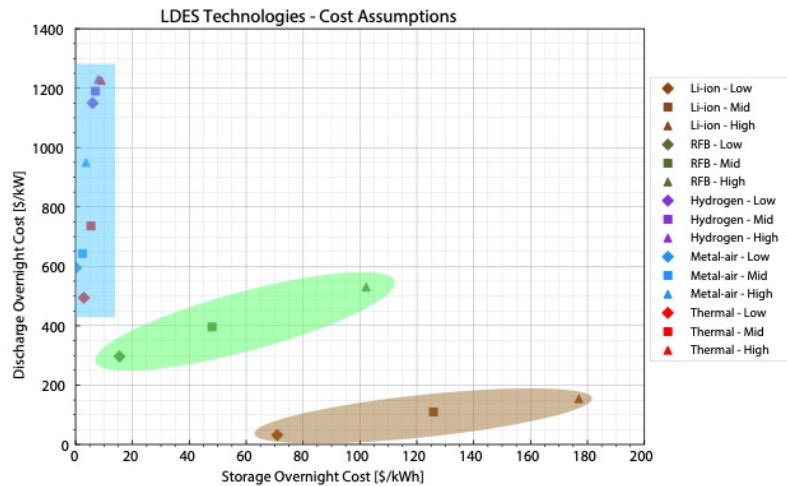


Figure 6.7: Classes of energy storage technologies, grouped by discharge power and storage overnight capital costs. We define the classes as: (1) technologies with the lowest power cost, relatively high energy capacity cost, high RTE; (2) technologies with mid-range power and energy capacity costs and RTE; and (3) technologies with high power costs, low energy capacity costs, and low RTE. Other salient design attributes can be seen in Table 6.3. Pumped hydro storage is modeled with a fixed duration of 12 hours for this study; since we do not have a breakdown of pumped hydro costs, we do not include this storage option on the chart.

In addition to the attributes displayed in Figure 6.7, other cost and performance attributes (shown in Table 6.3) are also important when comparing storage technologies within and across each class. For example, recent studies have shown that in addition to energy capacity cost, discharge efficiency is another important technology design attribute that affects the value (i.e., cost reduction potential) of LDES in zero-carbon power systems (Sepulveda, Jenkins, Edington, Mallapragada, & Lester, 2021).

Impact of Adding Flow Batteries (Class 1, 2)

We first explore the system impacts of adding RFB storage, using estimated cost and performance parameters discussed in Chapter 2. As we note there, RFBs offer potentially lower energy capital costs compared to Li-ion batteries; they also have the potential added advantage of being able to recover energy capacity loss at a lower cost (either via rebalancing or via the replacement of chemicals that make up RFB systems). From a system perspective, this results in lower capital and FOM costs for RFB energy capacity compared to Li-ion technology, along with comparable RTE. The downside of RFBs compared to Li-ion batteries is their relatively high fixed cost for power capacity. This implies that RFBs could be favored over Li-ion batteries for applications involving more long-duration storage.

Figure 6.8 compares capacity outcomes for the Northeast and Texas under plausible scenarios for future Li-ion and RFB costs.²⁴ When CO₂ constraints are binding, RFBs under mid-cost assumptions (third row from the bottom in each panel in Figure 6.8) largely (but not completely) displace Li-ion storage and increase deliverable energy storage capacity compared to the base case (shown in the bottom row in each panel in Figure 6.8). This shift from Li-ion to RFB storage has minor impacts on installed VRE capacity and VRE curtailment. Although it is difficult to see in the figure, RFBs displace substantial dispatchable fossil-fuel capacity. For the 5 gCO₂/kWh case, the availability of mid-cost RFB technology (defined in Table 6.3) results in a 9% decline in natural gas generation capacity in the Southeast, and a 16% decline in both the Northeast and Texas, compared to the base case. This effect increases with more stringent CO₂ constraints.

²⁴ Results for the Southeast are discussed in Appendix D.

Exploring the sensitivity of these findings to plausible low-, medium-, and high-cost assumptions for Li-ion and RFB storage (defined in Table 6.3), several points emerge: (1) Across all the scenarios we analyzed with RFB technology, RFB storage duration was between 7 and 27 hours compared to Li-ion storage duration of 1–5 hours. (2) When available, both technologies are deployed in all scenarios, indicating that neither technology is dominant from a power system perspective. (3) RFB availability enables more buildouts of VRE to substitute for gas capacity, reflecting the value of LDES with low energy capital costs. For example, mid-cost and low-cost RFB (and mid-cost Li-ion) reduces natural gas capacity in Texas by 9–27 GW and increases VRE capacity by 10–23 GW relative to the base case (compared to a system peak load of 151 GW). (4) The addition of RFB storage reduces system costs compared to the base case, with the largest cost reductions observed in the 5 gCO₂/kWh case that includes low-cost assumptions for both battery technologies (12% in the Northeast, 14% in Texas, and 16% in the Southeast).

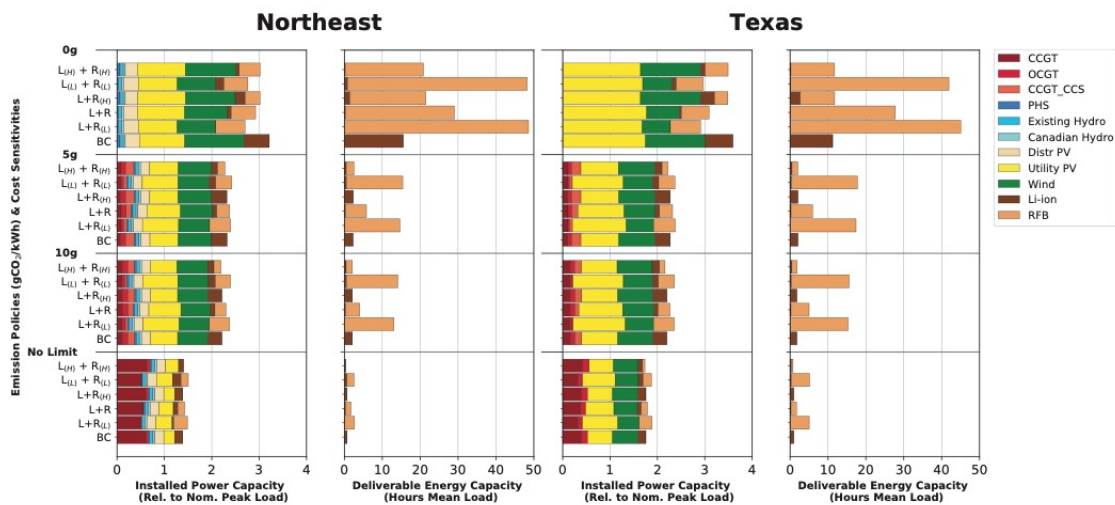


Figure 6.8: System impacts of adding RFB storage for the Northeast and Texas. Scenarios show the impacts of cost sensitivities around Li-ion and RFB technology in terms of installed power capacity and storage capacity, across a range of CO₂ emission policies. They are, in ascending order: (1) base case (i.e., mid-cost Li-ion only, BC); (2) mid-cost Li-ion + low-cost RFB (L+R_L); (3) mid-cost Li-ion + mid-cost RFB (L+R); (4) mid-cost Li-ion + high-cost RFB (L+R_H); (5) low-cost Li-ion + low-cost RFB (L_L+R_L); and (6) high-cost Li-ion + high-cost RFB (L_H+R_H). Low-, mid-, and high-cost assumptions for each storage technology are defined in Table 6.3.

Impact of Adding Emerging LDES Technologies (Class 1, 2, 3)

Class 3 LDES²⁵ technologies (represented by the blue box in Figure 6.7) have still lower energy capital costs than RFBs, but their power capacity costs are generally higher. Though they generally also have much lower round-trip efficiency than either Li-ion or RFB technology, they are potentially appealing for much longer-duration energy storage and near-complete displacement of dispatchable generation capacity. Given the relative immaturity of this class of LDES technologies, we evaluate their potential system impacts one technology at a time, with the assumption that any or all these technologies could be commercially scalable by 2050. Across the mid-range LDES cost and performance scenarios we evaluated, we find that LDES substitutes for natural gas and VRE capacity, leads to reduced curtailment of wind and solar generation, and modestly reduces SCOE compared to scenarios without LDES. Figure 6.9 and Figure 6.10 summarize key model outputs for different levels of LDES availability across the three regions.

²⁵ For this section, we use “LDES” to refer specifically to storage technologies with the potential for still lower energy capital costs compared to RFBs.

LDES technologies with lower energy capacity costs and lower discharge efficiency compared to Li-ion batteries have the greatest impacts on electricity system decarbonization when natural gas generation without CCS is not an option (as in the highly restrictive 0 gCO₂/kWh scenario). This is because LDES directly competes with natural gas generation in providing supply during long periods of low VRE output. How important this is depends on the region's relative VRE resource quality. In the 5 gCO₂/kWh case, optimal deployment of LDES (Class 3) resources reduces the need for thermal generating capacity (i.e., gas with and without CCS, and nuclear) by 9%–45% (Figure 6.9) relative to the base case. Thermal capacity is replaced by VRE capacity, which increases by 6%–9% in the Northeast, 5%–14% in the Southeast, and 4%–9% in Texas, relative to the base case. In effect, the availability of LDES makes VRE capacity more nearly dispatchable and thus increases its value to the power system. Under mid-cost assumptions, the incremental availability of low energy capital cost LDES technologies contributes to SCOE reductions of between 3% and 9% across the three regions for the 5 gCO₂/kWh scenarios shown in Figure 6.9.

Our analysis also reveals that there is a clear trade-off between installed storage capacity and VRE curtailment in the modeled regions. When it is optimal to employ LDES in the 5 gCO₂/kWh case, it is generally optimal to have storage durations much greater than those associated with Li-ion or RFB storage (Figure 6.10). Across the scenarios analyzed, the storage duration for LDES resources ranges between 39 and 59 hours, as compared to Li-ion storage duration of 1–2 hours and RFB storage duration of 6–11 hours.²⁶ These storage durations translate to total deliverable storage energy capacity (across the various technologies) of 6–18 hours of mean system load (across the LDES options and regions modeled). Optimal VRE curtailment in the Northeast and Southeast is reduced from 5%–6% without LDES deployment to 2%–6% with LDES deployment. Optimal VRE curtailment in Texas is reduced from 19% without LDES to 13%–17% with LDES. Relatively higher VRE curtailment in Texas, even with LDES, reflects the region's higher VRE resource quality, which reduces the cost penalty of "overbuilding" VRE capacity and, consequently, the marginal value of incremental storage additions.

²⁶ In absolute terms, results for the deliverable storage capacity of Li-ion batteries, RFB, and LDES in Figure 6.10, correspond to 15–41 GWh, 93–983 GWh and 38–1,422 GWh, respectively.

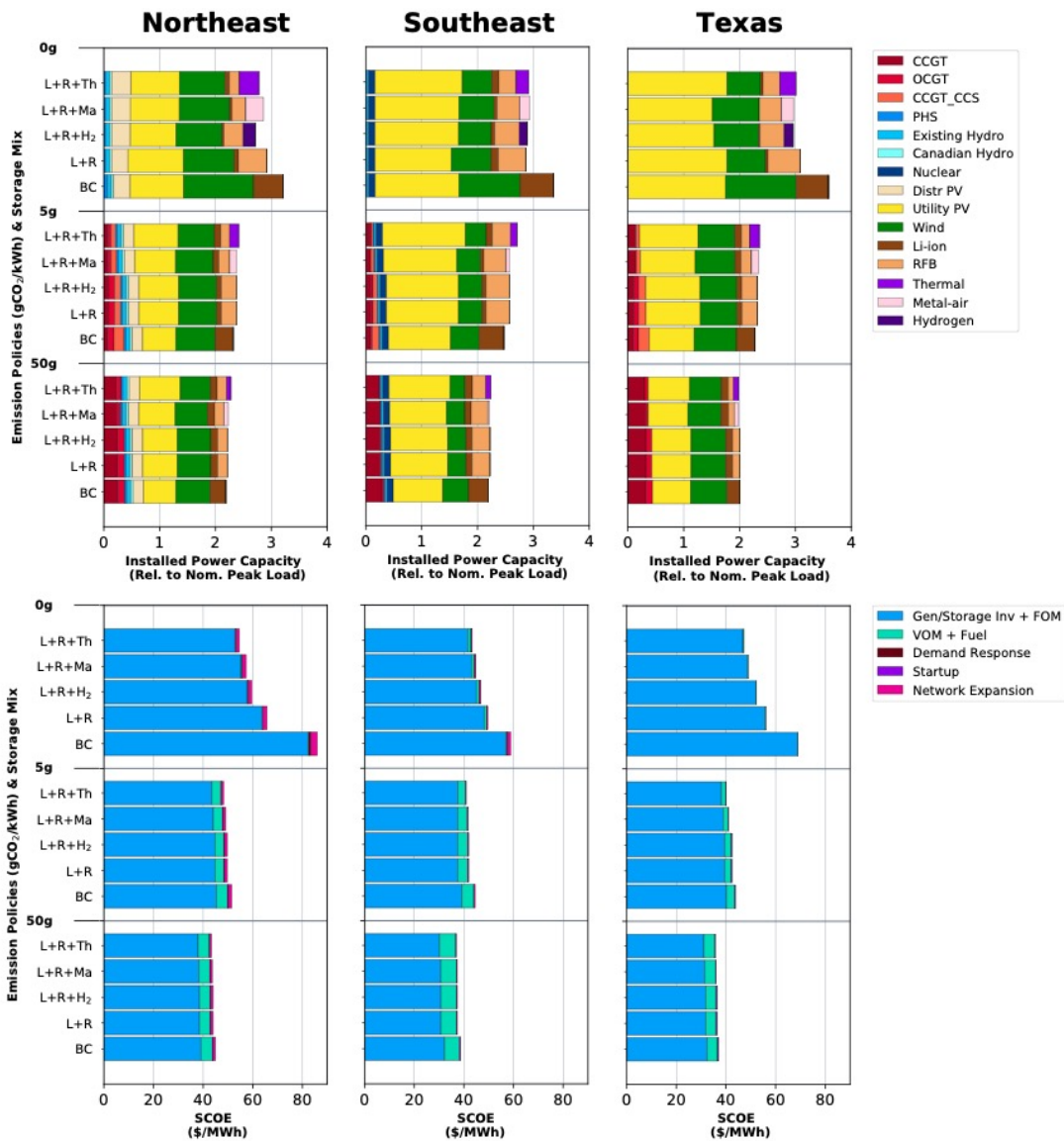


Figure 6.9: Impacts of adding RFB+ LDES on installed power capacity and SCOE, across a range of CO₂ constraints for the Northeast, Southeast and Texas regions. They are, in ascending order: (1) base case (i.e., Li-ion only, BC); (2) Li-ion + RFB (L+R); (3-5) Li-ion + RFB + incrementally adding an LDES option in the form of hydrogen (+H₂), metal-air batteries (+MA), or thermal storage (+Th)—all at mid-cost assumptions. As discussed previously, we evaluate the Class 3 LDES technologies one at a time, with the assumption that any or all these technologies could be commercially scalable by 2050. Mid-cost assumptions for each storage technology are defined in Table 6.3.

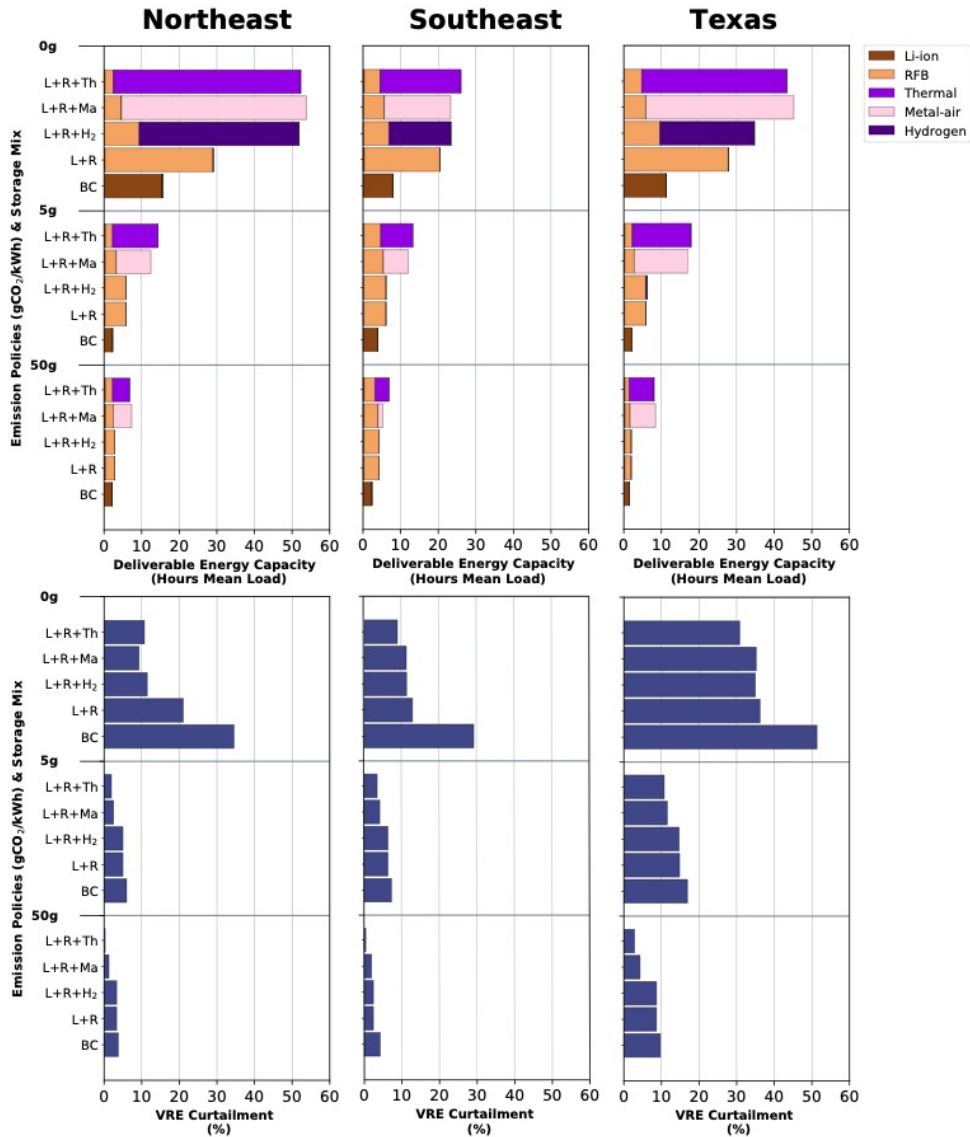


Figure 6.10: Impacts of adding RFB+ LDES on installed storage capacity and VRE curtailment, across a range of CO₂ emission constraints. They are, in ascending order: (1) base case (i.e., Li-ion only, BC); (2) Li-ion + RFB (L+R); (3-5) Li-ion + RFB + incrementally adding an LDES option in the form of hydrogen (+H₂), metal-air batteries (+MA), and thermal storage (+Th)—all at mid-cost assumptions (as defined in Table 6.3).

In scenarios where all three classes of storage technology (i.e., Li-ion, RFB, and one Class 3 LDES technology) are available, we observe partial substitution of Li-ion batteries by RFB and LDES. This substitution is more prominent for energy capacity. For example, in the 5 g CO₂/kWh case, the deliverable energy capacity of Li-ion storage in the Northeast decreases by 97%–98% when both RFB and an LDES technology are considered. This indicates that it is more economically efficient to build LDES facilities mainly for longer-duration storage cycles. The availability of LDES has less impact on Li-ion discharge power capacity since it remains more efficient to deploy Li-ion battery storage for short-duration cycles. Substitution is even stronger between Li-ion and RFB because these technologies are more similar to each other in terms of power/energy capacity costs and RTE.

Given the significant cost and operational variations associated with different classes of LDES technology (Table 6.3), we also explore how low- and high-cost assumptions for LDES resources affect system outcomes. These experiments lead to the following observations: (1) they underscore the finding that LDES has the greatest impacts on electricity system decarbonization

when natural gas generation without CCS is not an option (e.g., in the case of the 0 gCO₂/kWh scenario modeled here); (2) the availability of LDES resources even in our high-cost case enables increased VRE deployment and displaces natural gas capacity, relative to the base case; and (3) cost variations between Li-ion and RFB technologies have greater total system impacts than cost variations between the specific LDES technologies we modeled.

We show the 0 gCO₂/kWh case here, because in the Northeast hydrogen is only deployed in this extreme case (Figure 6.11). As discussed earlier, this is a stricter definition of a zero-carbon power system than the “net-zero” carbon goal being contemplated by policymakers. Still, the 0 gCO₂/kWh case is helpful for making comparisons across LDES technologies and across the modeled regions. In particular, differences in the deployment of hydrogen vs. metal-air batteries at this very stringent level of carbon constraint show that technologies with higher discharge efficiency are likely to be more valuable for grid-scale energy storage applications (Sepulveda, Jenkins, Edington, Mallapragada, & Lester, 2021). In Texas, hydrogen is deployed at lower (less stringent) levels of decarbonization—for example, at 5 gCO₂/kWh (Figure 6.12). At this emissions constraint, the availability of low-cost hydrogen changes the relative mix of wind and solar in Texas, but it does not produce a net change in optimal VRE capacity relative to the mid-cost hydrogen case. The availability of low-cost hydrogen does, however, reduce natural gas capacity by 9% while increasing total deliverable energy capacity by more than ten times (again assuming a 5 gCO₂/kWh carbon constraint).

Figure 6.11 shows that optimal VRE capacity mix and system costs for the Northeast region do not change appreciably in response to the LDES cost variations evaluated here (see results for the Texas and Southeast regions in Appendix D).²⁷ For the 5 gCO₂/kWh case, low-cost metal-air battery storage reduces SCOE by 1%, and high-cost metal-air battery storage increases SCOE by 1%, relative to mid-cost metal-air. Impacts on storage energy capacity and gas substitution are more pronounced than impacts on VRE capacity: with low-cost metal-air, optimal storage deliverable energy capacity is 123% higher relative to a scenario that assumes mid-cost metal-air (optimal storage capacity is 303% higher in the Southeast). This increase in storage capacity has the effect of displacing 23% of natural gas capacity (CCGT with and without CCS), relative to the scenario that assumes mid-cost metal-air. In terms of storage duration, low-cost metal-air makes 61 hours of storage optimal, compared to 34–41 hours in the high- and mid-cost scenarios. This translates to deliverable energy capacity equivalent to 21 hours of mean load in the low-cost case, 9 hours in the mid-cost case, and less than 3 hours in the high-cost case.

Cost variations for Li-ion and RFB storage affect system costs more strongly than cost variations across LDES technologies. In all regions and across all the LDES cost ranges we considered, the availability of low-cost Li-ion and RFB technology displaces all need for LDES capacity (top row in Figure 6.11 and Figure 6.12). This indicates that system reliability requirements can be met economically by shorter-duration storage technologies alone if the costs of those technologies are sufficiently low. We should note that the alternative cost assumptions for hydrogen considered here and defined in Table 6.3, still reflect costs for above-ground storage of compressed gas. Lower storage costs are possible with geological hydrogen storage in some locations (see Chapter 5 for further discussion). As discussed later, the availability of geological hydrogen storage significantly increases the value of hydrogen storage for grid decarbonization. Of course, the large-scale use of hydrogen outside the power sector would also increase the value of hydrogen storage.

²⁷ Results for the Southeast and Texas are discussed in Appendix D: Figure D-4 and Figure D-3, respectively.

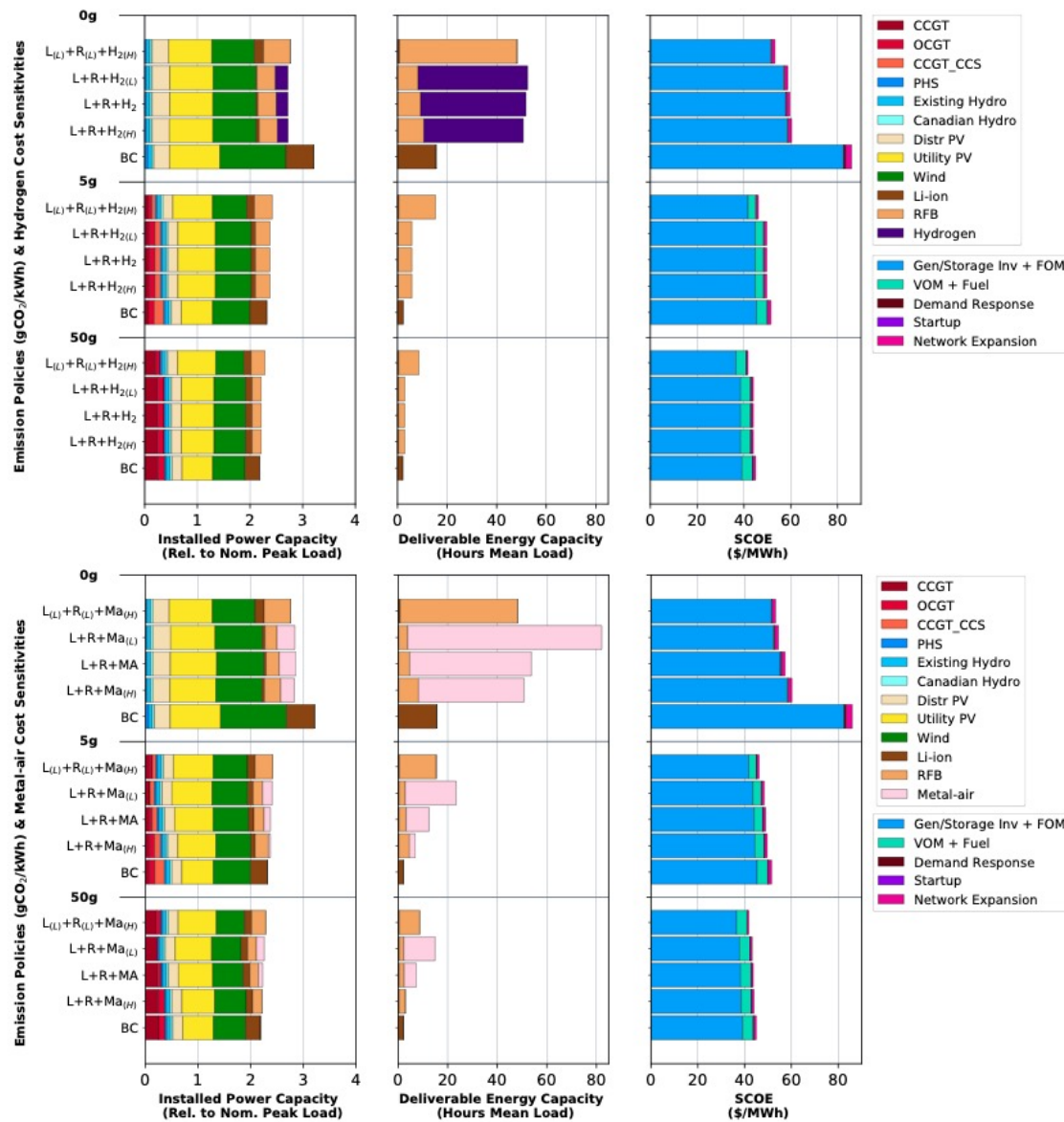


Figure 6.11: Impact of low-, mid-, and high-cost hydrogen (top row) and metal-air battery (bottom row) storage on installed power capacity, storage capacity, and SCOE, across a range of CO₂ constraints for the Northeast region. They are, in ascending order: (1) base case (i.e., mid-cost Li-ion only, BC); (2-4) mid-cost Li-ion and RFB + incremental additions of high-cost hydrogen or metal-air (L+R+H₂/MA_H), mid-cost hydrogen or metal-air (L+R+H₂/MA), and low-cost hydrogen or metal-air (L+R+H₂/MA_L); and (5) low-cost Li-ion and RFB + high-cost hydrogen or metal-air (L_L+R_L+H₂/MA_H). Low-, mid-, and high-cost assumptions for each storage technology are defined in Table 6.3.

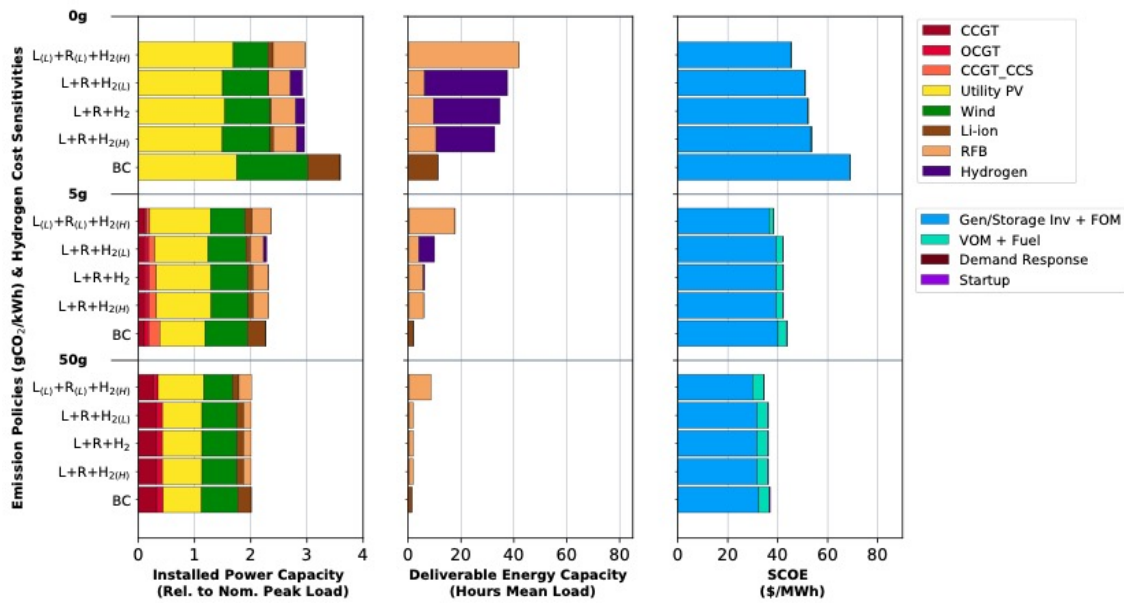


Figure 6.12: Impacts of low-, mid-, and high-cost hydrogen on installed power capacity, storage capacity, and SCOE, across a range of CO₂ constraints for the Texas region. They are, in ascending order: (1) base case (i.e., mid-cost Li-ion only, BC); (2-4) mid-cost Li-ion and RFB + incremental additions of high-cost hydrogen (L+R+H_{2H}), mid-cost hydrogen (L+R+H₂), and low-cost hydrogen (L+R+H_{2L}); and (5) low-cost Li-ion and RFB + high-cost hydrogen (L_L+R_L+H_{2H}). Low-, mid-, and high-cost assumptions for each storage technology are defined in Table 6.3.

Finding: With lower energy capacity costs and lower round-trip efficiency compared to Li-ion battery technology, LDES has the greatest impacts on electricity system decarbonization when natural gas generation without CCS is not an option (corresponding to our 0 gCO₂/kWh policy case), under the assumptions used in this analysis. Generally, LDES, when optimally deployed, substitutes for natural gas capacity, increases the value of VRE generation, and produces moderate reductions in system average electricity cost.

Operational Behavior of Short- vs. Long-Duration Storage Technologies

Our modeling highlights the differing operating patterns of various classes of storage technologies, as influenced by the attributes of individual technologies and by system conditions (such as the stringency of the CO₂ constraint). Figure 6.13 shows how frequently storage resources are cycled (deep discharge and charge cycle) in our model of the deeply decarbonized Texas system with Li-ion batteries and hydrogen as the available storage technologies. As expected, Li-ion batteries, with their relatively low power capacity cost, relatively high energy capacity cost, and high RTE are used primarily for short-cycle operations, while hydrogen storage, with higher power costs but much lower energy capacity costs and RTE than Li-ion, is mostly used for longer-cycle operations. These operational modes are not exclusive to each storage technology, however, and we see that Li-ion batteries sometimes perform relatively long charge/discharge cycles, while hydrogen systems are sometimes cycled rapidly. Moreover, the optimal operating pattern for storage technologies is also influenced by the CO₂ constraint: tighter constraints lead to longer cycles, as can be seen by comparing the top and bottom portions of Figure 6.13.

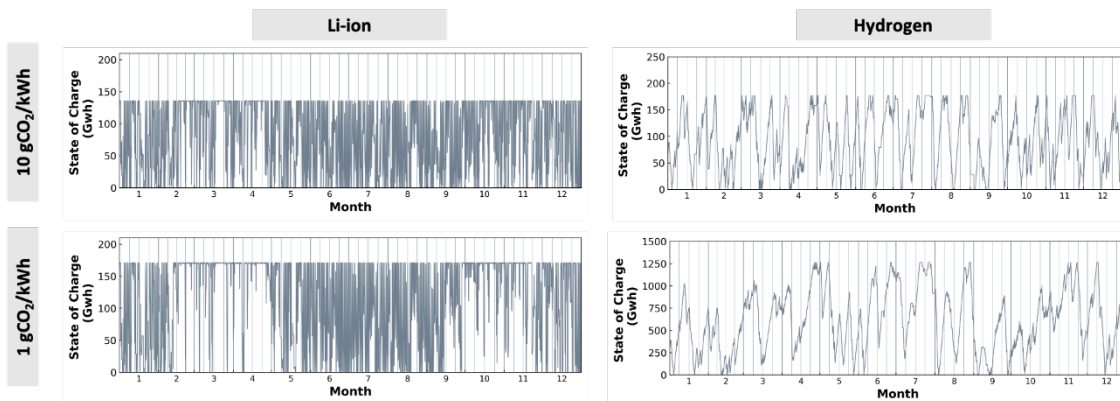


Figure 6.13: Example state of charge (SoC) of Li-ion battery and hydrogen storage systems in Texas. Scenarios show the hourly SoC for Li-ion and hydrogen storage for the scenario with mid-cost Li-ion, RFB (not shown), and hydrogen storage technologies available across two emissions constraints. Here, we show 12 months of operation. Results correspond to mid-cost assumptions for each storage technology as defined in Table 6.3.

As discussed in Junge, Mallapragada, and Schmalensee (2021), storage technologies do not follow simple cycling patterns. Optimal operation is more complex than the marginal cost dispatch rule for generation technologies. In effect, the marginal cost of using storage energy depends on the (shadow) value of stored energy, which changes from one period to the next.

Frequency analysis²⁸ applied to the time series of the state of charge of storage technologies is a useful way to unpack complexity and quantify operating behavior, since this type of analysis can be used to quantify the relative importance of different frequencies (or cycling patterns) in the modeled storage state of charge. The results of the frequency analysis, applied to the model outputs related to storage state-of-charge variables shown in Figure 6.13, are listed in Table 6.10. The table shows that for the 10 gCO₂/kWh case, hydrogen storage behaves mostly in cycles that occur within a month (intra-month charge and cycle); for the 1 gCO₂/kWh case,²⁹ which we consider here as an extreme example,³⁰ the cycles decrease in frequency and become mostly seasonal (64%). Conversely, Li-ion battery storage shows a tendency towards daily and weekly cycles. In the 10 gCO₂/kWh case, daily and weekly charge and discharge cycles account for 73% of the operational patterns; they account for only 52% of operational patterns in the 1 gCO₂/kWh case. It is worth highlighting the observation that Li-ion storage in the 1 gCO₂/kWh case also displays a significant proportion of seasonal cycling (35%), reflecting the fact that this technology is used less frequently during some periods of the year than during others.

²⁸ Frequency analysis is performed by applying a fast Fourier transform (FFT) to the time-dependent variable corresponding to the hourly storage state of charge. Next, the root mean square (RMS) contribution of selected frequency bands is computed. The frequency bands of interest are listed in Table 6.10.

²⁹ For the Texas case study, we also examined scenarios with the 1gCO₂/kWh emissions intensity constraint for certain technology and system assumptions. However, because we did not evaluate this emissions intensity constraint for other regions, we primarily rely on results from the 5g CO₂/kWh scenario when describing trends in system outcomes under deep decarbonization.

³⁰ See also note 19, above.

Frequency band	Mode of operation	10 gCO ₂ /kWh		1 gCO ₂ /kWh	
		Li-Ion	H ₂	Li-Ion	H ₂
Above 365 cycles/year	Daily	39%	1%	23%	0%
52 to 365 cycles/year	Weekly	34%	15%	29%	4%
12 to 52 cycles/year	Monthly	12%	59%	12%	32%
0 to 12 cycles/year	Seasonal	16%	25%	35%	64%

Table 6.10: Relative root mean square (RMS) contribution of different frequency bands to the storage's State of Charge.

Finding: When it is cost-optimal to deploy multiple storage technologies, the technologies with the lowest capital cost of energy storage capacity are generally best suited to provide long-term storage. However optimal storage operation, unlike optimal generation dispatch, is complicated by the changing shadow value of stored energy. As a result, all storage technologies deployed will operate with charge/discharge cycles of various durations. Simplified assessments of storage economics based on stylized charge/discharge profiles overlook such dynamics and may provide inaccurate assessments of storage value.

6.3.3 Storage Substitutes for Grid Resources

Energy market arbitrage involves buying when prices and net demand (the difference between demand and VRE output) are low and selling when prices (and net demand) are high. In performing arbitrage, energy storage can substitute for other grid resources (and vice versa). Candidate substitutes for grid resources include VRE “overbuilding” (i.e., deploying VRE capacity in excess of system peak load), demand flexibility, dispatchable generation, and increased network capacity (transmission and distribution). The degree to which storage can substitute for these resources depends not only on the cost and performance of storage technologies relative to competing resources, but also on system conditions, such as the stringency of the carbon constraint, the amount of storage deployed already, the availability of demand flexibility resources, and the ability to expand transmission. This section quantifies the cost-optimal substitution between various types of resources and storage under scenarios for deep grid decarbonization. We evaluate four potential substitutions: (1) storage vs. VRE generation capacity, (2) storage vs. demand-side resources, (3) storage vs. dispatchable low-carbon generation, and (4) storage vs. transmission. The systems modeling framework we employ to study the substitutability of storage with other resources (and vice versa) implicitly accounts for the fact that the marginal value of all resources, including storage, declines with increasing penetration.

Impact of VRE Cost on Storage Deployment

As discussed above, low-cost storage options can reduce the need to overbuild VRE capacity by more effectively balancing VRE intermittency and by, in effect, shifting generation to hours of high net demand. The degree to which storage substitutes for VRE capacity in our modeling depends on the cost and performance of storage technologies and on VRE resource availability and costs. Figure 6.14 explores the sensitivity of storage deployment across a range of VRE capital cost scenarios. We find, first, that storage deployment is relatively robust to VRE costs, as the deployment of VRE resources is driven more by policy considerations than by cost considerations. Second, we find that the impact of VRE costs is most pronounced in the No-Limit policy scenario. This is particularly true in regions with lower-quality VRE resources, such as the Northeast, relative to regions with higher-quality VRE resources, such as Texas.

When only Li-ion batteries are available as a storage technology and we apply a 5 gCO₂/kWh carbon constraint, low-cost VRE (where “low-cost” is defined as a 23% cost reduction for utility-

scale solar and a 33% cost reduction for onshore wind compared to our mid-cost assumptions) increases optimal VRE capacity by 2%–10% across the three regions (favoring wind over solar). This increased VRE deployment leads to 0%, 6%, and 16% lower delivered energy storage capacity compared to the mid-cost VRE scenario in Texas, the Northeast, and the Southeast, respectively (5 gCO₂/kWh policy case in Figure 6.14 and Figure D-5). The regional differences in the impact of low-cost VRE on storage capacity can be explained by differences in the availability of dispatchable generation (e.g., nuclear) and the quality of VRE output.³¹ As expected, overbuilding resulting from low-cost VRE increases VRE curtailment—for example, from 17% to 22% in Texas in the 5 gCO₂/kWh case. Most noticeably, VRE costs have significant impacts on system cost. At the 5 gCO₂/kWh emissions limit, assuming optimal deployment, SCOE is 14%–17% lower across the modeled regions in the low-cost VRE scenario compared to the mid-cost VRE scenario. Conversely, for the same emission policy constraint, SCOE is 12%–15% higher with optimal deployment in the high-cost VRE scenario (where “high-cost” is defined as a 29% cost increase for solar and a 16% increase for wind compared to mid-cost assumptions).

Across all scenarios we considered, system outcomes are most sensitive to VRE technology costs in the No Limit policy case, since this is where VRE deployment is most sensitive to capital costs (as opposed to binding carbon constraints). The substitution effect between VRE resources and natural gas is most pronounced in regions with lower-quality VRE resources (the Northeast) compared to regions with higher-quality VRE (Texas). For example, in the No Limit case, low VRE costs increase VRE capacity by 111% in the Northeast, compared to 19% in Texas. As with optimal storage deployment at higher levels of decarbonization, low costs for VRE have a greater impact in terms of natural gas capacity reductions in Texas (6%) than they do in the Northeast (1%). These results are robust to the addition of storage technologies with lower energy capital costs.

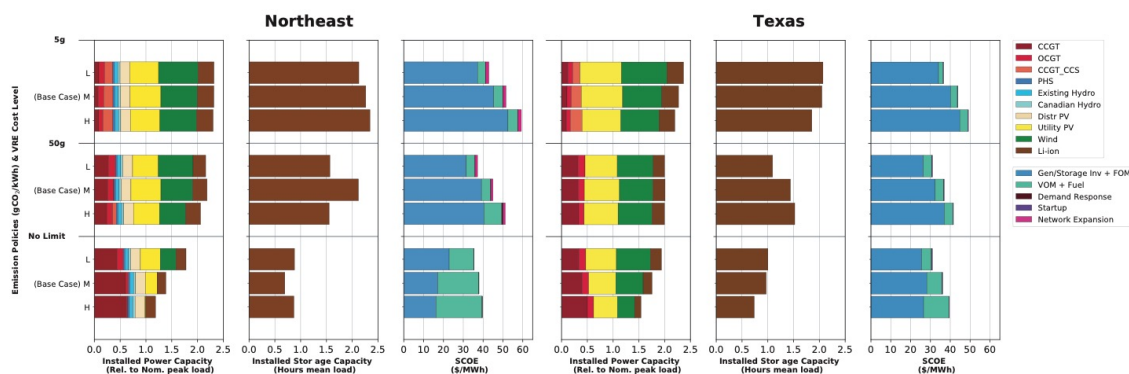


Figure 6.14: Impacts of low-, mid-, and high-cost VRE on installed power capacity, storage capacity, and SCOE across a range of CO₂ constraints for the Northeast and Texas regions. They are, in ascending order: (1) high-cost VRE (H), (2) mid-cost VRE (M), and (3) low-cost VRE (L). Low-, mid-, and high-cost assumptions for VRE are defined in Appendix A.

Impact of Intra-Day Demand Flexibility

The potential value of flexibility in electricity consumption for various end-uses increases with greater deployment of smart meters and related technologies and expanded electrification in sectors such as transportation. Here, we explore how enabling intra-day demand flexibility affects the cost-optimal grid configuration and, in particular, how it changes the role for energy

³¹ Low-cost VRE favors “overbuilding” VRE over deploying storage capacity. However, low-cost VRE also improves the competitiveness of VRE+ storage to displace dispatchable low-carbon generation (CCGT with CCS). Collectively, these two factors explain why storage capacity remains unchanged for Texas when modifying VRE costs from mid to low for the 5 gCO₂/kWh emissions case. With low-cost VRE, gas capacity declines by 6% compared to the mid-cost VRE scenario (Figure 6.14).

storage under various CO₂ constraints and different assumptions regarding storage technology. For these experiments, we consider a very optimistic version of demand flexibility: the ability to shift electricity consumption from specific demand subsectors, highlighted in Table 6.11, over constrained (feasible) time windows at zero cost and with zero energy efficiency losses.

Our assumptions about demand flexibility are based on the NREL EFS enhanced flexibility scenario, which provides potential hours of delay and advance for specific demand subsectors, along with the share of the load that can be shifted (Mai, et al., 2018). Since the load from each subsector changes over time, potential demand flexibility also varies from hour to hour. For this reason, Table 6.11 notes the maximum load that could be shifted for each subsector at any point in time for the Texas region in 2050 under the high-electrification load scenario. (Data for Northeast and Southeast are shown in Table A-6 in appendix A.) It is important to notice that these subsector peaks do not occur at the same time; the actual maximum potential demand flexibility in any single hour is 47 GW, which corresponds to 31% of total demand in that hour (Mai, et al., 2018).

Since the assumed temporal flexibility of demand-side resources spans hours rather than days, we focus on how demand flexibility affects the cost-optimal substitution of short-duration (Li-ion battery) storage rather than how it affects LDES resources. Figure 6.15 (and Figure D-6) **Error! Reference source not found.** shows the impact of short-term demand flexibility across the three regions under various carbon constraints. In all three modeled regions, the impact of demand flexibility on optimal deployment of Li-ion storage declines with more stringent emission policies. For example, in all regions, demand flexibility substitutes for almost 100% of short-duration storage in the No Limit case, while in the 5 gCO₂/kWh case, it substitutes for just 19% of Li-ion storage on an energy basis in the Southeast, 35% in Texas, and 37% in the Northeast. Differences in the impacts of demand flexibility across the three regions are partly explained by underlying differences in the temporal profiles for demand and zero-carbon resource availability (including the hydro available in the Northeast and Southeast, and nuclear in the Southeast).

Figure 6.16 illustrates how the system operates with and without demand flexibility under a carbon constraint of 5 gCO₂/kWh for the Texas region. The figure shows that charge and discharge cycles for Li-ion storage are less frequent when demand flexibility is implemented. For this case, the daily component of the frequency analysis, introduced in Table 6.10, decreases by 20%. The bottom panel in Figure 6.16 shows how the availability of short-duration demand flexibility shifts load toward hours with more VRE generation.

Lower requirements for short-term storage with flexible demand translate into reductions in SCOE, with cost reductions in line with how much Li-ion storage is displaced. In all three regions, cost reductions are modest, ranging from 5%–6 % in the No Limit case to 3% in the 5 gCO₂/kWh case (shown for the Southeast case in Figure D-6).

Demand Subsector	Hours Delay	Hours Advance	Share of End-Use That Is Flexible	Maximum Hourly Demand Flexibility [GW]
Commercial HVAC	1	1	25%	8.6
Residential HVAC	1	1	35%	7
Commercial Water Heating	2	2	25%	0.2
Residential Water Heating	2	2	25%	1
Light duty vehicles	5	0	90%	33
Medium duty trucks	5	0	90%	3
Heavy-duty trucks	3	0	90%	5

Table 6.11: Demand flexibility assumptions for Texas under 2050 load conditions. HVAC = heating, ventilation, and air conditioning. Data sourced from NREL Electrification Futures Study (Mai, et al., 2018).

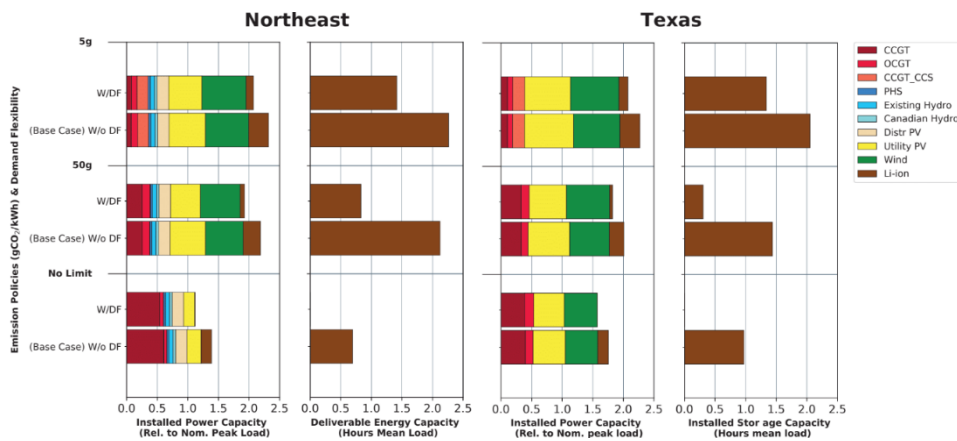


Figure 6.15: Impacts of demand flexibility in terms of installed power capacity, storage capacity, and SCOE, across a range of CO₂ constraints for the Northeast and Texas regions. Demand flexibility assumptions are summarized in Table 6.11.

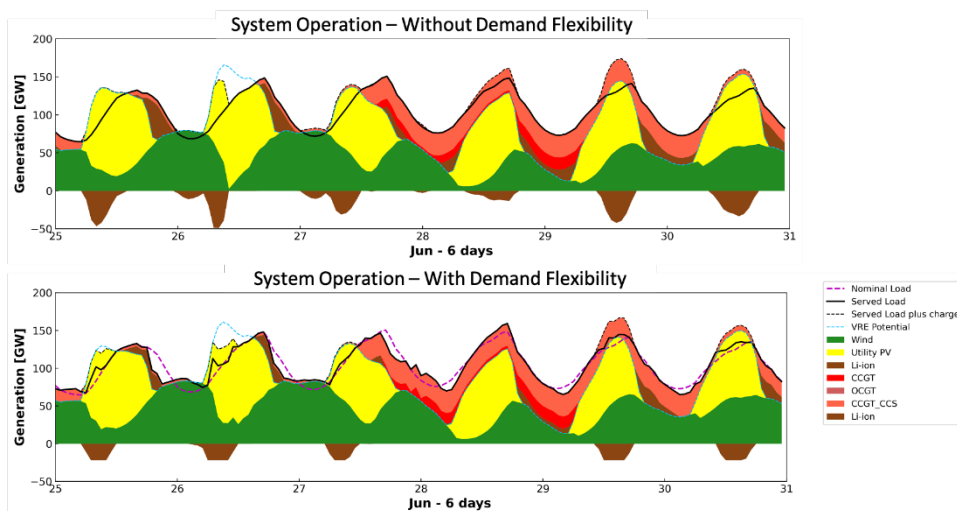


Figure 6.16: Impact of demand flexibility on system operations in Texas. The figure shows six days of stacked dispatch in winter under a CO₂ emissions constraint of 5 gCO₂/kWh. The upper plot shows the operation of the system without demand flexibility; the lower plot shows how the system operates with assumed levels of demand flexibility. Demand flexibility assumptions are summarized in Table 6.11.

Hydrogen Use in Industry

Whereas prior sections concerned with LDES technologies have focused exclusively on power system drivers that affect the value of these technologies, the value of long-duration storage options that involve hydrogen could also be affected by the co-existence of non-power-sector uses for hydrogen. This creates the opportunity to share hydrogen production technology and

associated costs across sectors. Here, we explore the impact of hydrogen demand outside the power sector on the cost-effectiveness of hydrogen storage that could be deployed by the power sector, using industrial decarbonization as an example. Figure 6.17 highlights the potential opportunity to share hydrogen technology components to serve both the power sector and external hydrogen demand simultaneously. This is a special case of demand flexibility, whereby the use of electricity to produce hydrogen via water-splitting (or electrolysis) can be flexibly scheduled because hydrogen can be stored at relatively low energy capital cost (see Table 6.3) even though external hydrogen demand is modeled to be constant and inflexible across all hours of the year.

We evaluate the impact of varying levels of hydrogen demand on power system outcomes under different CO₂ intensity constraints, with a focus on Texas because it is one of the largest energy consuming states in the country and one in which more than half of overall energy consumption comes from industrial activity (EIA 2021). Our industrial hydrogen demand scenarios are developed by assuming that this sector adopts hydrogen to substitute for natural gas used in process heating. We consider a range of scenarios based on different levels of hydrogen substitution for natural gas as a heat source in industrial applications: 0%, 25%, 50%, 75%, and 100%. Here 100% substitution corresponds to 19.7 GW_t (thermal) of hydrogen demand and the 0% case corresponds to no hydrogen demand. For comparison purposes, a constant 19.7 GW_t load is equivalent to average power demand of 25.6 GW_e assuming mid-range charging (electrolyzer) efficiency as per Table 6.3. (Note that 25.6 GW_e is equal to approximately 17% of projected 2050 peak demand in Texas.) Details of our approach to modeling hydrogen demand are provided in Appendix C.

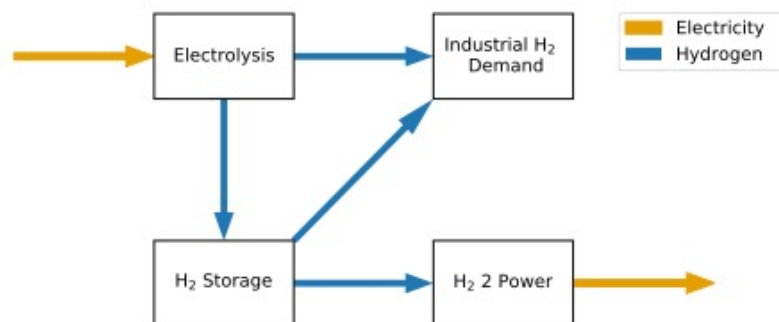


Figure 6.17 Representation of how industrial hydrogen demand is modeled within GenX. We assume that a portion (0%–100%) of industrial hydrogen demand is met by electricity; this hydrogen can be produced either directly through electricity from the grid (electrolysis to H₂ demand) or through electricity from storage (electrolysis to storage to H₂ demand). Storage in this framework can provide hydrogen either for industry (storage to H₂ demand) or to serve electric load (storage to H₂ to power).

Different levels of hydrogen demand were simulated under a range of power sector CO₂ intensity constraints, including 1, 5, 10, and 50 gCO₂/kWh and a No Limit case.³² Our initial results assume above-ground storage of hydrogen in tanks, with mid-level costs from Table 6.3. From the installed capacity perspective, our findings show that for a given CO₂ constraint, increased industrial hydrogen demand with incremental hydrogen production using flexible electrolysis

³²It should be noted that scenarios with industrial hydrogen demand are associated with greater annual electricity consumption than scenarios without hydrogen demand. For example, including constant external hydrogen demand at the level of 25.6 GW_e translates into incremental electricity consumption of 224.25 TWh or a 31% increase in total annual electricity consumption. Consequently, for the same CO₂ intensity constraint on dispatched generation, power sector CO₂ emissions in the case with industrial hydrogen demand will be greater than in the case without hydrogen demand. However, *overall* energy sector CO₂ emissions will be lower due to the substitution for natural gas by electrolytic hydrogen in the industrial sector.

favors the deployment of VRE generation and displaces gas generation (both with and without CCS) and Li-ion power capacity (Figure 6.18). For example, in the 5 gCO₂/kWh scenario, Li-ion and gas power capacities with 100% industrial hydrogen demand are 10% and 23% lower, respectively, than in the case without any industrial hydrogen demand (the 0% case).

Including industrial hydrogen demand reduces the percentage increase in power capacity optimally built to achieve increasingly stringent CO₂ constraints. Whereas installed power capacity increases 53% from the No Limit case to the 1 gCO₂/kWh case *without* hydrogen demand, the increase falls to 35% for the case of 100% hydrogen substitution. A second, related effect of increased hydrogen demand is a reduction in VRE curtailment. Across the range of carbon constraints we considered, VRE curtailment is 30% lower on average with 100% hydrogen substitution than with zero industrial hydrogen demand. (It is 46% lower in the 1 gCO₂/kWh case.)

Higher industrial hydrogen demand enables improved utilization of both electrolyzer and VRE assets, which leads to a lower SCOE to achieve the same CO₂ intensity target (Figure 6.19). The magnitude of the maximum SCOE reduction depends on the stringency of the CO₂ constraint; in our modeling results it ranges from a 3% reduction (in the No Limit case) to a 14% reduction (in the 1 gCO₂/kWh case). Stated another way: As compared to the No Limit case, achieving a grid emissions intensity of 1 gCO₂/kWh increases SCOE by 37% without industrial hydrogen demand and by 22% with 100% hydrogen substitution (Figure 6.19). For context, the modeled increase in SCOE as a result of going from the No Limit case to the 1 gCO₂/kWh case with LDES but without industrial hydrogen demand is 31%.

The diminishing marginal benefits of increasing industrial hydrogen demand are reflected in increasing marginal hydrogen production costs, shown in Figure 6.19. This suggests that strategies that are purely based on electrolytic production of hydrogen to meet non-power hydrogen demand may be limited in the quantity of hydrogen that can be cost-effectively supplied. As our analysis does not account for other means of hydrogen production or for hydrogen imports, and because we model industrial hydrogen demand as constant and inflexible, increasing industrial hydrogen demand under a given CO₂ intensity constraint results in increased marginal hydrogen production cost. This effect is explained by the fact that extra electricity generating capacity (mostly VRE) and hydrogen storage are needed to satisfy increased industrial demand.

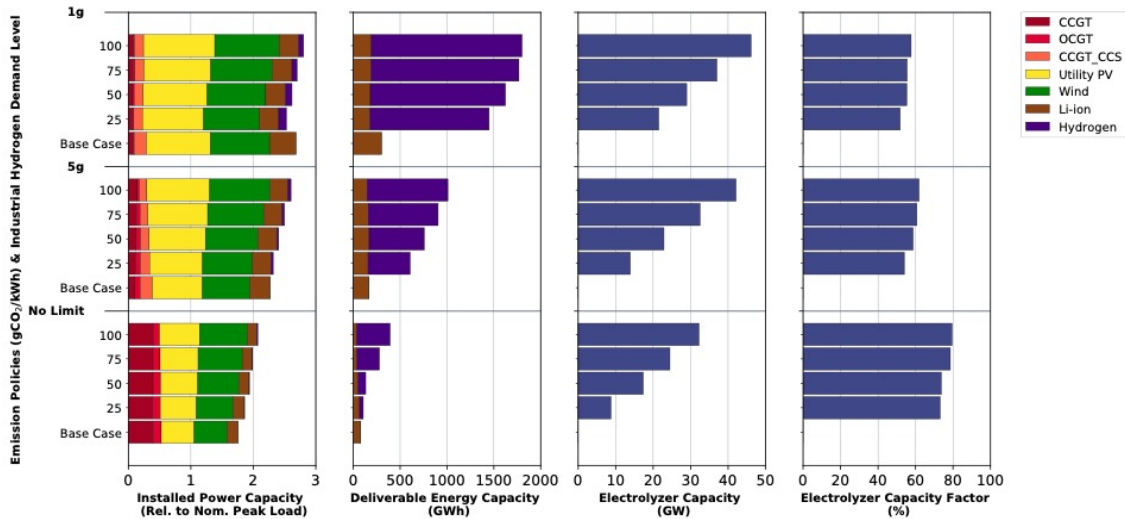


Figure 6.18. Impacts of serving 0%–100% of baseline industrial hydrogen demand (19.7 GW_e) with electricity in terms of installed power capacity, storage capacity, electrolyzer capacity, and electrolyzer capacity factor, across a range of annual CO₂ emission constraints for the Texas region. Hydrogen technology assumptions reflect mid-range costs as reported in Table 6.3. The base case corresponds to 0% industrial hydrogen demand.

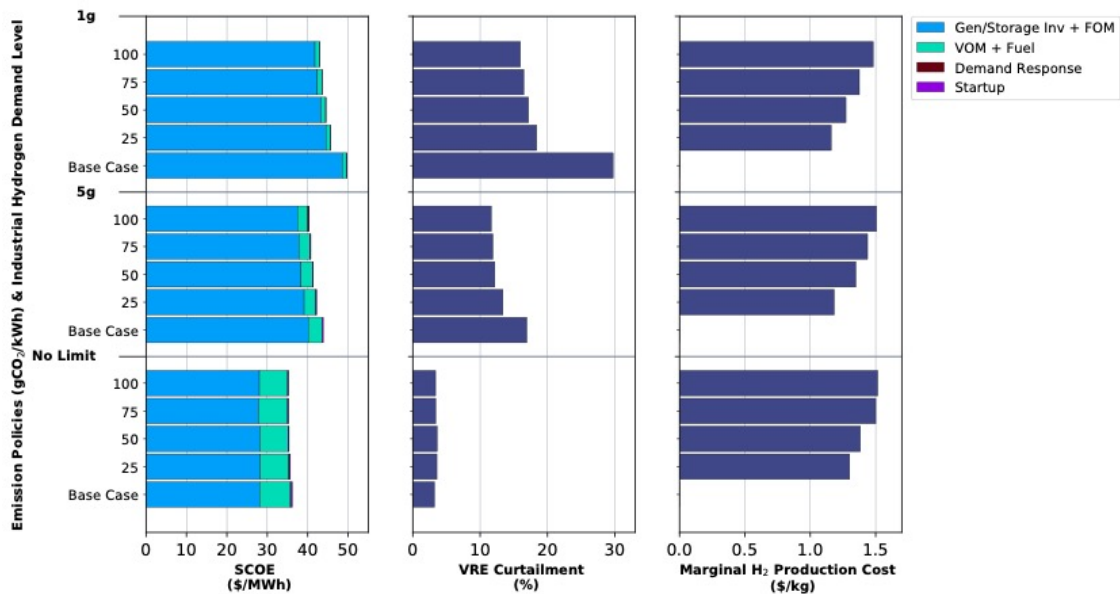


Figure 6.19. Cost and VRE curtailment impacts of alternative industrial hydrogen demand levels. Scenarios show the impacts of serving 0%–100% of baseline industrial hydrogen demand (19.7 GW_e) with electricity in terms of SCOE,³³ VRE curtailment, and marginal hydrogen production, across a range of CO₂ constraints for the Texas region. Hydrogen technology assumptions reflect mid-range costs as reported in Table 6.3.

To explore the broader potential of a system in which hydrogen is partly used to meet industrial demand for process heat as well as for storage in the electric power system, we consider the effects of the availability of underground geological storage as a potential technology that can be deployed by the model. The main difference between geological and tank storage of hydrogen is the investment needed per unit of stored energy (assumed to be 84% less for geologic storage compared to the mid-level cost projections for above-ground hydrogen

³³ In the context of producing hydrogen for industrial heat, the system cost of electricity (SCOE) is computed as the ratio of total system cost to total served demand, where the latter includes both the electric demand in the power system and the equivalent electrical energy used to produce hydrogen for industry.

storage; see "ultra-low" value reported in Table 6.3 and Chapter 5 for further discussion). Our findings (Figure 6.20) show that geological hydrogen storage has a positive effect across the different metrics we consider. In the 1 gCO₂/kWh case with 100% hydrogen substitution, relative to tank storage the availability of underground geological storage results in a 91% increase in optimal storage capacity, a 3.5% reduction in SCOE, a 30% reduction in natural gas capacity, an 11% decrease in VRE curtailments, and an 11% reduction in VRE capacity.

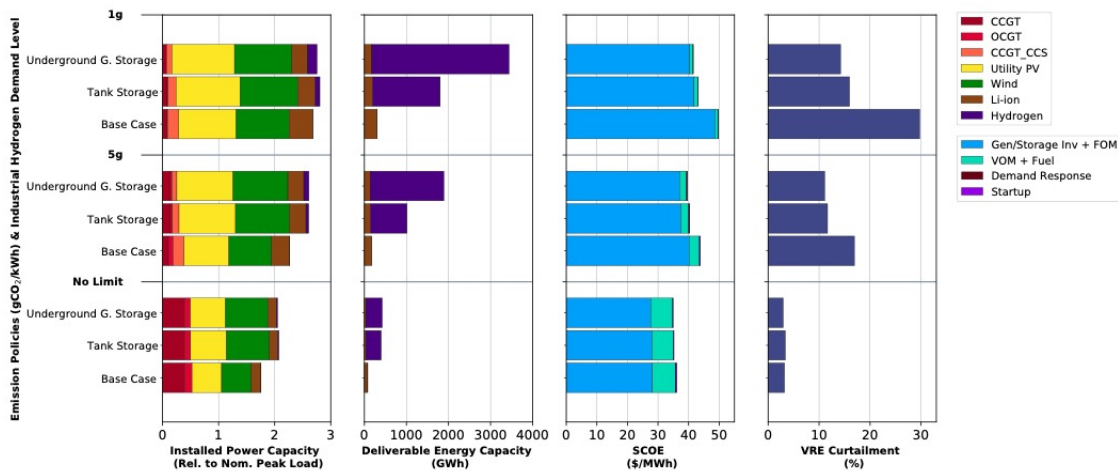


Figure 6.20 System impacts of the availability of underground geological hydrogen storage. The base case assumes 0% industrial hydrogen demand; the other scenarios involve 100% hydrogen substitution (19.7 GW_t). The Figure shows impacts on power capacity mix, storage capacity, SCOE and VRE curtailment across a range of CO₂ emissions constraints. Hydrogen technology assumptions reflect mid-range (tank storage) and ultra-low (underground storage) costs as reported in Table 6.3.

Competition with Low-Carbon Dispatchable Resources

Storage makes it possible to shift VRE generation over time, thus increasing the value of VRE resources. This can place storage resources in direct competition with dispatchable low- or zero-carbon resources. We examine this competition by comparing storage penetration and utilization with the deployment of two dispatchable low-carbon resources: (1) an advanced natural gas power plant with close-to-100% CO₂ capture (also known as “Allam” or “Allam-Fetvedt” cycle) (Weiland & White, 2019) and (2) new nuclear capacity. In our modeling, the advanced natural gas technology with CCS is made available in Texas, where CO₂ sequestration appears most viable (see cost assumptions in Table 6.5); substituting LDES with new nuclear capacity is an option in the Southeast region.

If the Allam cycle becomes commercially available,³⁴ our modeling predicts that it will dominate CCGT+CCS deployment in Texas. Compared to a scenario in which this technology is not available, the option to deploy the Allam cycle increases total gas capacity by 13% and reduces VRE capacity by 7% in the 5 gCO₂/kWh case, for mid-cost hydrogen in Texas (Table 6.12). The Allam cycle can serve as a partial substitute for storage, as evidenced by a reduction in modeled deliverable storage capacity of 28% with LDES in the form of hydrogen storage, 20% with LDES in the form of metal-air battery storage, and 3% with LDES in the form of thermal storage.³⁵ Table 6.12 documents the (relatively small) incremental SCOE reductions obtained by adding the Allam cycle to a system with hydrogen storage under different cost assumptions. Table D-2 in Appendix D presents the similar results obtained by adding the Allam cycle to a system with

³⁴ As per recent announcements, prototype near-zero-emission natural gas power plants are being developed and have reached various stages of technology readiness. For an example, see McMahon (2021).

³⁵ The results for metal-air systems can be found in (Appendix D, Table D-2).

metal-air storage. Collectively, the availability of the Allam cycle along with LDES enables SCOE reductions of 5%–13% relative to the base case across low-, mid-, and high-cost assumptions for all three LDES technologies under the 5 gCO₂/kWh emissions policy case.

	Low-Cost Hydrogen			Mid-Cost Hydrogen			High-Cost Hydrogen		
	Without Allam Cycle	With Allam Cycle	% Diff	Without Allam Cycle	With Allam Cycle	% Diff	Without Allam Cycle	With Allam Cycle	% Diff
Firm Dispatchable Installed Capacity (GW)									
CCGT	17.6	19.4	10%	17.0	19.3	14%	17.0	19.3	14%
OCGT	10.1	12.2	21%	12.1	13.1	8%	12.2	13.1	7%
CCGT_CCS	16.6	0.0	-100%	19.4	0.0	-100%	19.6	0.0	-100%
Allam	0.0	20.1	-	0.0	22.3	-	0.0	22.3	-
Total	44.2	51.7	17%	48.5	54.7	13%	48.8	54.7	12%
VRE Installed Capacity (GW)									
Wind	102.6	94.7	-8%	99.4	93.8	-6%	99.2	93.8	-5%
Utility PV	142.7	137.2	-4%	146.7	135.9	-7%	147.0	135.9	-8%
Total	245.3	231.9	-5%	246.1	229.6	-7%	246.2	229.6	-7%
Energy Storage (Li-ion + RFB + LDES)									
Power (GW)	55.3	48.8	-12%	55.4	46.0	-17%	55.3	46.0	-17%
Energy (GWh)	817	542	-34%	510	369	-28%	484	369	-24%
System Cost of Electricity									
Average \$/MWh	42.2	41.7	-1%	42.4	41.7	-2%	42.4	41.7	-2%

Table 6.12: System impacts of a dispatchable low-carbon generating technology in Texas. Scenarios show the impact of low-, mid-, and high-cost hydrogen with and without the Allam cycle in terms of installed power capacity, storage capacity, and SCOE, across 5 gCO₂/kWh emissions scenarios. Low-, mid-, and high-cost assumptions for hydrogen storage are given in Table 6.3. Cost assumptions for the Allam cycle are given in Appendix A.

We also tested the impact of allowing for new nuclear builds in the Southeast region. At an assumed completion cost of \$6,048/kW (2020 NREL ATB), the model does not choose to deploy new nuclear capacity under the 5 gCO₂/kWh emission constraint. This result differs from findings in the 2018 MIT study, *The Future of Nuclear in a Carbon-Constrained World*, for two main reasons. First, following NREL, we assume higher costs for new nuclear generation (\$6,048/kW vs. \$5,500/kW in the *Future of Nuclear* study). Second, this study assumes lower costs for solar (\$725/kW vs. \$917/kW) and wind (\$1,085/kW vs. \$1,550/kW) based on NREL's 2020 mid-cost projections for 2050. Together, these cost assumptions combine to make new nuclear builds less attractive. However, we also looked at the effect of applying low-cost assumptions for new nuclear capital costs from the 2018 MIT study.³⁶ At \$4,202/kW (the "low" cost for new nuclear from the 2018 study), and \$2,818/kW (the "ultra-low" cost from the 2018 study), the model deploys 21 GW and 78 GW, respectively, of new nuclear in the Southeast under the 5 gCO₂/kWh policy constraint. This new nuclear displaces mainly VRE capacity (15% and 49% in the low- and ultra-low nuclear cost scenarios, respectively) as well as some gas peaking capacity.

Role of Regional and Inter-Regional Transmission

The modeling results presented thus far assume the co-optimization of generation and transmission investments and operations. For transmission planning, this means that regional transmission systems have been sized to deliver the highest-value service at lowest total cost. In the Northeast and Southeast regions this means investments have been made to meet intra-regional demand by relieving transfer congestion (for example, in capacity-constrained areas such as New York City), enabling the integration of lower-cost VRE resources in other zones in the region, increasing system flexibility, and reducing overall balancing costs. However, current planning processes do not consider the full, stacked benefits of transmission upgrades, instead relying only on traditional metrics to assure reliability and meet local needs (Pfeifenberger, 2021). Permitting and siting challenges create further barriers to transmission expansion. In this sensitivity analysis, we assume no transmission expansion, meaning that regional transmission systems are limited to existing capacities, and assess the impact on VRE and storage deployment.³⁷

In the model, increased regional transmission capacity provides two main benefits: (1) it allows for increased VRE deployment in regions with higher-quality VRE resources (lower cost of energy), which in turn reduces overall system costs; and (2) it improves VRE integration, by balancing resource intermittency across connected regions and smoothing the effects of geographical differences. Thus, limiting the optimal deployment of transmission capacity to the levels that currently exist in these regions focuses VRE deployment into the same zone as the demand being served, rather than allowing deployment at sites with the highest-quality resources. For example, Table 6.13 shows that for the Northeast, in the 5 gCO₂/kWh case with intra-regional transmission expansion allowed, the model optimizes by adding 55 GW of new transfer capacity within the region to connect better-quality VRE resources from other zones. Restricting intra-region transmission expansion, on the other hand, increases average SCOE by \$3/MWh (or 5%) in the 5 gCO₂/kWh case, because it forces greater reliance on lower-quality VRE capacity that is located closer to demand (e.g., distributed and utility PV over wind). Limited regional supply–demand balancing increases the role for energy storage, particularly under very tight carbon constraints. For example, a scenario with no transmission expansion increases energy storage requirements in the Northeast by 36%, in the 5 gCO₂/kWh policy case. By contrast, enabling transmission expansion in the Southeast has little impact on VRE integration,

³⁶ Cost numbers are from Buongiorno, et al. (2018), plus a 2.49% inflation rate to bring them to 2018 dollars.

³⁷ For more expansive studies of the benefits of inter-regional transmission, see Brown and Botterud (2021) and Brinkman, et al. (2020) (Brinkman, Novacheck, Bloom, & McCalley, 2020).

because VRE resource quality is similar across all four modeled zones in that region. In the Southeast, restricting transmission expansion has the effect of increasing reliance on gas generation with CCS, which can be located closer to demand, in place of VRE and storage capacity (Table D-3).

	0 gCO ₂ /kWh			5 gCO ₂ /kWh			No Limit Policy		
	With Trans Exp	Without Trans Exp	% Diff	With Trans Exp	Without Trans Exp	% Diff	With Trans Exp	Without Trans Exp	% Diff
Firm Dispatchable Installed Capacity (GW)									
CCGT	0.0	0.0	-	7.1	9.2	29%	57.0	57.0	0%
OCGT	0.0	0.0	-	9.9	5.1	49%	5.0	5.0	0%
CCGT_CCS	0.0	0.0	-	17.0	18.9	12%	0.0	0.0	-
Total	0.0	0.0	-	34.0	33.2	-2%	62.0	62.0	0%
VRE Installed Capacity (GW)									
Wind	117.7	93.2	-21%	66.5	59.2	11%	0.1	0.1	0%
Utility PV	90.1	113.3	26%	56.0	62.0	11%	21.5	21.5	0%
Distr PV	28.1	63.0	124%	17.7	24.9	41%	17.7	17.7	0%
Total	235.9	269.4	14%	140.3	146.1	4%	39.3	39.3	0%
Energy Storage (Li-ion only)									
Power (GW)	50.2	69.3	38%	30.3	33.7	11%	16.0	16.0	0%
Energy (GWh)	797	1,258	58%	116	158	36%	36	36	0%
Transmission Expansion									
Total (GW)	98.4	-	-	55.4	-	-	0.0	-	-
System Cost of Electricity									
Average \$/MWh	86.0	105.9	23%	51.5	54.1	5%	37.9	37.9	0%

Table 6.13: System impacts of enabling intra-regional transmission expansion in the U.S. Northeast. Scenarios show the impacts of allowing transfer capacities to expand vs. restricting transfer capacities to existing levels, on installed power capacity, storage capacity, and SCOE, across a range of CO₂ constraints. Cost assumptions for transmission expansion are defined in Appendix A.

Brown and Botterud (2021) extend this analysis to the entire continental United States. While our analysis applies different cost assumptions and modeling approaches, the trends in the Brown and Botterud (2021) results are important to note because of the continental scope of their analysis and its implications for the impacts of expanding inter-regional transmission on zero-carbon power systems using today's VRE and storage technologies. Incrementally increasing the level of regional coordination (even without adding new transmission capacity) yields system cost savings and reduces the need for generation and storage capacities: SCOE decreases by \$22/MWh between Brown and Botterud's "isolated states" and "existing regional" transmission scenarios, and by \$16/MWh between their "new regional" and "existing inter-regional" transmission scenarios (Figure 6.21). Brown and Botterud's "new regional" transmission scenario corresponds to the assumptions made in the regional studies discussed above in the base case. Allowing new, inter-regional AC transmission within the three U.S. interconnects (Eastern, Western, and Texas) reduces SCOE by \$10/MWh compared to the "existing inter-regional" transmission scenario; allowing new DC transmission between interconnects reduces SCOE by a further \$8/MWh (Figure 6.21).

Since expanded transmission capacity partly substitutes for storage deployment, it follows that increased transmission and greater regional coordination (transmission expansion effectively increases the geographic extent of economic dispatch areas) leads to a decline in optimal storage deployment. The most connected scenario (“new inter-regional transmission across interconnects”) deploys 40% of the energy storage used in the “new regional” transmission scenario and 23% of the energy storage used in the “isolated states” scenario (Figure 6.21).

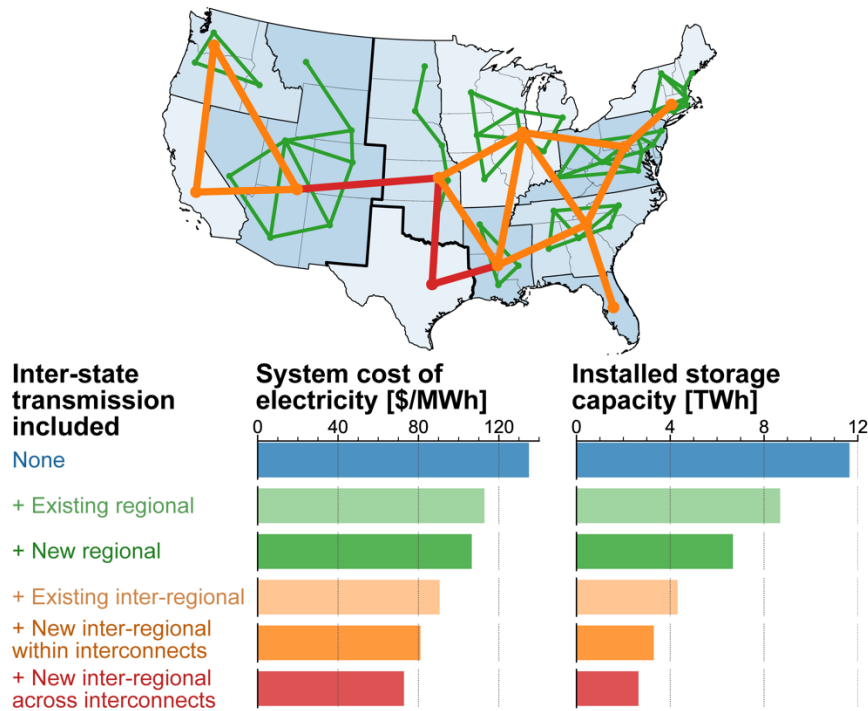


Figure 6.21: System impacts of incrementally expanding regional coordination and transmission capacity in a U.S.-wide context. Scenarios show the impacts on SCOE and optimal storage deployment if the country is modeled as isolated states (blue bars), isolated zones without and with new regional transmission (green bars), and a fully interconnected system with different levels of inter-regional transmission (orange and red bars). Source: (Brown & Botterud, 2021). The transmission assumptions in the regional case study discussed above are most similar to the “new regional” transmission scenario shown here.

Finding: In performing energy market arbitrage—that is, buying when prices (and net demand) are low and selling when prices (and net demand) are high—energy storage can substitute for other grid resources, both on the demand side and on the supply side.

6.3.4 Future Marginal Values of Electrical Energy

Wholesale Energy Price Variability

The modeled system’s time-dependent marginal value of energy³⁸ serves as a proxy for the spot price or locational marginal price in wholesale U.S. power markets organized by regional transmission organizations (RTOs) or independent system operators (ISOs). We study the impact

³⁸ The modeled marginal value of energy in each time period is computed as the dual variable of the hourly supply–demand balance constraint in the capacity expansion model and represents the increase in (minimized) objective function value to serve the next unit of demand. Because the model includes the option of adding new generation, storage, or transmission capacity, the computed marginal value of energy represents the long-run marginal value of electricity rather than the short-run value in which capacity decisions are fixed. Finally, the marginal value of energy computed here does not reflect the impact of short- and long-term capacity requirements that are often included in organized markets to ensure resource adequacy (Levin and Botterud 2015).

of CO₂ constraints and energy storage capacity on the frequency distribution of the marginal value of energy by examining the distribution of the marginal value using the bands shown in Figure 6.22. These bands include the following marginal values: (1) \$0–\$5/MWh, characterized mostly by periods of high VRE generation; (2) \$5–\$50/MWh when natural gas capacity is the marginal generator;³⁹ (3) \$50–\$200/MWh when natural gas capacity needs to be started up and associated start-up costs must be recovered; and (4) >\$200/MWh, which corresponds to scarcity events, including times when storage facilities operate (either charging to dispatch in higher-price periods or discharging based on charging in lower-price periods) and load-shedding events, if any. Because the marginal cost of generation from storage is based on opportunity cost rather than being physically defined, it varies from period to period—consequently, storage charging and discharging can occur in all of the price bands.

Consistent with prior research (Levin and Botterud 2015), we find that increasing VRE penetration leads to many hours of very low prices interspersed with a few periods when prices are very high (approaching the value of lost load, which is assumed to be \$50,000/MWh in our modeling) owing to scarcity events (e.g., high load and low VRE output). Counter-intuitively, the volatility in the price distribution, as measured by the coefficient of variation (CoV), declines with increasing stringency of CO₂ emissions constraints (Table 6.14), since the limited number of high-priced hours increase the unweighted average value. Thus, the level, range, and variation in wholesale spot prices is likely to be drastically different from that seen in RTO/ISO-managed wholesale markets today, as illustrated for Texas in Figure 6.22.⁴⁰

Our findings show a consistent increase in the number of hours at less than \$5/MWh and a consistent decrease in the price band of \$5–\$50/MWh as the CO₂ constraint tightens. These trends reflect an increase in the share of VRE generation and a decline in natural gas generation. Figure 6.22 shows that the \$0–\$5/MWh price band includes up to 62% of hours in the 5 gCO₂/kWh case. As discussed earlier, the 0 gCO₂/kWh case modeled here reflects a strict definition of a net-zero carbon power system—one that relies solely on VRE and storage resources and leads to large increases in both ends of the distribution for the marginal value of generation. Thus, although decarbonization increases the number of hours with near-zero prices, it also increases the number of hours with high prices. This leads to a consistent increase in the mean price as the carbon constraint is tightened.

Our model findings are based on what is effectively a representation of a pure, energy-only electricity market structure, in which all wholesale (and, implicitly, all retail) transactions occur at the spot market price of electricity. While not directly comparable, we pull the most recent available (2019) spot prices from ERCOT and summarize their distribution below. It is clear from Figure 6.22 that the wholesale energy price distribution would change rather dramatically as the Texas system decarbonizes. Our model results imply many more very low-price hours and many

³⁹ When carbon emissions from natural gas generation are penalized, the penalty (the shadow price of carbon emissions) is reflected in the marginal prices when natural gas generators are on the margin. Under stringent CO₂ emissions constraints, natural gas marginal costs, therefore, could be much higher than \$50/MWh and might be responsible for high prices (i.e., \$200/MWh or greater).

⁴⁰ The precise implementation of short- and long-term resource adequacy requirements will impact the volatility of wholesale electricity prices in each region, but the trend of increasing hours of near-zero marginal value of electricity interspersed with high prices, is a robust conclusion supported by other modeling in the literature as well. See for example, (Levin & Botterud, Electricity market design for generator revenue sufficiency with increased variable generation, 2015), (Levin, Kwon, & Botterud, The long-term impacts of carbon and variable renewable energy policies on electricity markets, 2019), and (Ela, et al., 2014).

more high-price hours compared to ERCOT in 2019. We note, however, that we are not trying to model ERCOT in any detail. ERCOT employs market intervention and capacity remuneration mechanisms that may affect price signals. Moreover, the ERCOT energy-only wholesale market model has not been adopted by other RTOs/ISOs in the United States or by grid operators in the European Union. Most U.S. systems also have capacity markets and relatively low price caps on energy markets, which will shift some spot price variation (and revenue variation, as we discuss presently) to capacity prices. Since any system must satisfy break-even constraints, however, total revenues and revenues earned by each technology should, in theory, be unaffected, though the addition of capacity markets may affect the break-even capacity mix.

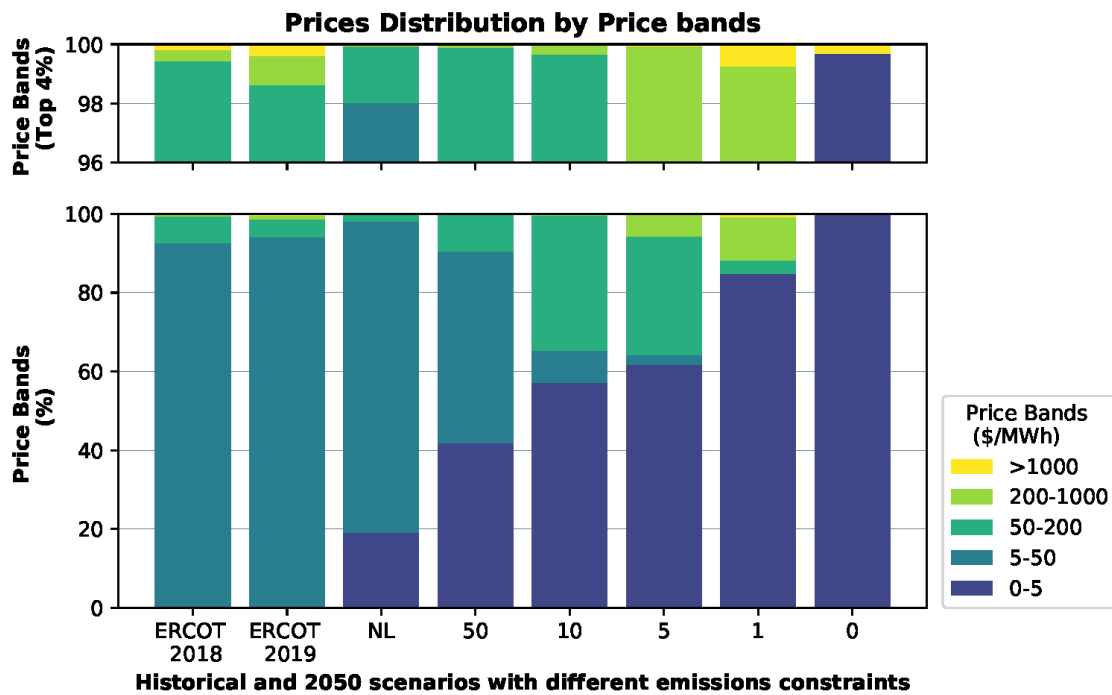


Figure 6.22: Marginal value of energy under base case assumptions (Li-ion battery storage only) for Texas. The price bands are based on the known marginal cost of various generation technologies; we zoom in on the top 4% to show the price distributions at that extreme. Results for the Northeast and Southeast are presented in Appendix D. ERCOT historical prices are from ERCOT (2021).

To illustrate how the marginal value of energy relates to system operation and VRE resource availability, we compare two timeframes in Figure 6.23. The time interval on the left side has high VRE resource availability, which leads to frequent periods of VRE curtailment (shown as the area between VRE potential and served load)—consequently marginal values of energy are near \$0/MWh. Prices of about \$60/MWh are realized when natural gas generation with CCS needs to operate for specific intervals, and peaks of around \$250/MWh are also observed when storage is discharging to meet load. In contrast, the right side of the figure shows a period of low VRE availability, in which gas generation is often needed to meet load requirements that exceed VRE output. When CCGT with CCS is on the margin, price levels are about \$60/MWh. If CCGT without CCS is also needed, prices climb to \$100–\$130/MWh and when OCGT without CCS operates (days 29–30) prices are in the range of \$150–\$180/MWh.

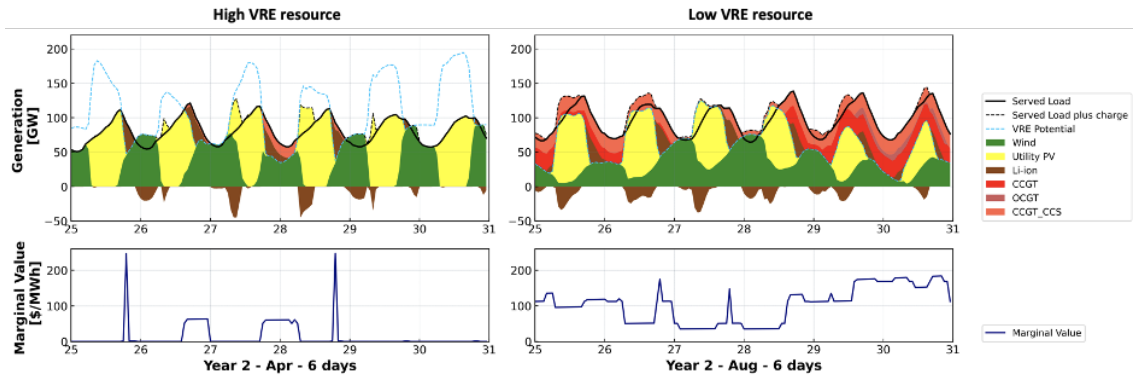


Figure 6.23: System operation and marginal value of energy under Base Case assumptions (Li-ion battery storage only) for Texas at 10 gCO₂/kWh. The figure shows two periods of time with high (left side) and low (right side) VRE resource availability.

Figure 6.24 shows that the cost-optimal deployment of LDES (redox flow batteries plus metal-air batteries, thermal storage, or hydrogen) primarily serves to reduce the frequency of periods when the marginal value of energy is high, i.e., above \$200/MWh, and increases instances of marginal value near or below \$50/MWh. The latter effect is consistent with the reduced VRE curtailment seen with LDES deployment (Figure 6.10). Table 6.14 shows that LDES tends to reduce the unweighted average value of energy while also reducing the volatility of the marginal value of energy, as measured by the CoV, relative to the base case (TM0 in Table 6.14). Across the different CO₂ constraints modeled, volatility decreases by 33% on average compared to the base case when LDES resources are present in the system. While the dispatch of LDES can help to smooth out some fluctuations in the marginal value of energy, the presence of LDES alone does not alter the broader trend of increasing hours with near-zero marginal value of energy and increasing peak prices under tightening CO₂ constraints.

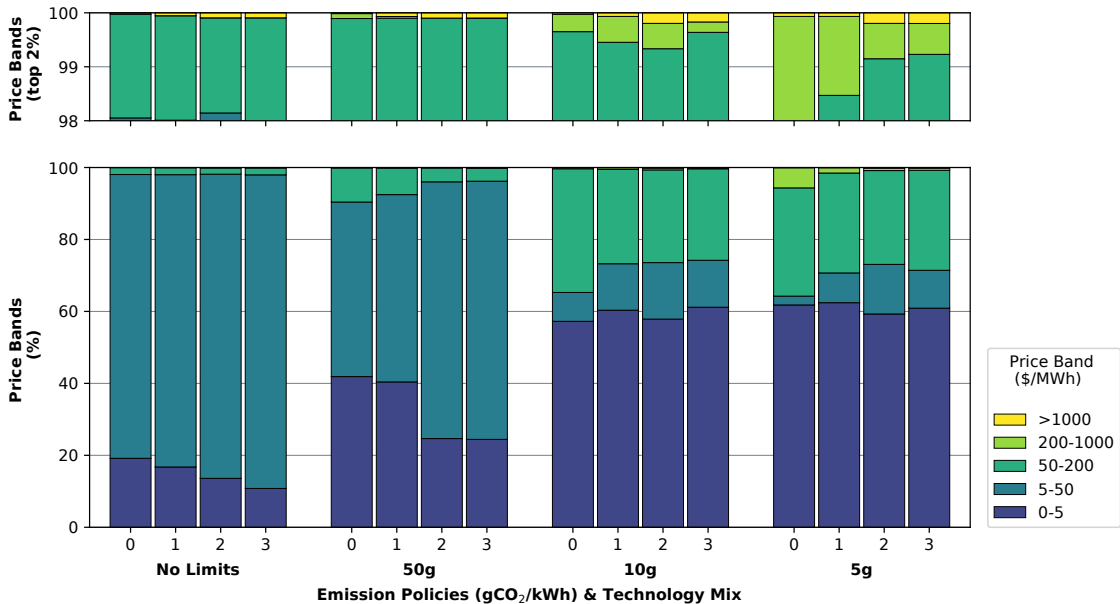


Figure 6.24: Marginal value of energy across different storage mixes for Texas. Scenarios shown are, from left to right: (0) base case (i.e., Li-ion battery storage only), (1) Li-ion + RFB + H₂, (2) Li-ion + RFB + metal-air, and (3) Li-ion + RFB + thermal. The price bands reflect the costs of the marginal technology; we zoom in on the top 2% to show the price distributions at that extreme.

Emission policy (gCO ₂ /kWh)	Unweighted average value of energy				Price volatility (CoV)			
	Base case	TM1	TM2	TM3	Base case	TM1	TM2	TM3
5	42.1	39.6	38.0	37.3	9.8	7.4	6.9	7.7
10	40.5	38.8	37.5	36.8	10.9	7.5	7.0	7.9
50	34.1	34.9	33.4	33.0	17.6	8.8	10.2	11.6
NL	31.0	31.4	31.4	31.3	18.3	12.5	12.3	12.7

Table 6.14: Comparison of the average marginal value of energy (simple average of prices over time) and volatility, as measured by the coefficient of variation (standard deviation divided by mean) for modeled 2050 prices in Texas. For comparison, actual figures for ERCOT in 2019 were \$37.6/MWh for the average value of energy and 4.4 for price volatility (CoV). The technology mixes in the table correspond to (TMO) base case (i.e., Li-ion battery storage only); (TM 1) Li-ion + RFB + H2; (TM 2) Li-ion + RFB + Metal-air; and (TM 3) Li-ion + RFB + Thermal.

Finding: The level, range, and variation in the marginal value of energy in future low-carbon electricity systems will be drastically different than values seen in ISO/RTO-managed wholesale markets today.

Revenue Analysis

In the CEM modeling used here, which involves least-cost linear optimization with perfect foresight and constant returns to scale, all resources just break even, meaning that annual revenues over the modeled period equal annualized investment and operational costs (Junge, Mallapragada, & Schmalensee, 2021). Analyzing system operation and revenue distribution by price bands, we find that different technologies operate at different price bands and earn revenue in different ways, based on the likelihood that a given technology is the marginal resource (Figure 6.25). With more stringent CO₂ constraints, VRE technologies operate more at lower prices and begin to rely on fewer hours of higher prices to earn the revenue required to break even. For example, for wind generation in the 10 and 5 g CO₂/kWh cases, 90% and 96% of revenues come from the 33% and 35% of energy delivered by wind during periods when prices are high (above \$50/MWh), respectively. We find similar results for solar photovoltaics, Li-ion battery storage, and gas generation (OCGT, CCGT, CCGT_CCS), meaning that these resources would need to earn most of their revenue in a handful of hours under an energy-only wholesale power market design. Moreover, optimization ensures full cost recovery in the model because the model assumes perfect foresight of load and VRE availability. In reality, it could be difficult to finance investments in generation and storage assets that have to rely for most of their revenues on a handful of operating hours in any given year.

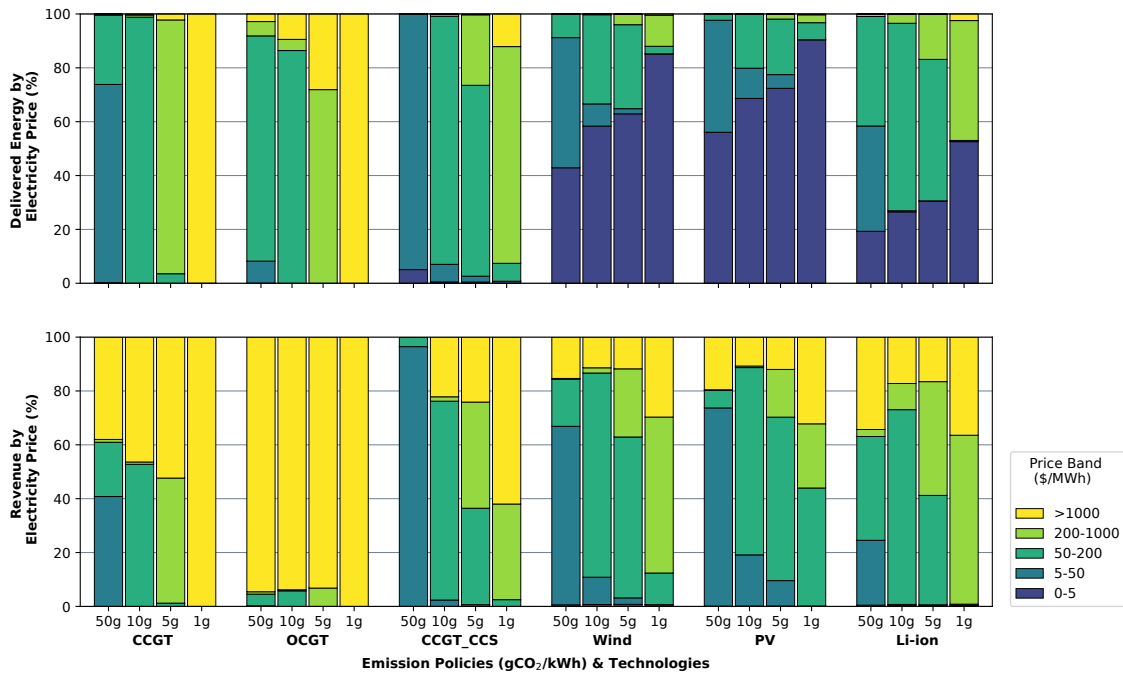


Figure 6.25: Technology operation by price band in Texas – base case. The upper panel shows the distribution of delivered energy by price band for different technologies and emission constraints. The lower panel shows the revenue distribution by price band.

6.4 Conclusion and Key Takeaways

This chapter, detailing the results of our modeling analysis, explores the drivers for adopting energy storage in the transition to low-carbon power systems by 2050. We consider the interplay between storage technology cost and performance attributes and other factors, including the costs of alternative generation technologies, demand growth, demand flexibility, and VRE resource quality, among others. We also examine how varying the stringency of the carbon constraint affects these interactions.

We find that the near-complete decarbonization of power systems (i.e., average emissions intensity of 5 gCO₂/kWh) can be achieved with VRE deployment, in conjunction with available (Li-ion) battery energy storage, along with infrequent use of dispatchable natural generation, with bulk power cost increases of 21% (Texas) to 36% (Northeast) compared to a scenario with no emission limits, without creating reliability issues for hourly grid operations. At the same time, we find that full decarbonization based on deploying VRE and Li-ion storage technologies while ruling out any use of natural gas generation (in other words, targeting “zero” CO₂ emissions rather than “net-zero” emissions) is significantly more expensive at the margin. Put another way, the incremental cost of increasing the share of carbon-free electricity generation⁴¹ from around 90%–93% (as seen in the 5 gCO₂/kWh emission case in Table 6.9) to 100%, via a combination of VRE and Li-ion storage, is quite high. This observation is consistent with findings from other studies modeling zero-carbon power systems based on VRE and Li-ion storage (Cole, et al., 2021; Brown & Botterud, 2021; Sepulveda, Jenkins, de Sisternes, & Lester, 2018). It

⁴¹ As noted in the caption of Table 6.9, carbon-free electricity generation is defined to include VRE, nuclear, and hydro resources, but it excludes generation from CCGT with CCS. Such a definition decreases the perceived level of decarbonization achieved in each case since it does account for the substantially reduced carbon intensity of the remaining generation. See footnote 22 for further discussion.

provides a compelling reason to focus public and private RD&D resources on further improving the cost and performance attributes of a range of technologies, including emerging long-duration energy storage (LDES) technologies, alternative low- or no-carbon generation technologies that are dispatchable, and negative emissions technologies that can remove CO₂ from the atmosphere.

While these broad observations apply across all regions studied here, our modeling reveals significant regional variation in system costs, optimal storage capacity deployment, and optimal generation mix under different emission constraints. The differences primarily reflect differences in the quality of wind and solar resources and thus in the cost of zero-carbon generating technologies in the three regions we examine. Notably, among these regions, the Northeast has the lowest-quality VRE resources and the highest CO₂ emissions under a No Limits policy scenario. Relative to other regions, the Northeast also generally sees the highest system average electricity cost to achieve a given CO₂ emissions goal for the same technological assumptions. That is, without policies that significantly constrain CO₂ emissions, the Northeast would not “naturally” reduce its emissions per unit of electricity generated.⁴² By contrast, Texas, due to its excellent wind and solar resources, sees a significant “natural” reduction in CO₂ per kWh in our modeling without any additional policy interventions, though policy interventions are necessary to get to complete decarbonization of the electricity sector in that state also. The Southeast falls between the Northeast and Texas on these dimensions. In short, the challenges of “getting to zero” vary across regions based on their resource endowments.

Our modeling highlights the multiple impacts of LDES availability on decarbonized power systems, which includes reducing the need for dispatchable generation, lowering the system average cost of electricity, reducing VRE curtailment, and reducing variability in wholesale electricity prices. The strength of these effects depends on LDES cost and performance attributes but also on system factors and on the attributes of other technologies (for example, VRE capital cost and availability). The most important LDES performance parameters (in terms of value to the system) are energy storage capacity cost followed by discharge efficiency—this finding is supported by our modeling as well as by a recent paper that uses the same analytical approach (Sepulveda, Jenkins, Edington, Mallapragada, & Lester, 2021). The latter paper also notes that charge and discharge power capacity costs and charge efficiency are of secondary importance. Similarly, our findings suggest that when LDES is deployed, the cost-optimal storage duration ranges over days rather than weeks or months. Among LDES technology options, we find that hydrogen (and other forms of derived chemical energy storage) offers a unique value proposition if it is produced with electricity and used as a fuel to decarbonize other end-uses, thereby creating a large flexible load that supports VRE integration in the power sector.

The fact that the cost-optimal dispatch of storage, unlike the cost-optimal dispatch of generation resources, cannot be reduced to simplistic merit-order or time-invariant economic principles highlights the increased complexity of actual power system dispatch with significant storage deployment. Whereas our modeling results assume perfect foresight with respect to load and VRE availability in future periods, uncertainty in real-world power system operations (regarding both load and VRE availability) will make optimal storage dispatch more challenging. Thus, there is a need to improve the software tools used for power system dispatch to support cost-efficient

⁴²As noted earlier (in footnote 8), many northeastern states have passed legislation that mandates reductions in economy-wide greenhouse gas (GHG) emissions of at least 80% by 2050, with a few states committing to more ambitious targets. In this context, our “No Limits” policy scenario for the Northeast is mainly a consistent internal benchmark to systematically quantify the impact of other technology or demand drivers that encourage electrification outside the power sector.

utilization of resources like storage as well as demand flexibility and VRE in future low-carbon power systems. In this context, knowledge sharing forums between industry and academia, such as the annual technical conference on improved software organized by the Federal Energy Regulatory Commission (FERC) are noteworthy.⁴³ From the U.S. perspective, recommendation 1 can be implemented by (1) increasing funding for demonstration activities to be undertaken by the Energy Delivery Grid Operations Technology program proposed by DOE's Office of Electricity in its FY22 budget request, and (2) expanding the grid resilience, reliability, and flexibility programs proposed by the Advanced Research Projects Agency–Energy (ARPA–E) to support research and commercialization of software for reliable grid operations.

Our modeling of least-cost power systems and alternative storage technology deployments considered inter-annual and intra-annual variations in VRE availability as well as increased demand from expanded electrification in other sectors of the economy, assuming perfect foresight with respect to future costs and operational conditions. While this approach represents an improvement over previous studies that have explored power and energy system decarbonization pathways (Larson, et al. 2020; Phadke, et al. 2020; Cochran, et al. 2021), it still does not fully address all the factors that will impact the evolution of future low-carbon power systems and the role of energy storage.

First, due to data limitations, we did not model the demand-side impacts of very extreme weather events. Such events, which can affect both electricity demand and supply, are likely to become more important in the future owing to climate change. Thus, further work to characterize weather-driven demand and supply uncertainty would be very useful. Second, for reasons of computational tractability, we had to resort to approximating annual grid operations using representative weeks for two of the study regions (Southeast and Northeast) using multi-zonal grid representation. Collectively, these factors, coupled with our assumption of perfect foresight, mean that our results likely *underestimate* the value of storage and the magnitude of storage deployment that would be cost-effective in low-carbon power systems. Clear opportunities exist to advance understanding of these issues through further data collection, data analysis, and optimal system modeling.

At the same time, other assumptions in our modeling may contribute to results that overestimate the value of storage. First, as is common practice in state-of-art power system planning studies, we ignore use-based degradation of electrochemical storage (instead we account for degradation as a fixed O&M cost related to battery cell replacement). If degradation were included, it might limit the value of these storage resources. Second, our modeling does not consider the availability of bioenergy-based power generation with or without carbon capture or other dispatchable renewable generation sources such as geothermal. If, when, and where such sources become available, their deployment could help minimize the cost impacts of going from near-complete decarbonization to full decarbonization and could significantly reduce the value of LDES. If bioenergy systems with CCS or direct air capture were feasible at reasonable cost, for example, the negative CO₂ emissions that they could produce could make it possible to reach a “net-zero” carbon power system while still allowing for some use of natural-gas-based generation. A few recent studies have shown that access to negative emissions, generated either within or outside the power sector, reduces the value of energy storage technologies in the power sector (Daggash, Heuberger and Dowell 2019; Larson, et al. 2020; Williams, et al. 2021). Finally, our analysis is based on least-cost investment planning for a future year (2050) with corresponding technology cost projections for that year. In reality, VRE

⁴³ FERC convenes this technical conference annually to discuss opportunities to enhance operational efficiency through improved software (FERC, 2021).

and other resource investments will be added incrementally over time, likely leading to higher investment costs than were assumed here. Higher system costs would almost certainly be incurred if the target date for power sector decarbonization is brought forward, say between 2035 and 2050, owing to the cost associated with potentially stranding some existing thermal generation and the reduced opportunity for learning-induced cost reductions in emerging storage technologies. We have not attempted to quantify the cost and system implications of these factors in our analysis.

The discussion in this chapter illustrates the complexity of long-term investment planning aimed at efficiently achieving deeply decarbonized and reliable power systems. It also highlights the importance of fundamental research to advance the state-of-art in models used for investment planning, as well as the need for system operators to continuously review and update their planning approaches to incorporate best-available methodologies. Existing practices for power system planning and reliability assessment in various jurisdictions increasingly recognize the importance of incorporating increased temporal resolution of grid operations as well as inter-annual variability (CPUC 2019; FERC 2021; National Academies of Sciences, Engineering, and Medicine 2021), but these are only two of several factors to be addressed. As the grid outages that occurred in Texas in February 2021 highlighted, system planning needs to account more effectively for variability in demand and supply, especially under extreme weather events, and for correlations between the supplies from individual generators in the portfolio and between total generator output and demand. This variability is likely to increase with climate change, and recent studies have highlighted its impacts on grid operations and planning (Ralston Fonseca, et al. 2021; Steinberg, et al. 2020). Demand response and demand flexibility, as well as distributed energy resources, also can play an important role and deserve much more attention than we were able to give them in this analysis. Similar to other CEM studies (Mai, et al., 2018), our modeling assumes inelastic demand that is either very responsive to economic signals, such as when modeling demand flexibility from certain end-uses (e.g., electric vehicle charging), or completely inflexible. This representation overlooks the potential for differentiated consumer responses (flexibility as well as elasticity) to economic signals noted in empirical research; it also does not consider potential behavioral changes caused by the adoption of new technologies. While our modeling shows that increased demand flexibility generally tends to reduce storage needs and costs, understanding the impact of demand flexibility on storage needs and grid operations in practice requires further analysis and efforts to model the realistic responses of different customer classes. Another aspect of electricity demand that is not considered here concerns the relative merits of electrification vs. other approaches for decarbonizing end-use sectors that currently rely on fossil fuels (e.g., industry). As shown by our case study of industrial hydrogen demand in Texas, technological approaches to decarbonizing these end-uses can directly affect cost-effective decarbonization pathways for the electricity sector. This suggests that integrated energy systems analysis—not just electricity systems analysis—would be essential to understand the costs and benefits of technology choices in the electricity sector from the perspective of economy-wide decarbonization.

Finally, our modeling points to increased variability in the marginal value of energy, used here as a proxy for wholesale energy prices in an energy-only wholesale market, in future low-carbon electricity systems. This creates challenges for financing investments since, although assets recover costs under assumptions of perfect foresight for purposes of the modeling analysis, in reality, the risk of negative returns is high when many assets generate the dominant portion of their overall revenues from just a handful of operating hours in the year. As discussed in Chapter 8, this potential for increased price variability also points to the value of retail rate reform that can encourage electrification by enabling flexible consumers to increase demand in the many hours in which the social marginal cost of electricity is at or close to zero. This issue impacts all

resources, including energy storage, and points to the need for electricity market reforms, which are the focus of Chapter 8.

Key takeaways based on the findings from our modeling analysis and from the discussion in this chapter are summarized below (recommendations for future work in this area appear in italics):

- Near-complete decarbonization of electricity systems appears feasible, from an hourly energy supply and demand balance perspective, using renewables, natural gas, and lithium-ion battery storage alone, without creating significant reliability issues or very large increases in system average cost.
- In the absence of any CO₂ constraint on the power sector, the three U.S. regions studied here (Texas, the Northeast, and the Southeast) achieve very different CO₂ emission intensities for the same 2050 technology cost assumptions. These differences primarily result from regional variations in renewable resource quality and load profiles.
- With lower energy capacity costs and lower round-trip efficiency compared to lithium-ion battery technology, long-duration energy storage has the greatest impacts on electricity system decarbonization when natural gas generation without carbon capture and sequestration (CCS) is not an option. Generally, LDES, when optimally deployed, substitutes for natural gas capacity, increases the value of variable renewable (VRE) generation, and produces moderate reductions in system average electricity cost.
- When it is cost-optimal to deploy multiple storage technologies, the technologies with the lowest capital cost of energy storage capacity are generally best suited to provide long-term storage. However, while optimal generation dispatch is determined by roughly constant marginal costs, optimal storage operation is driven by the changing and unobservable shadow values of stored energy. As a result, all storage technologies deployed will operate with charge/discharge cycles of various durations. Simplified assessments of storage economics based on stylized charge/discharge profiles overlook such dynamics and may provide inaccurate assessments of storage value.
- In performing energy market arbitrage—that is, buying when prices (and net demand) are low and selling when prices (and net demand) are high—energy storage can substitute for other grid resources, both on the demand side and on the supply side.
- The level, range, and variation in the marginal value of energy in future low-carbon electricity systems will be drastically different than values seen in ISO/RTO-managed wholesale markets today.
- Our results highlight the multi-dimensional value of long-duration energy storage to decarbonized power systems. However, the presence of significant storage capacity also greatly increases the complexity of cost-optimal power system dispatch, especially under real-world conditions of imperfect information about load and VRE availability in future time periods.
- Improved modeling and software tools are needed to accurately represent the inter-temporal complexity introduced by extensive deployment of storage as well as demand-side resources in future high-VRE electricity systems. *The U.S Department of Energy, in cooperation with ISO/RTOs, state regulators and other institutions, should support*

fundamental research and demonstration projects to accelerate the development and deployment of advanced software tools for enabling cost-efficient grid operations.

- Scalable methodologies are also needed to model the least-cost planning and dispatch of future low-carbon electricity systems while considering imperfect information about future costs, resource availability, wholesale market prices, and demand. *The U.S. Department of Energy, in cooperation with ISO/RTOs, state regulators and other institutions, should support research to develop such methodologies.*
- Our findings with respect to increased price variability in decarbonized electricity systems—specifically, the potential for many hours of very low or zero marginal energy value but a small number of hours with very high value—also point to increased challenges for financing future investments in grid assets, including storage. This issue impacts all resources and underscores the need for thoughtful electricity market reforms and retail rate design to encourage efficient economy-wide decarbonization.

Bibliography

- Black, J. (2021). *Final 2021 PV Forecast*.
- Brinkman, G., Novacheck, J., Bloom, A., & McCalley, J. (2020). *Interconnection Seams Study*. Golden, CO: National Renewable Energy Laboratory.
- Brown, M., Cole, W., Eurek, K., Becker, J., Bielen, D., Chernyakhovskiy, I., . . . Mai, T. (2020). *Regional Energy Deployment System (ReEDS) Model Documentation Version 2019*. Golden, CO: National Renewable Energy Laboratory.
- Brown, P. R., & Botterud, A. (2021). The value of inter-regional coordination and transmission in decarbonizing the US electricity system. *Joule*, 115-134.
- Brown, T., & Reichenberg, L. (2021). Decreasing market value of variable renewables can be avoided by policy action. *Energy Economics*.
- Brown, T., Hörsch, J., & Schlachtberger, D. (2018). PyPSA: Python for Power System Analysis. *Journal of Open Research Software*.
- Buongiorno, J., Corradini, M., Parsons, J., & Petti, D. (2018). *The future of nuclear energy in a carbon-constrained world: An interdisciplinary MIT Study*.
- Cochran, J., Denholm, P., Mooney, M., Steinberg, D., Hale, E., Heath, G., . . . Jain, H. (2021). *Los Angeles 100% Renewable Energy Study (LA100)*. Golden, CO: National Renewable Energy Laboratory.
- Cole, W. J., Greer, D., Denholm, P., Frazier, A. W., Machen, S., Mai, T., . . . Baldwin, S. F. (2021). Quantifying the challenge of reaching a 100% renewable energy power system for the United States. *Joule*.
- Cole, W., & Frazier, A. W. (2020). *Cost Projections for Utility-Scale Battery Storage: 2020 Update*. Golden, CO: National Renewable Energy Laboratory.
- Cole, W., Frew, B., Mai, T., & Sun, Y. (2017). *Variable Renewable Energy in Long-Term Planning Models: A Multi-Model Perspective*. NREL.
- CPUC. (2019). *Unified Resource Adequacy and Integrated Resource Plan Inputs and Assumptions: Guidance for Production Cost Modeling and Network Reliability Studies*. California Public Utilities Commission.
- Daggash, H. A., Heuberger, C. F., & Dowell, N. M. (2019). The role and value of negative emissions technologies in decarbonising the UK energy system. *International Journal of Greenhouse Gas Control*, 181-198.
- Darghouth, N. R., Barbose, G., Zuboy, J., Gagnon, P. J., Mills, A. D., & Bird, L. (2020). Demand charge savings from solar PV and energy storage. *Energy Policy*.
- DNV GL. (2017). *Safety, operation and performance of gridconnected energy storage systems*.
- DOE. (2017). *Staff Report to the Secretary on Electricity Markets and Reliability*.
- Draxl, C., Clifton, A., Hodge, B.-M., & McCaa, J. (2015, 8). *The Wind Integration National Dataset (WIND) Toolkit*. Retrieved from <https://linkinghub.elsevier.com/retrieve/pii/S0306261915004237>
- EIA. (2020). *Annual Electric Power Industry Report, Form EIA-861 detailed data files*. Retrieved from <https://www.eia.gov/electricity/data/eia861/>
- EIA. (2020). *Battery Storage in the United States: An Update on Market Trends*.
- EIA. (2020, June 3). *Form EIA-860 detailed data with previous form data (EIA-860A/860B)*. Retrieved from <https://www.eia.gov/electricity/data/eia860/>
- EIA. (2021, June 11). *Form EIA-923 detailed data with previous form data (EIA-906/920)*. Retrieved from <https://www.eia.gov/electricity/data/eia923/>
- EIA. (2021). *Independent Statistics and Analysis*. Retrieved from <https://www.eia.gov/outlooks/aeo/data/browser/>
- EIA. (2021, March 26). *Net Generation by State by Type of Producer by Energy*. Retrieved from Electricity Data: <https://www.eia.gov/electricity/data/state/>
- EIA. (2021). *Open Data*. Retrieved 6 2021, from <https://www.eia.gov/opendata/>

- EIA. (2021, March 26). *U.S. Electric Power Industry Estimated Emissions by State*. Retrieved from Electricity Data: <https://www.eia.gov/electricity/data/state/>
- EIA. (2021). *U.S. Nuclear Generation and Generating Capacity*. Retrieved from Nuclear & Uranium: <https://www.eia.gov/nuclear/generation/>
- EIA. (2021, May 14). *What are U.S. energy-related carbon dioxide emissions by source and sector?* Retrieved June 3, 2021, from <https://www.eia.gov/tools/faqs/faq.php?id=75&t=11>
- Ela, E., Milligan, M., Bloom, A., Botterud, A., Townsend, A., & Levin, T. (2014). *Evolution of Wholesale Electricity Market Design with Increasing Levels of Renewable Generation*. Golden, CO: National Renewable Energy Laboratory.
- EPA. (2018). *Documentation for EPA's Power Sector Modeling Platform v6 Using the Integrated Planning Model*. Washington DC: U.S. Environmental Protection Agency.
- EPA. (2021). *Inventory of U.S. Greenhouse Gas Emissions and Sinks: 1990-2019*. Environmental Protection Agency.
- EPA's Clean Air Markets Division. (2018). *Documentation for EPA's Power Sector Modeling Platform v6 Using the Integrated Planning Model*. Washington DC: U.S. Environmental Protection Agency.
- EPRI and RFF. (2017). *Systems Analysis in Electric Power Sector Modeling: Evaluating Model Complexity for Long-Range Planning*. Palo Alto: Electric Power Research Institute and Resources for the Future.
- ERCOT. (2021). *Historical RTM Load Zone and Hub Prices*. Retrieved May 2021, from <http://mis.ercot.com/misapp/GetReports.do?reportTypeId=13061&reportTitle=Historical%20RTM%20Load%20Zone%20and%20Hub%20Prices&showHTMLView=&mimicKey>
- Fajardy, M., Morris, J., Gurgel, A., Herzog, H., Dowell, N. M., & Paltsev, S. (2021). The economics of bioenergy with carbon capture and storage (BECCS) deployment in a 1.5 °C or 2 °C world. *Global Environmental Change*, 102262.
- FERC. (2021). *Increasing Efficiency through Improved Software*. Retrieved June 2021, from <https://www.ferc.gov/industries-data/electric/power-sales-and-markets/increasing-efficiency-through-improved-software>
- Gamesa. (2017). *G126-2.5 MW*. Retrieved from <https://docplayer.net/24040007-Gamesa-gmw-greater-energy-produced-from-low-wind-sites-minimum-power-density-improved-coe-maximum-profitability.html>
- He, G., Mallapragada, D. S., Bose, A., Heuberger, C. F., & Gençer, E. (2021). Sector coupling via hydrogen to lower the cost of energy system decarbonization. *Energy & Environmental Science*, 14, 4635-4646. Retrieved from <https://pubs.rsc.org/en/content/articlelanding/2021/ee/d1ee00627d>
- Heuberger, C. F., Staffell, I., Shah, N., & Dowell, N. M. (2017). A systems approach to quantifying the value of power generation and energy storage technologies in future electricity networks. *Computers & Chemical Engineering*, 247-256.
- Holmgren, W. F., Hansen, C. W., & Mikofski, M. A. (2018). *pvlip python: a python package for modeling solar energy systems*. Retrieved from <http://joss.theoj.org/papers/10.21105/joss.00884>
- Hulbert, D., Chernyakhovskiy, I., & Cochran, J. (2016). *Renewable Energy Zones: Delivering Clean Power to Meet Demand*. Golden, CO: National Renewable Energy Laboratory. Retrieved from <https://www.nrel.gov/docs/fy16osti/65988.pdf>
- IEA. (2019). *The Future of Hydrogen: Seizing Today's Opportunities*.
- IEA. (2021). *Global Energy Review 2021: CO2 Emissions*. Retrieved June 2021, from <https://www.iea.org/reports/global-energy-review-2021/co2-emissions>
- IEA. (2021). *Net Zero by 2050: A Roadmap for the Global Energy Sector*.
- ISO New England. (2020). *2018 ISO New England Electric Generator Air Emissions Report*. Holyoke, MA: ISO New England, Inc.

- Jafari, M., Botterud, A., & Sakti, A. (2020). Estimating revenues from offshore wind-storage systems: The importance of advanced battery models. *Applied Energy*, 115417.
- Jenkins, J., & Sepulveda, N. (2017). Enhanced Decision Support for a Changing Electricity Landscape: The GenX Configurable Electricity Resource Capacity Expansion Model. *MIT Energy Initiative Working Paper*.
- Jenkins, J., Ponciroli, R., Vilim, R., Ganda, F., Sisternes, F., & Botterud, A. (2018). The benefits of nuclear flexibility in power system operations with renewable energy. *Applied Energy*, 872-884.
- Johnston, J., Henriquez-Auba, R., Maluenda, B., & Fripp, M. (2019). Switch 2.0: A modern platform for planning high-renewable power systems. *SoftwareX*, 100251.
- Junge, C., Mallapragada, D., & Schmalensee, R. (2021). Energy Storage Investment and Operation in Efficient Electric Power Systems. *MIT CEEPR Working Paper*, 1-48.
- Kotzur, L., Markewitz, P., Robinius, M., & Stolten, D. (2018). Time series aggregation for energy system design: Modeling seasonal storage. *Applied Energy*, 213, 123-135. Retrieved from <https://www.sciencedirect.com/science/article/abs/pii/S0306261918300242>
- Kuepper, L. E., Teichgraeber, H., & Brandt, A. R. (2020). Capacity Expansion: A capacity expansion modeling framework in Julia. *Journal of Open Source Software*, 2034.
- Larson, E., Greig, C., Jenkins, J., Mayfield, E., Pascale, A., Zhang, C., . . . Socolow, R. (2020). *Net-Zero America: Potential Pathways, Infrastructure, and Impacts (Interim Report)*. Princeton, NJ: Princeton University.
- Levin, T., & Botterud, A. (2015). Electricity market design for generator revenue sufficiency with increased variable generation. *Energy Policy*, 392-406.
- Levin, T., Kwon, J., & Botterud, A. (2019). The long-term impacts of carbon and variable renewable energy policies on electricity markets. *Energy Policy*, 53-71.
- Mai, T., Barrows, C., Lopez, A., Hale, E., Dyson, M., & Eureka, K. (2015). *Implications of Model Structure and Detail for Utility Planning: Scenario Case Studies Using the Resource Planning Model*. Golden, CO: National Renewable Energy Laboratory. Retrieved from <https://www.nrel.gov/docs/fy15osti/63972.pdf>
- Mai, T., Jadun, P., Logan, J., McMillan, C., Muratori, M., Steinberg, D., . . . Nelson, B. (2018). *Electrification Futures Study: Scenarios of Electric Technology Adoption and Power Consumption for the United States*. Golden, CO: National Renewable Energy Laboratory.
- Mallapragada, D. S., Papageorgiou, D. J., Venkatesh, A., Lara, C. L., & Grossmann, I. E. (2018). Impact of model resolution on scenario outcomes for electricity sector system expansion. *Energy*, 1231-1244.
- Mallapragada, D. S., Sepulveda, N. A., & Jenkins, J. D. (2020). Long-run system value of battery energy storage in future grids with increasing wind and solar generation. *Applied Energy*, 115390.
- Massachusetts Executive Office of Energy and Environmental Affairs. (2021). *GWSA Implementation Progress*. Retrieved June 2021, from <https://www.mass.gov/service-details/gwsa-implementation-progress>
- McMahon, J. (2021, January 8). *NET Power CEO Announces Four New Zero-Emission Gas Plants Underway*. Retrieved 2021, from <https://www.forbes.com/sites/jeffmcmahon/2021/01/08/net-power-ceo-announces-four-new-zero-emission-gas-plants-underway/?sh=3b4e9e86175b>
- McMillan, C. (2019, November 14). *2018 Industrial Energy Data Book*. Retrieved March 21, 2021, from <https://data.nrel.gov/submissions/122>
- MITEI and Princeton University. (2021). *GenX*. Retrieved from <https://energy.mit.edu/genx/#publications>
- MITEI and Princeton University. (2021). *GitHub: GenX Project*. Retrieved June 2021, from <https://github.com/GenXProject/GenX>
- National Academies of Sciences, Engineering, and Medicine. (2021). *The Future of Electric Power in the United States*. Washington, DC: The National Academies Press.

- National Renewable Energy Laboratory (NREL). (2020). *Electricity Annual Technology Baseline (ATB) Data Download*. Retrieved from <https://atb-archive.nrel.gov/electricity/2020/data.php>
- National Renewable Energy Laboratory (NREL). (2021). *NSRDB Data Viewer*. Retrieved from https://maps.nrel.gov/nsrdb-viewer/?aL=x8Cl3i%255Bv%255D%3Dt%26Jea8x6%255Bv%255D%3Dt%26Jea8x6%255Bd%255D%3D1%26VRLt_G%255Bv%255D%3Dt%26VRLt_G%255Bd%255D%3D2%26mcQtmw%255Bv%255D%3Dt%26mcQtmw%255Bd%255D%3D3&bL=clight&cE=0&IR=0&mC=4.740675384778373%2C22.8515
- Neubauer, J., & Simpson, M. (2015). *Deployment of Behind-The-Meter Energy Storage for Demand Charge Reduction*. Golden, CO: National Renewable Energy Laboratory.
- New York ISO. (2020). *2020 Load & Capacity Data*. Rensselaer, NY: NYISO.
- NREL ATB. (2019). *Regional CAPEX Parameter Variations and Adjustments*. Retrieved June 2021, from <https://atb.nrel.gov/electricity/2019/regional-capex.html>
- NYSERDA. (2021, January 26). *Governor Cuomo Announces More Than \$17 Million to Help Communities Drive High Impact Clean Energy Actions and Combat Climate Change*. Retrieved June 2021, from <https://www.nysersda.ny.gov/About/Newsroom/2021-Announcements/2021-01-26-Governor-Cuomo-Announces-More-Than-17-Million-to-Help-Communities-Drive-High-Impact-Clean-Energy-Actions-and-Combat-Climate-Change>
- Oak Ridge National Laboratory. (2020). *Existing Hydropower Assets Plant Dataset, 2020*. Retrieved 2020, from <https://hydrosourc.ornl.gov/dataset/existing-hydropower-assets-plant-dataset-2020>
- Palmintier, B. S. (2013). Incorporating operational flexibility into electric generation planning: Impacts and methods for system design and policy analysis. *MIT Thesis*.
- Pfeifenberger, J. (2021). *Transmission Planning and Benefit-Cost Analyses*. Boston, MA: The Brattle Group.
- Phadke, A., Paliwal, U., Abhyankar, N., McNair, T., Paulos, B., Wooley, D., & O'Connell, R. (2020). *The 2035 Report*. Berkeley, CA: Goldman School of Public Policy, UC Berkeley.
- Poncelet, K., Delarue, E., & D'haeseleer, W. (2020). Unit commitment constraints in long-term planning models: Relevance, pitfalls and the role of assumptions on flexibility. *Applied Energy*.
- Ralston Fonseca, F., Craig, M., Jaramillo, P., Bergés, M., Severnini, E., Loew, A., . . . Yearsley, J. (2021). Effects of Climate Change on Capacity Expansion Decisions of an Electricity Generation Fleet in the Southeast U.S. *Environmental Science & Technology*, 2522-2531.
- Sakti, A., Gallagher, K. G., Sepulveda, N., Uckun, C., Vergara, C., de Sisternes, F. J., . . . Botterud, A. (2017). Enhanced representations of lithium-ion batteries in power systems models and their effect on the valuation of energy arbitrage applications. *Journal of Power Sources*, 279-291.
- Sepulveda, N. A., Jenkins, J. D., de Sisternes, F. J., & Lester, R. K. (2018). The role of firm low-carbon electricity resources in deep decarbonization of power generation. *Joule*, 2403-2420.
- Sepulveda, N. A., Jenkins, J. D., Edington, A., Mallapragada, D. S., & Lester, R. K. (2021). The design space for long-duration energy storage in decarbonized power systems. *Nature Energy*, 1-11.
- Steinberg, D., Mignone, B., Macknick, J., Sun, Y., Eurek, K., Badger, A., . . . Averyt, K. (2020). Decomposing supply-side and demand-side impacts of climate change on the US electricity system through 2050. *Climatic Change*, 125-139.
- Sunny, N., Mac Dowell, N., & Shah, N. (2020). What is needed to deliver carbon-neutral heat using hydrogen and CCS? *Energy & Environmental Science*, 13, 4204-4224.
- Szilard, R., Sharpe, P., Kee, E., Davis, E., & Grecheck, E. (2017). *Economic and Market Challenges Facing the U.S. Nuclear Commercial Fleet - cost and revenue study*.

- U.S. Department of Energy. (2016). *Hydropower Vision: A new chapter for America's 1st Renewable Electricity Source*. Washington, DC: U.S. Department of Energy.
- U.S. Department of Energy. (2018). *Hydropower Vision*. Oak Ridge, TN: Office of Scientific and Technical Information.
- U.S. DOE, Office of Energy Efficiency & Renewable Energy. (2019). *2018 Industrial Energy Data Book*.
- Weiland, N., & White, C. (2019). *Performance and Cost Assessment of a Natural Gas-Fueled Direct sCO₂ Power Plant*. Pittsburgh, PA: National Energy Technology Laboratory. Retrieved from [https://www.netl.doe.gov/projects/files/Performance%20and%20Cost%20of%20a%20NG-Fueled%20Direct%20sCO₂%20Plant.pdf](https://www.netl.doe.gov/projects/files/Performance%20and%20Cost%20of%20a%20NG-Fueled%20Direct%20sCO2%20Plant.pdf)
- Williams, J. H., Jones, R. A., Haley, B., Kwok, G., Hargreaves, J., Farbes, J., & Torn, M. S. (2021). Carbon-neutral pathways for the United States. *AGU Advances*.
- Wiser, R., & Bolinger, M. (2018). *2018 Wind Technologies Market Report*. Oak Ridge, TN: Office of Scientific and Technical Information.

Appendix

Appendix A. Cost and Operational Assumptions

Transmission. Existing inter-zonal transfer capacity is approximated from the EPA Integrated Planning Model (IPM) model (EPA, 2018). The IPM model uses a selection of 64 regions based on North American Electric Reliability Corporation (NERC) regions, which represents fractions of states. We follow these zonal definitions to get the aggregate transfer capacities between zones within each region. Existing transmission capacity is assumed to be available at no cost in our modeling. When transmission expansion is enabled, new capacities can be added along the existing network paths. Transmission upgrades on 345 kV lines (U.S. Northeast and Texas) are assumed to be \$1,670/MW-km; upgrades on 500 kV for the Southeast are assumed to be \$960/MW-km (Brown, Cole, et al. 2020).⁴⁴

Brownfield Capacity. We assume a mainly greenfield modeling of the U.S. Northeast, Southeast, and Texas, apart from existing hydropower in all regions and nuclear capacity in the Southeast. For existing hydropower generators, we classify individual plants into run-of-river (ROR) or reservoir generators using the ORNL HydroSource database (Oak Ridge National Laboratory, 2020). ROR generators are modeled as must-run or non-dispatchable resources that do not have the ability to spill water (i.e., they do not respond to economic dispatch). Hydro reservoir generators are modeled as storage devices that receive exogenous inflows to their storage reservoirs, but cannot charge from the grid. We get hydropower generators' installed capacities from Form EIA-860 (EIA, 2020), and historical monthly generation from Form EIA-923 (EIA, 2021), then aggregate them up to the zonal level.

In the Southeast, we assume that a portion of the existing fleet of nuclear generators will remain operational in 2050. That is, based on each generator's start date, we assume that plants that could run to 2055 or beyond with a second life extension license (80 years from start date) are available. These include Vogtle 3 and 4 (with a combined capacity of 2,500 MW), which are still under construction in Georgia (see Table A- 1).

In the Northeast, we enforce a minimum build for distributed solar PV to reflect existing policies.⁴⁵ The minimum build is based on a projection of new capacity installed through 2050 (i.e., not including existing capacity, see Table A- 2). For states in ISO-NE, the projections are extrapolated to 2050 using the implied EIA Annual Energy Outlook 2030–2050 growth factor of 110%. For zones in the New York ISO, the projections are directly taken and aggregated from the 2020 Gold Book (New York ISO, 2020).

⁴⁴ Distances between zones are measured as the shortest distance between the urban areas of the respective zones.

⁴⁵ As discussed in the main text, distributed PV is always more expensive than utility-scale PV; therefore, the model would not choose to optimally build distributed PV endogenously, unless there are transmission constraints that prevent other forms of intra-zonal generation.

EIA Plant-Generator	EIA Nameplate Capacity (MW)	EIA Start Date	Date Entering Extended Operations
Browns Ferry_3	1,190	3/1/1977	7/2/2016
Brunswick Nuclear_1	1,002	3/1/1977	9/8/2016
Catawba_1	1,205	6/1/1985	12/5/2023
Catawba_2	1,205	8/1/1986	12/5/2023
Edwin I Hatch_2	865	9/1/1979	6/13/2018
Grand Gulf_1	1,440	7/1/1985	11/2/2024
Harris_1	951	5/1/1987	10/24/2026
Joseph M Farley_1	888	12/1/1977	6/25/2017
Joseph M Farley_2	888	7/1/1981	3/31/2021
McGuire_1	1,220	9/1/1981	6/12/2021
McGuire_2	1,220	3/1/1984	3/3/2023
Sequoyah_1	1,221	7/1/1981	9/17/2020
Sequoyah_2	1,221	6/1/1982	9/15/2021
St Lucie_1	1,080	5/1/1976	3/1/2016
St Lucie_2	1,080	6/1/1983	4/6/2023
V C Summer_1	1,030	1/1/1984	8/6/2022
Vogtle_1	1,160	5/1/1987	1/16/2027
Vogtle_2	1,160	5/1/1989	2/9/2029
Vogtle_3	1,250	1/1/2021	-
Vogtle_4	1,250	1/1/2022	-
Watts Bar Nuclear Plant_1	1,270	5/1/1996	-
Watts Bar Nuclear Plant_2	1,270	6/1/2016	-

Table A- 1: Brownfield nuclear capacity in the Southeast. List of nuclear generators that could run to 2055 or beyond with a Second Life Extension License (80 years from start date). Plant-level detail from Form EIA-860.

		Existing Capacity (MWdc)	Cumulative Installations through 2050 (MWdc)	Existing Capacity (MWac)	Cumulative Installations through 2030 (MWac)	Cumulative Installations through 2050 (MWac)	New Installations through 2050 (MWac)
ISO-NE Projections							
[1]	CT	-	-	682.3	1,242.8	2,607.1	1,924.8
[2]	MA	-	-	2,502.3	2,738.2	5,744.1	3,241.8
[3]	ME	-	-	68.8	320.6	672.5	603.7
[4]	NH	-	-	125.3	259.5	544.4	419.1
[5]	RI	-	-	223.8	196.7	412.6	188.8
[6]	VT	-	-	393.5	607.2	1,273.8	880.3
NYISO Projections							
[7]	A	125.0	1,276.0	108.7	-	1,109.6	1,000.9
[8]	B	63.0	371.0	54.8	-	322.6	267.8
[9]	C	169.0	977.0	147.0	-	849.6	702.6
[10]	D	5.0	101.0	4.3	-	87.8	83.5
[11]	E	123.0	974.0	107.0	-	847.0	740.0
[12]	F	299.0	1,168.0	260.0	-	1,015.7	755.7
[13]	G	251.0	705.0	218.3	-	613.0	394.8
[14]	H	34.0	70.0	29.6	-	60.9	31.3
[15]	I	46.0	109.0	40.0	-	94.8	54.8
[16]	J	210.0	791.0	182.6	-	687.8	505.2
[17]	K	537.0	880.0	467.0	-	765.2	298.3

Table A- 2: Rooftop PV minimum build. Assumes a DC-AC ratio of 1.15. Capacities from the ISO-NE Final 2021 PV Forecast (Black, 2021), pp. 23–28, extrapolated to 2050 forecasts using the EIA AEO implied 2030–2050 growth rate of 110%. Source: NYISO 2020 Gold Book (New York ISO, 2020), Table I-9a.

Load. Electricity demand is from the NREL Electrification Futures Study (Mai, et al., 2018). These demand data include assumptions around electrification and its impacts on the load profile; they are available on an hourly basis (8,760 hours per year) as well as on a state-by-state basis. The “2050 High-Moderate” profiles are used for the bulk of the study, except for the Reference Electrification scenario, which is based on the “2050 Reference_Moderate” profiles. These profiles reflect different levels of electrification (“High” vs. “Reference” and a “moderate” pace of energy-efficiency improvements). To align these state-based demand data to our IPM-based zonal definitions, we use 2018 utility state-level sales data (Form EIA-861) to allocate fractions of state demand to our defined zones.

GWh	TVA	Carolinas	SOCO	Florida
Tennessee	100.81	0.01	0.00	102.91
Alabama	23.66	0.00	66.62	90.28
North Carolina	0.79	131.74	0.00	138.29
South Carolina	0.00	81.64	0.00	81.64
Georgia	3.40	0.00	136.12	139.87
Florida	0.00	0.00	13.25	238.57
Mississippi	16.29	0.00	11.73	50.39

% Total	TVA	Carolinas	SOCO	Florida
Tennessee	98.0%	0.0%	0.0%	0.0%
Alabama	26.2%	0.0%	73.8%	0.0%
North Carolina	0.6%	95.3%	0.0%	0.0%
South Carolina	0.0%	100.0%	0.0%	0.0%
Georgia	2.4%	0.0%	97.3%	0.2%
Florida	0.0%	0.0%	5.6%	94.4%
Mississippi	32.3%	0.0%	23.3%	0.0%

Table A- 3: Load allocation from states to IPM zones. Utility bundled retail sales by state from Form EIA-861 (EIA 2020). Utility to IPM zonal mapping from EPA IPM model documentation (EIA 2018). SOCO refers to the territory serviced by the Southern Company. TVA refers to the territory serviced by the Tennessee Valley Authority.

VRE Supply Curves. We developed zonal VRE supply curves based on the methodology described in Brown and Botterud (2021). Hourly PV capacity factors are simulated using 2007–2013 weather data from the NREL National Solar Radiation Database (NREL 2021) through the PVLIB model framework (Holmgren, Hansen, & Mikofski, 2018), at a 4 km by 4 km spatial resolution. Hourly wind capacity factors are simulated using the same temporal and spatial resolution using the NREL Wind Integration National Dataset Toolkit (Draxl, Clifton, Hodge, & McCaa, 2015) and power curve data for the commercially available Gamesa:G126/2500 wind turbine (Gamesa, 2017) at 100-meter height. To reduce the spatial resolution of the VRE capacity factor data, we aggregate sites within a zone on the basis of average LCOE (including the cost of interconnecting to the nearest substation). Thus, for each resource and zone, we get a supply curve, with each bin representing increasing resource quality with an associated maximum availability (based on land area), interconnection cost and hourly capacity factor profile.

Generator and Storage Costs. Fossil-powered generation and VRE capital and operational costs are shown in Table 6.5. The gas, nuclear, VRE, and Li-ion costs are taken from the 2020 NREL Annual Technology Baseline 2045 “Mid” cost projections (NREL 2020). “Low” VRE and Li-ion costs are also taken from the NREL ATB for the sensitivity analysis.⁴⁶ Additionally, we apply a small, non-zero VOM for wind, hydropower, and storage to distinguish their dispatch as part of the economic dispatch modeled within GenX – this addition does not meaningfully affect resulting system costs.

For storage, system costs are separated as energy-only components (e.g., battery packs for Li-ion, tanks for LDES), or power-only components (e.g., inverter, interconnection and permitting

⁴⁶ The mid-cost and low-cost Li-ion cost assumptions for 2050 from NREL are broadly consistent with estimates reported in Chapter 2. We chose to use the NREL estimates since they are widely used by other power system modeling studies. See further discussion on Li-ion cost in Chapter 2.

fees, land acquisition costs). Power-only components can further be parsed into charging or discharging power costs, depending on the type of storage technology (see Table 6.2). This separation of function-based costs enables the model to independently vary the energy, discharging power, and charging power capacities of energy storage systems for optimal sizing. Low-, mid-, and high-cost Li-ion estimates are taken from the NREL ATB 2050 cost projections (NREL 2020); cost projections for other storage technologies are from the analysis described in the technology-focused chapters of this report (see Table 6.3).

Operations and Fuel Assumptions. Operational assumptions for gas- and nuclear-powered generators are from best-in-class technology in the industry (see Table A- 4). Fuel price assumptions are taken from the EIA AEO 2020 Reference (EIA 2021) 2050 case (see Table A-5).

Tech	Capacity Size (MW)	Start Cost (\$)	Start Cost (\$/MW/start)	Start Fuel (MMBTU/ start)	Start Fuel (MMBTU/ MW/start)	Heat Rate (MMBTU/ MWh)
[1] OCGT	237	33,147	140	45	0.19	9.51
[2] CCGT	573	34,982	61	115	0.20	6.40
[3] CCGT + CCS	377	36,419	97	75	0.20	7.12
[4] Existing Nuclear	1,000	1,000,000	1,000	0	0.00	10.46
[5] New Nuclear	1,000	1,000,000	1,000	0	0.00	10.46

Tech	Min Stable Output (%)	Ramp Up (%)	Ramp Down (%)	Up Time (Hours)	Down Time (Hours)
[1] OCGT	25	100	100	0	0
[2] CCGT	30	100	100	4	4
[3] CCGT + CCS	50	100	100	4	4
[4] Existing Nuclear	50	25	25	36	36
[5] New Nuclear	20	100	100	36	36

Table A- 4: Thermal generator operational characteristics. Compiled from multiple sources: Buongiorno, et al. 2018; Sepulveda, Jenkins and de Sisternes 2018; NREL 2020; GE 2017; Jenkins, et al. 2018.

Fuel	\$/MMBtu
Uranium	0.75
Coal	2.00
Natural Gas	4.16
Coal CCS	2.00
NG + CCS	4.16

Table A-5: Technology-specific fuel prices. Fuel prices from EIA AEO 2020 Reference (EIA 2021) 2050 case. CCS option assumes a \$20-per-metric-ton CO₂ transport and sequestration cost.

Demand Flexibility. As described in the main text, modeling assumptions for simulated demand flexibility are based on the NREL EFS enhanced flexibility scenario, which proposes hours of delay and advance for specific demand subsectors, along with the share of the load that can be shifted (Mai, et al., 2018). Table 6.11 in the main report shows assumptions for how many hours demand in each demand subsector can be advanced or delayed, as well as the maximum hourly demand that can be flexible in Texas. Table A 6 shows the maximum hourly demand flexibility for all three regions. Coincident maximum potential demand flexibility is 37 GW (39% of hourly demand) for the Northeast and 113 GW (37% of hourly demand) for the Southeast; both figures are proportionately higher than the maximum demand flexibility potential (47 GW or 31% of hourly demand) in Texas.

Demand Subsector	Northeast	Southeast	Texas
Commercial HVAC	1.5	3.0	8.6
Residential HVAC	2.0	6.2	7.0
Commercial Water Heating	0.0	0.1	0.2
Residential Water Heating	0.2	0.7	1.0
Light duty vehicles	27.6	79.4	33
Medium duty trucks	1.6	4.6	3.0
Heavy-duty trucks	1.2	6.0	5.0

Table A 6: Non-coincident maximum hourly demand flexibility in GW across the three modeled regions under 2050 load conditions. HVAC = heating, ventilation and air conditioning. Data sourced from NREL Electrification Futures Study (Mai, et al., 2018).

Appendix B. Time Domain Reduction Approach

Capacity expansion models (CEMs) rely on a compact temporal, spatial, and network representation of the system to maintain computational tractability. Traditional CEMs have relied on a time slice approach (e.g., 12 representative days across the year) that is usually based on disaggregating the load duration curve based on seasonal and time-of-day blocks. The intuition of the “time-slice” approach is to represent conditions of system peak, based on the idea that if there is sufficient generating capacity to cover the peak, then reliability can be ensured at all other times too. However, recent studies show that systems with high penetrations of VRE will require increased temporal resolution and operational detail to adequately capture the temporal and spatial dynamics of a highly decarbonized electricity grid. Specifically, with increasing VRE penetration, the system peak “net load” (i.e., the residual load after accounting for VRE generation) is likely to be more important than the system peak load for resource planning purposes.

In this study, we use model hourly grid operations that look to capture intra and inter-annual variability in load and VRE generation. For the Northeast and Southeast case studies, involving multi-zonal representations of the regions, we approximate annual grid operations outcomes based on modeling hourly operations over a set of representative periods that are selected

through a hybrid clustering scheme described below. The use of representative periods via clustering represents an improvement over time-slice approaches since it is based on prevailing variability in all time series, not just load, and since it also allows for preserving chronology in operations as well as inter-period energy transfer in the case of energy storage.

The hybrid clustering employed here to select representative periods is adapted to provide both sufficient temporal resolution and extreme weather coverage. While the clustering procedure seeks to closely approximate the underlying temporal distributions of historical load and VRE capacity factor profiles, the extreme periods selection procedure seeks to incorporate sufficient “reliability” events corresponding to extended periods of low VRE output and high demand (e.g., heat waves, cold snaps). We outline our iterative approach to selecting the periods used in the CEM below (Figure B-1).

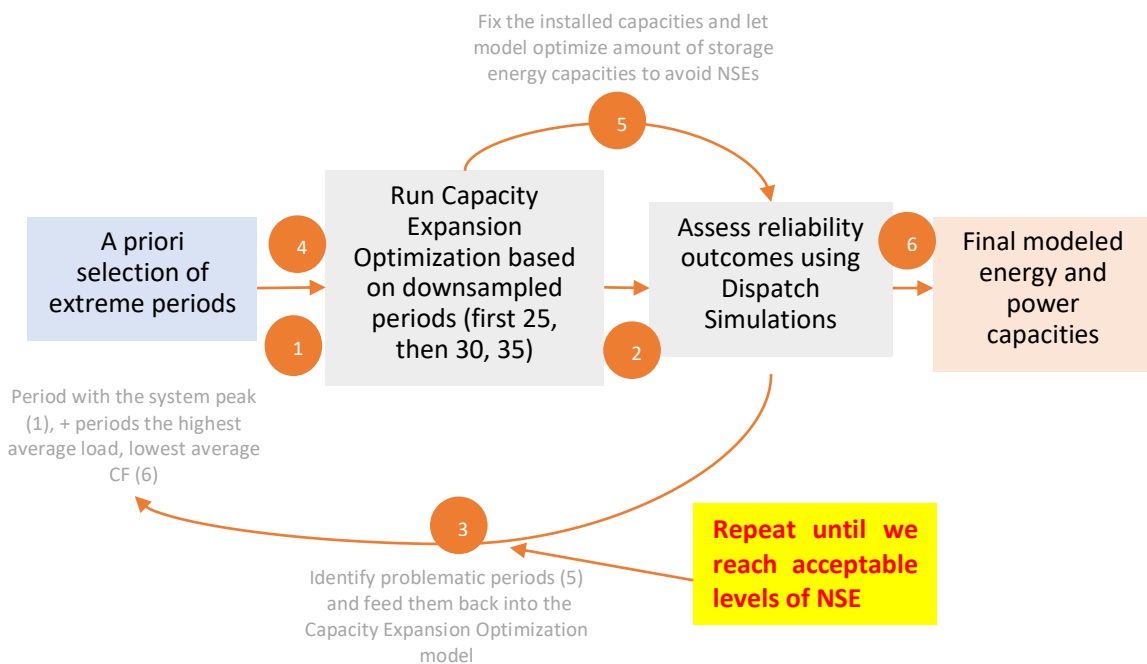


Figure B-1: Hybrid clustering approach used to select representative periods for CEM in the case of the Northeast and Southeast regions. Steps are further described in the text.

Step 1. We slice the zonal load and VRE capacity factor data into 10-day periods. For each period, we calculate average load, solar capacity factor (CF), and wind CF; and identify some “a priori extreme periods,” defined as those periods that have the highest system peak, highest average load, and lowest PV and onshore wind output, at a zonal level. We then stitch together the time series of all resources (solar, onshore wind, hydro) for each period, to create a single concatenated time series for each 10-day period; thus, each vector is of length: 24 hours/day x 10 day/period x 4 time series (load, solar, onshore wind, hydro) x number of modeled zones. Due to overlap between the extreme periods that meet the above criteria, we identify six extreme periods for the Northeast through this process and eight for the Southeast.

Step 2. We employ the *k*-means clustering technique to group the remaining (non-extreme periods, 255.5 equality the number of extreme periods) into 25 clusters. For each cluster, we select the historical period closest to the centroid of the cluster as the most representative period. This is because the centroid of the cluster may not reflect actual conditions that may exist in the system; thus, the most representative periods are indeed based on actual data. We then weigh each representative period based on cluster size, to achieve a total weight of 8,760 hours to approximate annual grid operations. To preserve the system peak, we did not scale the

weighted time series to match the annual load in the original data; this results in a 2%–3% increase in annual load relative to the NREL EFS data.

Step 3. The iterative process starts by inputting the CEM outputs into a simplified production cost model to simulate overall reliability under the proposed portfolios. This process is more effective at identifying periods of great reliability importance, which were not already flagged to be “a priori extreme” or “representative” periods. We call the periods causing the most reliability issues (i.e., frequent and long-lasting non-served energy events), “reliability periods.” We repeat this last step one or two times to ensure that we’re optimizing for system reliability at each hour (i.e., no significant load shedding due to capacity shortages). The threshold we are using is the often-used reliability standard of 1-in-10 years, which we interpret as one day in ten years of involuntary load shedding.

Steps 4–6. After we reach an acceptable level of reliability, we can finalize the selection of representative and extreme periods and interpret the model results (shown in the main report). Step 5 is optional; it can allow the CEM to re-optimize for storage power and energy capacities over the full seven years of weather data once the capacities for the other technologies and transmission have been fixed. We did not end up needing this step.

To test this approach, we assessed reliability outcomes, which we define as the frequency, duration, and magnitude of resulting non-served energy (NSE) events, across multiple model configurations. We start with a simple chronology-based approach that selects 25 periods across one single year of weather data (2012) to resolve the optimal capacity mix (S25-CEM). Then, we consider a suite of chronological C-CEMs resolved over seven years of weather data, while incrementally increasing the number of selected periods (therefore, number of hours the model “sees” to make its investments and dispatch decisions). This corresponds to the 25, 30, and 35 representative periods as annotated in Figure B-1.

Figure B-2 and Figure B-3 show the breakdown of all NSE events. As expected, a CEM based on one year of weather data (S25-CEM) yields a lower level of reliability than one based on multiple years of weather data (C25-CEM), particularly around extended periods of low VRE output (especially with respect to wind, since solar follows a fairly consistent diurnal pattern). We can also see how the individual events break down in terms of their duration (e.g., consecutive hours of NSE) and magnitude (e.g., as a proportion of total system load during each hour). We see that for the Southeast (Figure B-2), moving from the S25-CEM to the C25-CEM configuration decreases total NSE by 12% (or 1,535 GWh) and the total duration of such events by 33% (or 234 hours), across the seven weather years considered. The decrease in frequency of NSE events that last for more than four hours (shown in different shades of green), as well as the frequency of NSE hours with more than 10% of total system load is particularly noteworthy.

The reliability outcomes for the Northeast (Figure B-3) are a bit different in that the frequency of outage events actually seems to increase between S25-CEM and C25-CEM, and between C30-CEM and C35-CEM. Upon closer inspection, however, we can see that the number of severe events (i.e., with duration longer than 12 hours, or shedding more than 25% of hourly load) actually decreases, which is what we would expect. In general, because the Northeast does not have other forms of firm capacity (e.g., existing nuclear) and has poorer VRE resource quality, we'd expect to see more instances of NSE events, relative to the Southeast.

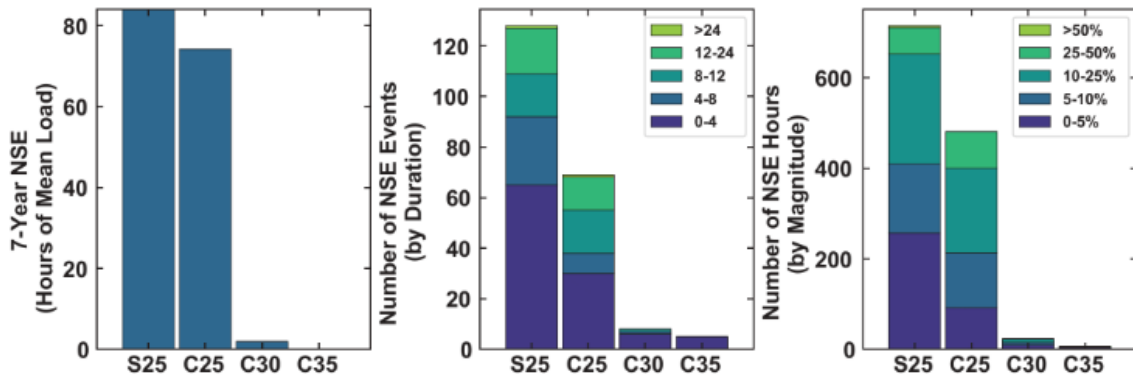


Figure B-2: Reliability outcomes in the Southeast across different model configurations. From left to right: (1) Total magnitude of NSE events across the seven test years, standardized to the system mean load (157.6 GW). (2) Number of NSE events by duration buckets. (3) Number of NSE hours by magnitude (as a percentage of hourly load) buckets.

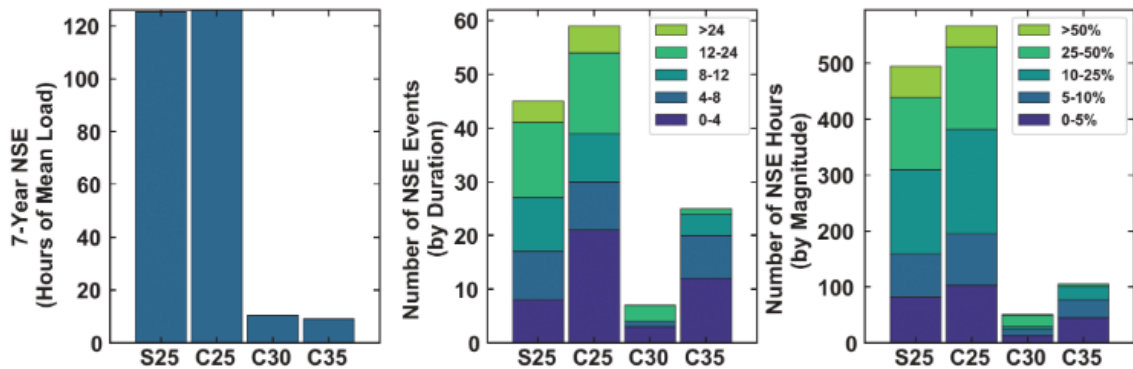


Figure B-3: Reliability outcomes in the Northeast across different model configurations. From left to right: (1) Total magnitude of NSE events across the seven test years, standardized to the system mean load (49.9 GW). (2) Number of NSE events by duration buckets. (3) Number of NSE hours by magnitude (as a percentage of hourly load) buckets.

Most striking in both regions is the large improvement in reliability that comes with the exogenous addition of extreme periods into the initial capacity expansion optimization problem, which allows the model to “see” these extended periods of low VRE output that are particularly prone to reliability issues. Moving from S25-CEM to C35-CEM decreases total NSE by almost 100% in the Southeast and by 93% in the Northeast. It also decreases the total duration of such events by 99% in the Southeast and by 78% in the Northeast. Thus, we have shown that using the proposed methodology, we are able to dramatically reduce the frequency, duration, and magnitude of expected NSE events.

Appendix C. Modeling Hydrogen Demand in Industry and Its Impact on Power Sector Evolution

The configuration of Figure C-1 is included in the GenX model, where along with specifying cost and performance assumptions for the elements as used previously (e.g., electrolyzer, storage tank and gas turbines for hydrogen storage), we add a constraint that requires the specified hydrogen (H₂) demand from industry to be met by either the electrolyzer or by discharging H₂ storage. This single constraint then enables the utilization of a traditional power-to-H₂-to-power storage system to be also optimized, in terms of component sizes and utilization, to meet H₂ demand in the industrial sector.

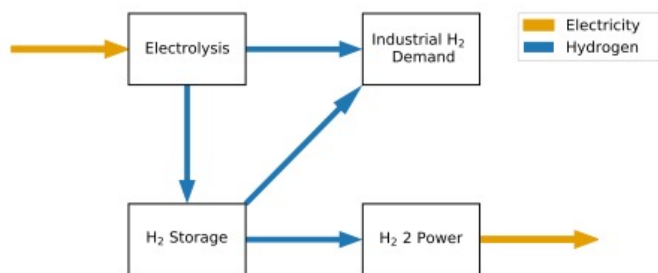


Figure C-1: Representation of the power to H₂ to power system within GenX and hydrogen's use for meeting industrial hydrogen demand.

Since we are primarily interested in understanding impacts on the power system from external H₂ demand, we make the following approximations to simplify the representation of the H₂ supply chain: (1) We ignore potential sources of H₂ supply, such as that produced from natural gas with and without carbon capture to meet this demand. Instead, we vary the H₂ demand from industry that is to be met by electrolyzer-driven H₂ supply and thereby account for the possibility of other sources of H₂ supply. (2) We are not considering any spatial distribution in H₂ production and industrial demand and are thus ignoring H₂ transportation. (3) We are not including source-dependent delivery costs for H₂ supply that could be associated with adjusting the state of delivered H₂ from different sources to meet industrial customer requirements. Other studies have included these factors in the hydrogen supply chain while also contemplating their impacts on the evolution of the power system (He, Mallapragada, Bose, Heuberger, & Gençer, 2021; Sunny, Mac Dowell, & Shah, 2020).

Hydrogen demand is modeled as exogenous and uniform throughout the year. Hydrogen demand was estimated using NREL's 2018 Industrial Data Book as a reference (McMillan, 2019). This publication contains a dataset detailing the annual energy consumed by large energy-using facilities⁴⁷ in 2016. Here, we focus on hydrogen demand from substituting for the use of natural gas for heating purposes.

Total natural gas consumption by large energy users in Texas accounted for 0.93 quadrillion BTU (QBTU) in 2016, which represents about 44% of the 2.1 QBTU of natural gas consumed by the industry in Texas, as reported by EIA (Figure C- 2). From that 0.93 QBTU, we considered for the analysis process heaters, furnaces, boilers and other combustion sources as potential units that use natural gas for heating purposes. Moreover, we excluded units whose unit name suggests natural gas is being used as feedstock. This results in 0.59 QBTU of natural gas used for heating. By assuming flat demand, the total of 0.59 QBTU/year of natural gas heat is equivalent to 19.7 GW_t of hydrogen.

⁴⁷ Defined as those facilities that are required to report greenhouse gas emissions under EPA's Greenhouse Gas Reporting Program.

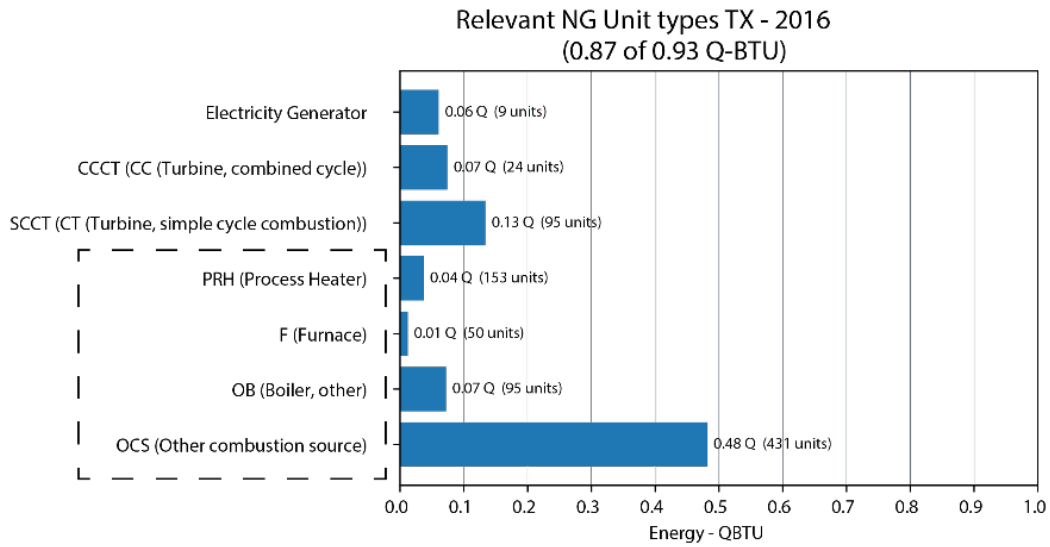


Figure C- 2: Natural gas consumption by Large Energy Users in Texas.

		Hydrogen demand as % of baseline Hydrogen demand (19.7 GWt)					
		0	25%	50%	75%	100%	125%
Emission policy (gCO2/kWh)	1	2.68	2.50	2.60	2.70	2.80	2.90
	5	2.27	2.39	2.49	2.60	2.72	2.83
	10	2.20	2.38	2.47	2.58	2.69	2.80
	50	2.01	2.03	2.13	2.24	2.35	2.45
	NL	1.76	1.90	1.99	2.11	2.20	2.32

Table C-1: Installed Power Capacity (relative to peak load). Increasing hydrogen demand and imposing a more stringent CO₂ constraint increases the total installed power capacity.

		Hydrogen demand					
		0	25%	50%	75%	100%	125%
Emission policy (gCO2/kWh)	1	29.7	12.0	11.7	11.4	10.8	10.2
	5	16.9	10.0	9.5	9.5	9.4	9.3
	10	15.3	10.1	9.7	9.0	8.6	8.3
	50	9.7	2.9	2.7	2.5	2.4	2.3
	NL	3.2	1.4	1.0	1.0	0.7	0.8

Table C-2: VRE Curtailment level (%). Increasing the stringency of the CO₂ constraint increases VRE curtailment levels but increasing industrial hydrogen demand decreases it.

Table 3. Average system cost (\$/MWh)

		Hydrogen demand					
		0	25%	50%	75%	100%	125%
Emission policy (gCO ₂ /kWh)	1	49.8	40.6	39.2	38.1	37.2	36.4
	5	43.9	39.0	37.7	36.6	35.7	35.0
	10	42.2	37.9	36.6	35.6	34.7	34.1
	50	37.0	34.8	33.8	33.0	32.4	31.9
	NL	36.2	34.6	33.6	32.8	32.2	31.7

Table C-3: Average system cost of energy, SCOE (\$/MWh). Increasing the stringency of the CO₂ constraint increases SCOE, but increasing industrial hydrogen demand decreases it.

Appendix D. Additional Modeling Results

	5g	10g	50g	NL
Northeast	2%	7%	31%	66%
Southeast	5%	9%	29%	54%
Texas	3%	7%	24%	36%

Table D-1: Capacity factors of CCGTs without CCS in the base case for various emission policy constraints (gCO₂/kWh).

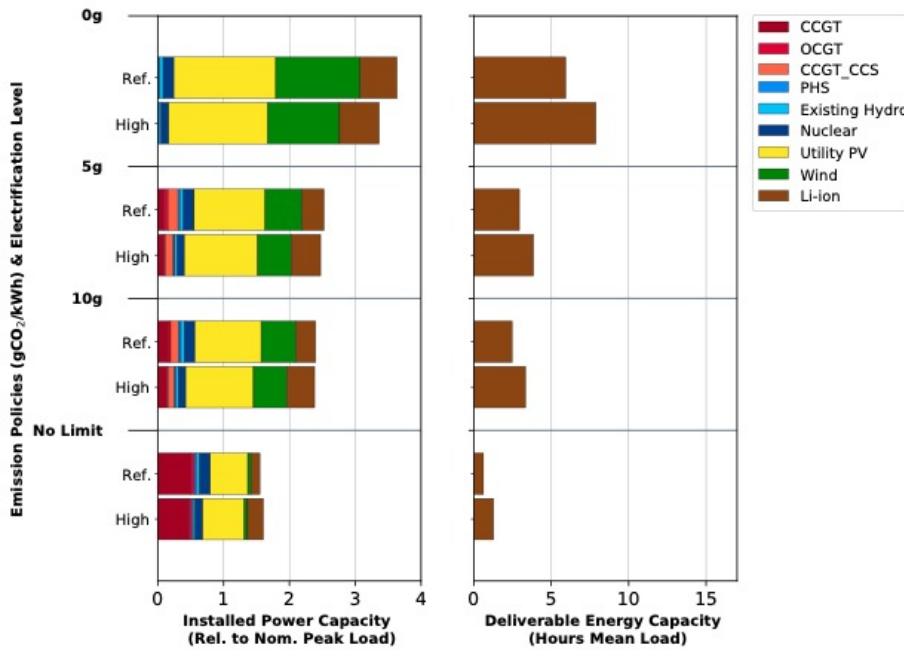


Figure D-1: Impacts of assuming the NREL EFS Reference vs. High Electrification load scenarios in the Southeast on installed power capacity, storage capacity, and VRE curtailment, across a range of CO₂ emission policies. Under the High Electrification scenario, both system peak and annual demand are higher, see Table 6 for details. See discussion of the impacts of electrification around Figure 6.5 in the main text.

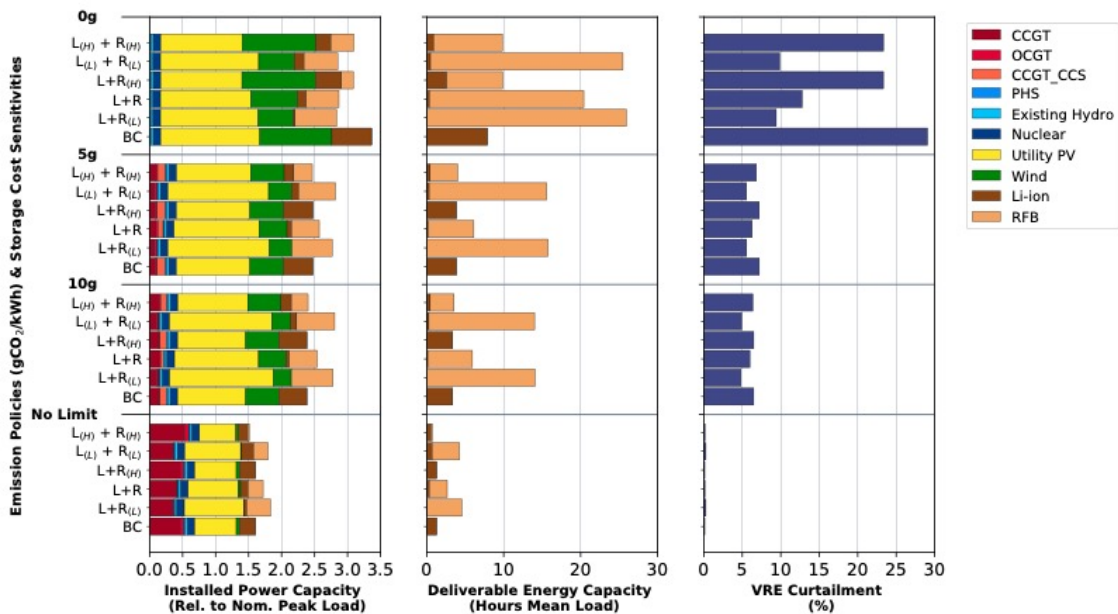


Figure D-2: Scenarios showing the impacts of cost sensitivities around Li-ion and RFB technology in the Southeast on installed power capacity, storage capacity, and VRE curtailment, across a range of CO₂ policies. They are, in ascending order: (1) base case (i.e., mid-cost Li-ion only, BC); (2) mid-cost Li-ion + low-cost RFB (L+R_L); (3) mid-cost Li-ion + mid-cost RFB (L+R); (3) mid-cost Li-ion + high-cost RFB (L+R_H); (4) low-cost Li-ion + low-cost RFB (L_L+R_L); and (5) high-cost Li-ion + high-cost RFB (L_H+R_H). Low-, mid-, and high-cost assumptions for each storage technology are defined in Table 6.3. See discussion of the impacts of Li-ion and RFB costs around Figure 6.8 in the main text.

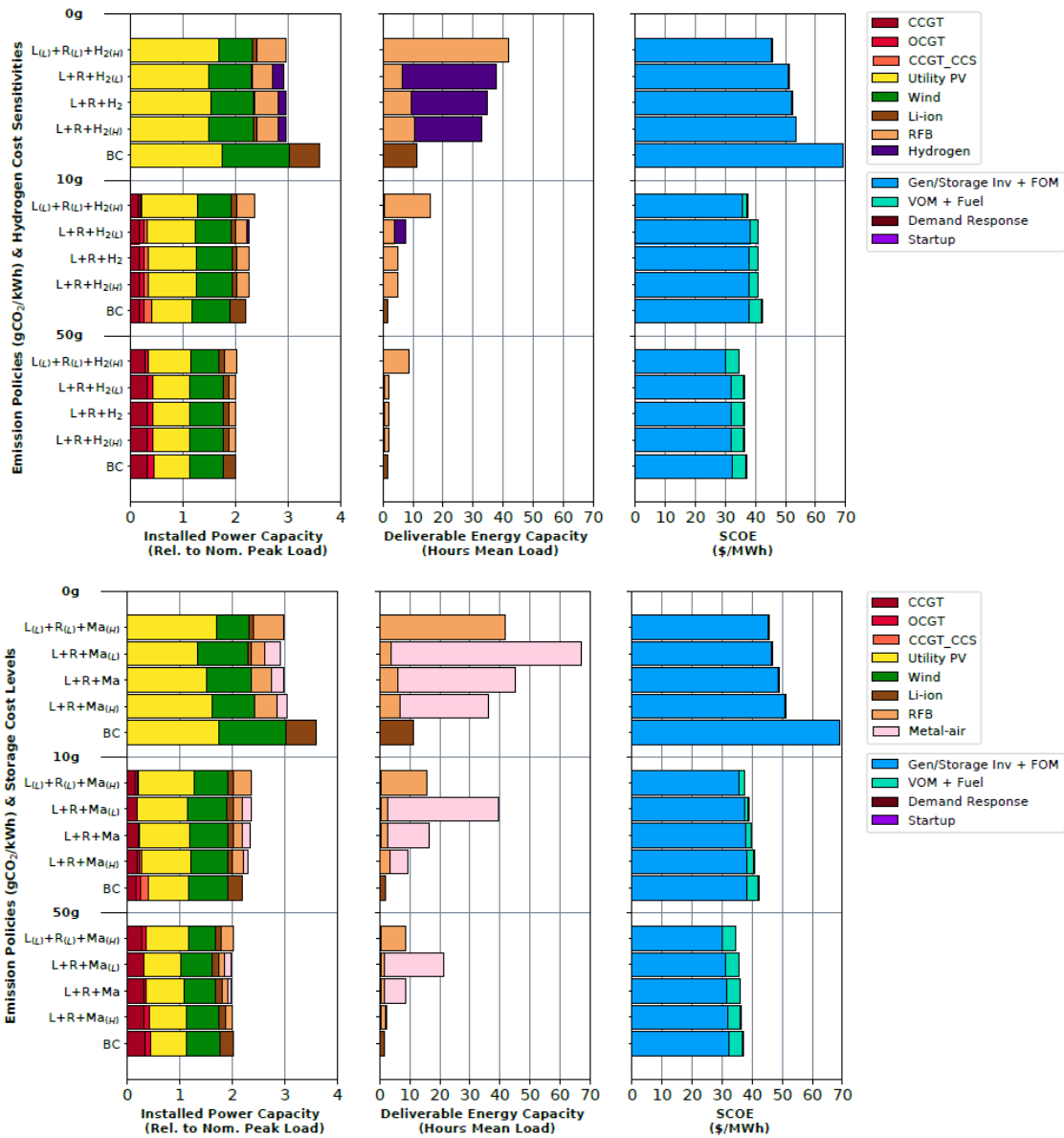


Figure D-3: System impacts of LDES availability at different assumed cost levels in Texas. Scenarios show the impacts of low-, mid-, and high-cost hydrogen and metal-air batteries on installed power capacity, storage capacity, and SCOE, across a range of CO₂ policies. They are, in ascending order: (1) base case (i.e., mid-cost Li-ion only, BC); (2–4) mid-cost Li-ion and RFB + incrementally adding high-cost hydrogen or metal-air batteries (L+R+H₂/MA_H), mid-cost hydrogen) or metal-air (L+R+H₂/MA), and low-cost hydrogen or metal-air (L+R+H₂/MA_L); and (5) low-cost Li-ion and RFB + high-cost hydrogen or metal-air (L_L+R_L+H₂/MA_H). Low-, mid-, and high-cost assumptions for each storage technology are defined in Table 6.3. See discussion of the impacts of LDES costs around Figure 6.11 and Figure 6.12 in the main text.

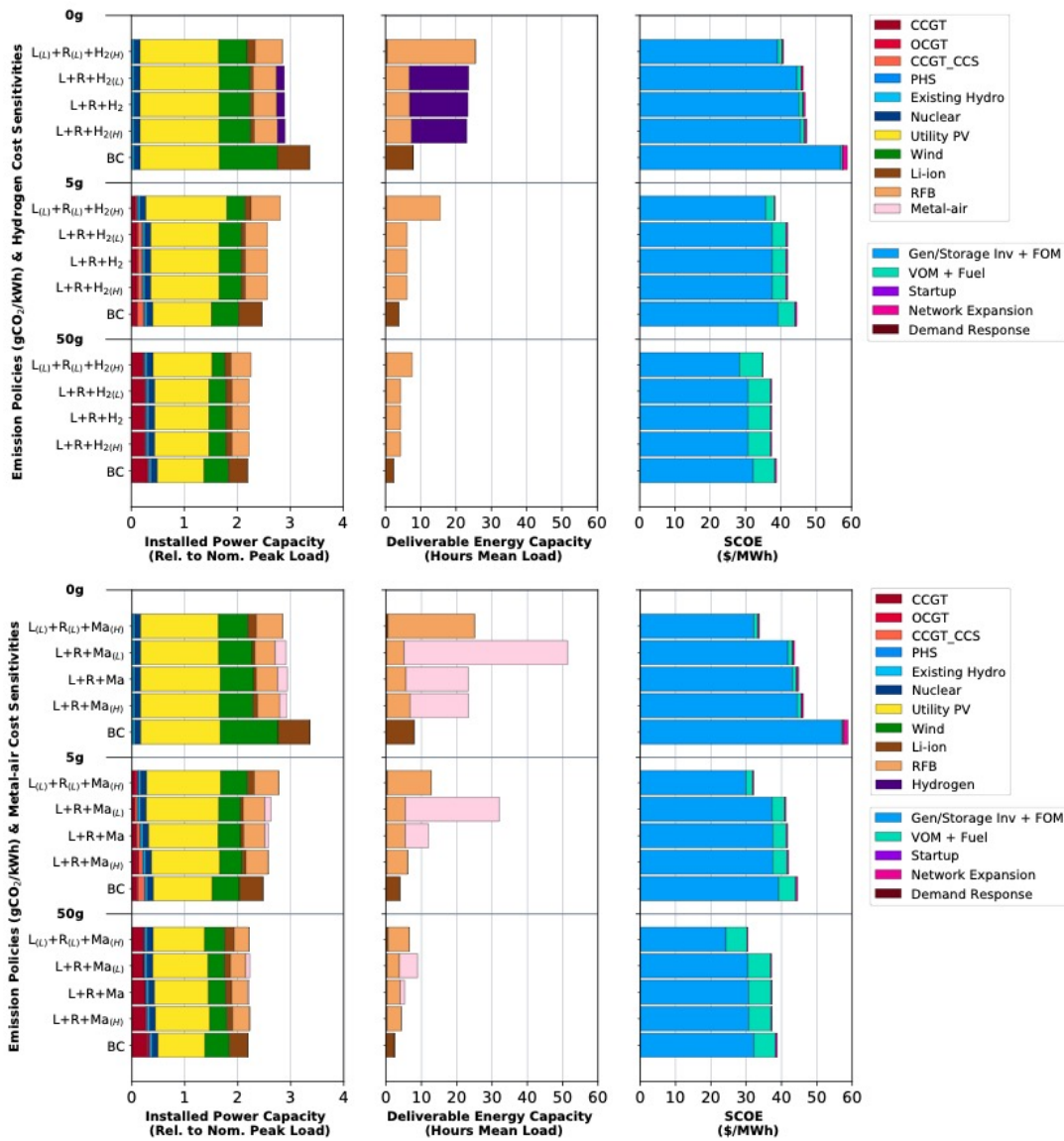


Figure D-4: System impacts of LDES availability at different assumed cost levels in the Southeast. Scenarios show the impacts of low-, mid-, and high-cost hydrogen and metal-air batteries on installed power capacity, storage capacity, and SCOE, across a range of CO₂ policies. They are, in ascending order: (1) base case (i.e., mid-cost Li-ion only, BC); (2-4) mid-cost Li-ion and RFB + incrementally adding high-cost hydrogen or metal-air (L+R+H₂/MA_H), mid-cost hydrogen or metal-air (L+R+H₂/MA), and low-cost hydrogen or metal-air (L+R+H₂/MA_L); and (5) low-cost Li-ion and RFB + high-cost hydrogen or metal-air (L_L+R_L+H₂/MA_H). Low-, mid-, and high-cost assumptions for each storage technology are defined in Table 6.3. See discussion of the impacts of LDES costs around Figure 6.11 and Figure 6.12 in the main text.

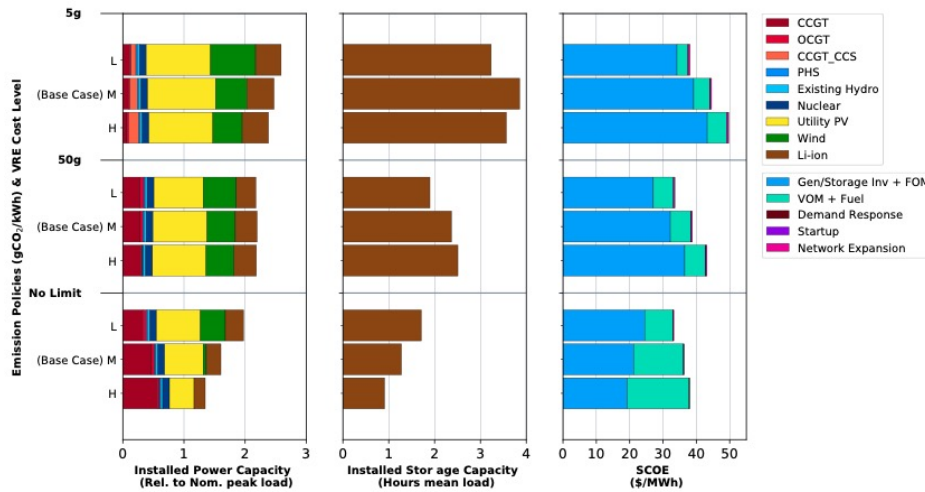


Figure D-5: System impacts of VRE at varying cost levels in the Southeast. Scenarios show the impacts of low-, mid-, and high-cost VRE on installed power capacity, storage capacity, and SCOE, across a range of CO₂ policies. They are, in ascending order: (1) high-cost VRE (H), (2) mid-cost VRE (M), and (3) low-cost VRE (L). Low-, mid-, and high-cost assumptions for VRE are defined in Appendix A. See discussion of the impacts of VRE costs around Figure 6.14 in the main text.

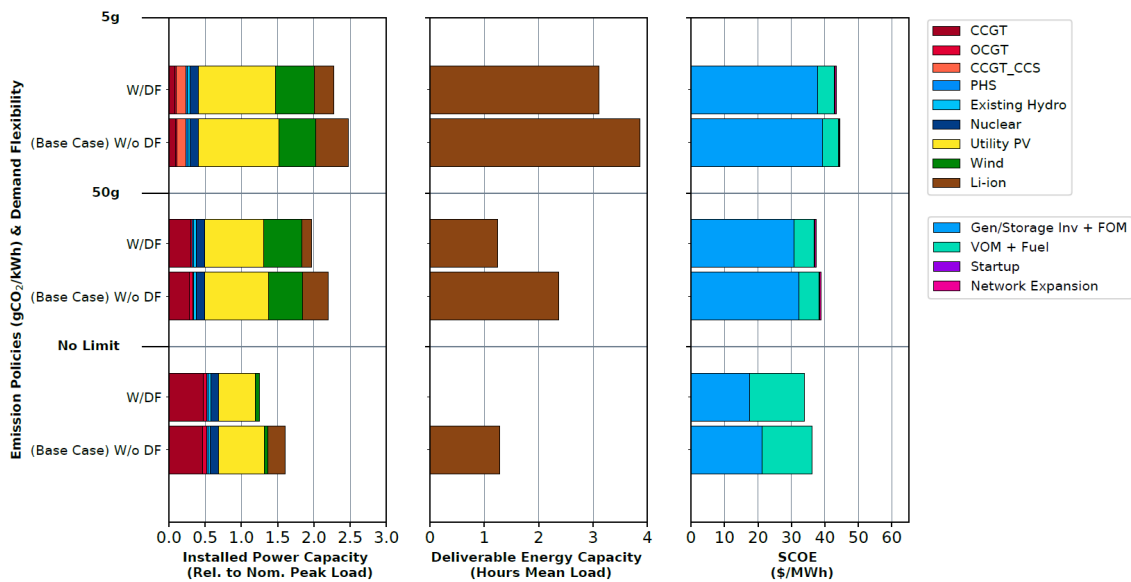


Figure D-6: System impacts of demand flexibility availability in the Southeast. Scenarios show impacts with and without demand flexibility in terms of installed power capacity, storage capacity, and SCOE, across a range of CO₂ policies. Demand flexibility assumptions are reported in Table 6.11. See discussion of the impacts of demand flexibility around Figure 6.15 in the main text.

	Low-Cost Metal-air			Mid-Cost Metal-air			High-Cost Metal-air		
	Without Allam Cycle	With Allam Cycle	% Diff	Without Allam Cycle	With Allam Cycle	% Diff	Without Allam Cycle	With Allam Cycle	% Diff
Firm Dispatchable Installed Capacity (GW)									
CCGT	19.5	20.2	4%	22.6	23.0	2%	19.0	20.1	6%
OCGT	0.0	0.0	-	0.1	2.1	2294%	6.2	9.2	47%
CCGT_CCS	7.7	0.0	100%	11.2	0.0	-100%	15.4	0.0	-
Allam	0.0	9.8	-	0.0	13.9	-	0.0	18.7	-
Total	27.2	30.0	10%	33.9	25.1	15%	40.6	29.3	18%
VRE Installed Capacity (GW)									
Wind	113.2	108.6	-4%	107.6	102.3	-5%	104.4	97.3	-7%
Utility PV	147.5	142.8	-3%	148.0	140.6	-5%	145.4	137.0	-6%
Total	260.7	251.4	-4%	255.6	243.0	-5%	249.8	234.3	-6%
Energy Storage (Li-ion + RFB + LDES)									
Power (GW)	70.7	68.6	-3%	64.6	60.4	-6%	58.7	52.3	11%
Energy (GWh)	3,168	3,121	-2%	1,399	1,114	-20%	840	626	25%
System Cost of Electricity									
Average \$/MWh	40.1	39.9	-1%	41.0	40.7	-1%	42.0	41.6	-1%

Table D-2: System impacts of a dispatchable low-carbon generating technology in Texas. Scenarios show the impact of low-, mid-, and high-cost metal-air batteries with and without the Allam cycle in terms of installed power capacity, storage capacity, and SCOE, for a 5 gCO₂/kWh scenario. Low-, mid-, and high-cost assumptions for each storage technology are defined in Table 6.3. Cost assumptions for the Allam cycle are presented in Appendix A.

	0 gCO ₂ /kWh			5 gCO ₂ /kWh			No Limit Policy		
	With Trans Exp	Without Trans Exp	% Diff	With Trans Exp	Without Trans Exp	% Diff	With Trans Exp	Without Trans Exp	% Diff
Firm Dispatchable Installed Capacity (GW)									
CCGT	0.0	0.0	-	26.4	21.7	-18%	139.9	144.9	4%
OCGT	0.0	0.0	-	8.1	18.1	124%	14.9	15.7	5%
CCGT_CCS	0.0	0.0	-	36.7	43.9	20%	0.0	0.0	-
Nuclear	32.9	32.9	-	32.9	32.9	0%	32.9	32.9	-
Total	32.9	32.9	-	104.1	116.6	12%	187.7	193.4	3%
VRE Installed Capacity (GW)									
Wind	325.6	297.2	-9%	152.7	145.4	-5%	15.3	14.0	-8%
Utility PV	447.7	470.8	5%	331.3	326.2	-2%	187.6	181.3	-3%
Total	773.3	768.0	-1%	484.1	471.6	-3%	202.9	195.3	-4%
Energy Storage (Li-ion only)									
Power (GW)	179.4	195.1	9%	132.0	130.1	-1%	71.3	66.3	-7%
Energy (GWh)	1,307	1,873	43%	639	612	-4%	212	189	11%
Transmission Expansion									
Total (GW)	145.3	-	-	45.5	-	-	2.0	-	-
System Cost of Electricity									
Average \$/MWh	58.8	64.9	10%	44.6	44.9	1%	36.3	36.3	0%

Table D-3: System impacts of expanding inter-zonal transfer capacity in the Southeast. Scenarios show the impacts of allowing transfer capacities to expand vs. restricting transfer capacities to existing levels in terms of installed power capacity, storage capacity, and SCOE, across a range of CO₂ policies. Cost assumptions for transmission expansion are presented in Appendix A.



MIT Center for Energy and
Environmental Policy Research

**MIT Center for Energy and
Environmental Policy Research**
Massachusetts Institute of Technology
77 Massachusetts Avenue, E19-411
Cambridge, MA 02139-4307
USA

ceepr.mit.edu



MASSACHUSETTS INSTITUTE OF TECHNOLOGY